

**PREPARATION OF ION-IMPRINTED  
POLY(N-ISOPROPYLACRYLAMIDE-2-  
METHACRYLOYLAMIDOCYSTEINE), P(NIPA-MAC),  
THERMOSENSITIVE HYDROGELS**

**İYON BASKILANMIŞ POLİ(N-İZOPROPİLAKRİLAMİD-2-  
METAKRİLAMİDOSİSTEİN), P(NIPA-MAC), ISIYA DUYARLI  
HİDROJELLERİN HAZIRLANMASI**

**AYŞENUR SAĞLAM**

Submitted to Institute of Sciences of Hacettepe University  
as a partial fulfilment to the requirements for the award of the degree of

DOCTOR OF PHILOSOPHY

in

CHEMISTRY

2010

**TO MY FATHER & MOTHER**

Graduate School of Natural and Applied Sciences,

This is to certify that we have read this thesis and that in our opinion it is fully adequate, in scope and quality, as a thesis for degree of **Doctor of Philosophy** in **Chemistry**.

Chairman : .....  
Prof. Dr. A. Rehber TÜRKER

Member  
(Advisor) : .....  
Prof. Dr. Sema BEKTAŞ

Member : .....  
Prof. Dr. Elmas GÖKOĞLU

Member : .....  
Prof. Dr. Nuray ÖĞÜN ŞATIROĞLU

Member : .....  
Assoc. Prof. Dr. Serdar ABACI

#### APPROVAL

This thesis has been certified as a thesis for degree of Doctor of Philosophy by the above Examining Committee Members on .... / .... / ....

.... / .... / ....

Prof. Dr. Adil DENİZLİ  
Director of the Graduate School of  
Natural and Applied Sciences

# PREPARATION OF ION-IMPRINTED POLY(N-ISOPROPYLACRYLAMIDE-2-METHACRYLOYLAMIDOCYSTEINE), P(NIPA-MAC), THERMOSENSITIVE HYDROGELS

**Ayşenur Sağlam**

## **ABSTRACT**

Ion-imprinted poly(N-isopropylacrylamide-methacryloylamidocysteine), p(NIPA-MAC) thermosensitive hydrogels were prepared with the aim of reversibly adsorb and release Cd(II) ions, for the selective removal of Cd(II) ions from aqueous media.

The present work was organized in two main parts. During the first part of the study, Cd(II) imprinted p(NIPA-MAC) hydrogel was synthesized by free radical polymerization technique. The effects of amount of the cross-linker and the amount of MAC monomer used in the synthesis of the hydrogel were investigated in order to improve the swelling/deswelling behavior of the hydrogel. For comparison, pNIPA and non-imprinted p(NIPA-MAC) hydrogels were also prepared. The characterization of the prepared thermosensitive hydrogels was carried out by using swelling test, Fourier Transform Infrared Spectroscopy (FTIR), elemental analysis, SEM images, and energy dispersive x-ray (EDX) techniques. In the second part of the study, adsorption and desorption of Cd(II) ions from aqueous solutions onto the template removed Cd(II) imprinted p(NIPA-co-MAC), non-imprinted p(NIPA-MAC), and pNIPA hydrogels was investigated in batch processes. The effect of the initial Cd<sup>2+</sup> concentration, pH of the medium, temperature, and adsorption time on the adsorption capacity were studied both on the p(NIPA-MAC) and Cd(II)-imprinted p(NIPA-MAC) hydrogels. Selectivity studies of Cd(II) ions versus other interfering metal ion mixture Pb<sup>2+</sup>, Cu<sup>2+</sup>, Cr<sup>3+</sup>, and Fe<sup>3+</sup>, was reported. Repeated use of the Cd<sup>2+</sup>-imprinted p(NIPA-MAC) thermosensitive hydrogels from aqueous solutions and the recovery of Cd(II) ions from a certified water sample was also studied.

**Keywords:** pNIPA, thermosensitive hydrogels, MAC, molecular imprinting, Cd(II).

Advisor: Prof.Dr. Sema Bektaş, Hacettepe University, Department of Chemistry, Analytical Chemistry Division

# İYON BASKILANMIŞ POLİ(N-İZOPROPİLAKRİLAMİD-2 METAKRİLAMİDOSİSTEİN), P(NİPA-MAC), ISIYA DUYARLI HİDROJELLERİN HAZIRLANMASI

**Ayşenur Sağlam**

## ÖZ

Bu çalışmada Cd(II) iyonlarının sulu ortamlardan seçimli olarak uzaklaştırılması için, sıcaklığın etkisi ile hidrofilitik/hidrofobik karakterini değiştirerek metal iyonunu tersinir olarak adsorbe ve desorbe edebilen, Cd(II) baskılanmış poli(N-izopropilakrilamid-2-metakrilamidosisistein), p(NİPA-MAC), ısıya duyarlı hidrojeller hazırlanmıştır.

Bu amaçla öncelikle Cd(II) iyonu baskılanmış p(NİPA-MAC) ısıya duyarlı hidrojel adsorbent radikal polimerizasyonu yöntemi kullanılarak sentezlenmiştir. Karşılaştırma yapmak amacıyla pNİPA ve iyon baskılanmamış p(NİPA-MAC) hidrojellerde aynı koşullarda hazırlanmıştır Hidrojellerin şişme ve büzülme özelliğini geliştirmek amacıyla polimerizasyonda kullanılan çapraz bağlayıcı ve şelatlaştırıcı monomer MAC miktarlarının şişme ve büzülmeye etkisi incelenmiştir. Hazırlanan ısıya duyarlı hidrojellerin karakterizasyonu için, şişme testi, Fourier Transform Infrared Spektroskopisi (FTIR), elemental analiz, SEM görüntüleri, enerji dispersive x-ışınları yöntemleri kullanılmıştır. Sulu ortamlardaki Cd(II) iyonlarının ısıya duyarlı Cd(II) baskılanmış p(NİPA-MAC) hidrojeller kullanılarak adsorpsiyonu ve desorpsiyonu için optimum koşulların belirlenmesinde, ortamın pH'sı, adsorpsiyon süresi, sıcaklığın etkisi ve başlangıç Cd<sup>2+</sup> çözelti derişimi kesikli sistemle incelenmiştir. Seçicilik çalışmalarında ise Cd(II) iyonlarına karşı Cu<sup>2+</sup>, Pb<sup>2+</sup>, Cr<sup>3+</sup> ve Fe<sup>3+</sup> metal iyonları karışımları kullanılmıştır. Sertifikalı su örneği kullanılarak Cd(II) iyonlarının geri kazanımı belirlenen optimum koşullarda çalışılmıştır. Cd<sup>2+</sup> baskılanmış p(NİPA-MAC) ısıya duyarlı hidrojellerin ard arda kullanıma uygunluğu denenmiştir.

**Anahtar Kelimeler:** pNİPA, hidrojel, MAC, moleküler baskılama, Cd(II).

Danışman: Prof.Dr. Sema Bektaş, Hacettepe Üniversitesi, Kimya Bölümü, Analitik Kimya Anabilim Dalı

## ACKNOWLEDGEMENT

I would like to express my special thanks to:

My advisor **Prof. Dr. Sema Bektaş**, for her valuable guidance, professional advice, constructive criticism and suggestion throughout the research with great patience;

**Prof. Dr. Adil Denizli**, for his undeniable contribution in building up the thesis;

**Prof. Dr. Nuray Ögün Şatıroğlu**, for her suggestions and ideas;

**Dr. Mutlu Sönmez Çelebi** and **Dr. Filiz Kuralay**, for their good fellowship and motivation;

My dear friends Assoc. **Prof. Dr. Hatice Kaplan Can**, **Dr. Bora Garipcan**, **Dr. Lokman Uzun**, **Dr. Müge Andaç**, **Research Assist. Cafer Çakal**, **Research Assist. Serhat Döker** and **Funda Altın** for their friendship, help, support and encouragement during the preparation of this thesis;

And finally, **my father, mother, brothers, sister and brother in law (my precious family)** for their love, support, encouragement, patience and invaluable contribution during my whole academic life.

## TABLE OF CONTENTS

ABSTRACT.....	I
ÖZ.....	II
ACKNOWLEDGEMENT.....	III
TABLE OF CONTENTS.....	IV
LIST OF FIGURES .....	VII
LIST OF TABLES.....	XI
1. INTRODUCTION.....	1
2. THEORETICAL INFORMATION .....	5
2.1. SMART POLYMERS .....	5
2.1.1. <i>pH-Responsive Smart Polymers</i> .....	7
2.1.2. <i>Thermoresponsive Smart Polymers</i> .....	8
2.1.3. <i>Reversibly Cross-Linked Polymer Networks</i> .....	11
2.2. HYDROGELS .....	11
2.2.1. <i>Fundamental Interactions</i> .....	14
2.2.1.1. Van der Waals .....	14
2.2.1.2. Hydrophobic.....	16
2.2.1.3. Hydrogen bonding.....	16
2.2.1.4. Electrostatic .....	17
2.3. APPROACHES TO MOLECULAR IMPRINTING .....	17
2.3.1. <i>Imprinting in Hydrogels</i> .....	20
2.3.2. <i>The Tanaka Equation</i> .....	21
2.3.3. <i>Temperature-Sensitive Imprinted Hydrogels</i> .....	22
2.4. TOXICITIES OF HEAVY METALS .....	29
2.5. CADMIUM, AN OVERVIEW .....	31
2.6. ANALYTICAL TECHNIQUES .....	33
2.6.1. <i>Fourier Transform Infrared Spectroscopy (FTIR)</i> .....	33
2.6.2. <i>Scanning Electron Microscopy (SEM)</i> .....	34
2.6.3. <i>Energy Dispersive X-Ray Spectroscopy</i> .....	35
2.6.4. <i>Elemental Analysis (EA)</i> .....	37
2.6.5. <i>Atomic Absorption Spectroscopy (AAS)</i> .....	38

3. EXPERIMENTAL.....	41
3.1. PREPARATION OF POLYMERIC HYDROGELS .....	41
3.1.1. <i>Materials</i> .....	41
3.1.2. <i>Synthesis of 2-methacryloylamidocysteine (MAC) Chelating Monomer and the Complex with Cd(II) Ions</i> .....	41
3.1.3. <i>Preparation of Cd(II)-imprinted p(NIPA-MAC) Hydrogels</i> .....	42
3.1.4. <i>Removal of the Template Cd(II) ions</i> .....	43
3.2. CHARACTERIZATION OF THE HYDROGELS .....	44
3.2.1. <i>Temperature Dependence of Swelling Ratios</i> .....	44
3.2.2. <i>Swelling kinetics</i> .....	44
3.2.3. <i>FTIR Characterization</i> .....	45
3.2.4. <i>Elemental Analysis</i> .....	45
3.2.5. <i>Morphologies of Hydrogels</i> .....	45
3.2.6. <i>Energy Dispersive X-Ray Analysis</i> .....	45
3.3. ADSORPTION AND DESORPTION STUDIES .....	46
3.3.1. <i>Reagents and Apparatus</i> .....	46
3.3.2. <i>Temperature-Dependent Adsorption Studies</i> .....	47
3.3.3. <i>Desorption and Reusability Studies</i> .....	47
3.3.4. <i>Selectivity Experiments</i> .....	48
4. RESULTS AND DISCUSSION .....	49
4.1. PREPARATION OF HYDROGELS .....	49
4.2. CHARACTERIZATION OF Cd <sup>2+</sup> IMPRINTED P(NIPA-MAC) HYDROGELS .....	50
4.2.1. <i>Temperature Dependence of Swelling Ratio of the Hydrogels</i> .....	50
4.2.2. <i>Swelling Kinetics of the Hydrogels</i> .....	55
4.2.3. <i>Elemental Analysis</i> .....	56
4.2.4. <i>FT-IR Characterization</i> .....	57
4.2.5. <i>SEM Observation of Synthesized Hydrogels</i> .....	57
4.2.6. <i>Energy Dispersive X-ray (EDS) Analysis</i> .....	61
4.3. ADSORPTION STUDIES .....	63
4.3.1. <i>Adsorption Rate</i> .....	63
4.3.2. <i>Effect of pH</i> .....	64
4.3.3. <i>Adsorption Capacity</i> .....	65
4.3.4. <i>Temperature-Dependent Adsorption</i> .....	68



4.3.5. <i>Selectivity Experiments</i> .....	68
4.3.6. <i>Desorption and Reusability</i> .....	73
4.3.7. <i>Determination of Cd(II) Ions in a Certified Sample</i> .....	75
5. CONCLUSION .....	77
REFERENCES .....	81
CURRICULUM VITAE .....	89

## LIST OF FIGURES

Figure 2.1. Potential stimuli and responses of synthetic polymers.....	5
Figure 2.2. (a) Copolymer of sodium 2-(acrylamido)-2-methylpropanesulfonate) (NaAMPS) with a series of monomers bearing long chain alkyl carboxyl pendants. (b) Schematic illustration of pH responsive unimer micelle (Yusa et al., 2002).....	8
Figure 2.3. Temperature response for thermosensitive polymers: (a) soluble phase (below LCST); (b) insoluble phase (above LCST).....	9
Figure 2.4. Structures of thermoresponsive homopolymers.....	10
Figure 2.5. Fundamental interactions in polymer gels. a) For polar solvents, hydrophobic interaction use to dominate, b) while in the case of non polar solvent Van der Waals is specially relevant. The other two interaction usually present in polymer gels are c) electrostatic and d) hydrogen bonds. Change of the interaction balance by specific external modifications makes these systems suitable for a great deal of applications.....	15
Figure 2.6. Schematic representation of the molecular imprinting process in synthetic polymers. Pre-assembly of functional monomers is achieved by virtue of their interaction with the template molecule. Polymerization in the presence of a high concentration of crosslinking agent “freezes” the bound groups, thus effectively forming a well defined cavity of molecular recognition. Removal of the template molecule either by solvent extraction, chemical or enzymatic scission generates binding sites with the capacity for specific recognition of the original template molecule.....	19
Figure 2.7. Schematic view of the imprinting process: (a) covalent approach, in which the template is covalently bound to polymerizable binding groups that are reversibly broken after polymerization; and (b) noncovalent approach, in which the template interacts with functional monomers through noncovalent interactions (e.g., ionic interaction, ii; hydrophobic interaction, hi; or hydrogen bond, hb) before and during polymerization.....	20

Figure 2.8. The volume phase transition of the hydrogel (induced by external stimuli such as a change in pH, temperature, or electrical field) modifies the relative distance of the functional groups inside the imprinted cavities. This alters their affinity for the template. The affinity is recalled when the stimulus reverses and the gel returns to its original conformation. ....	22
Figure 2.9. Chemical structures of some monomers used to create imprinted smart gels: <i>N</i> -isopropylacrylamide (NIPA, temperature-sensitive), <i>N,N'</i> -methylene-bisacrylamide (BIS, cross-linker), methacrylamidopropyl trimethylammonium chloride (MAPTAC, cationic adsorber), and acrylic acid (AA, anionic adsorber). Structures of some ionically charged derivatives of pyranine used as targets are also shown. ....	23
Figure 2.10. Two-step procedure to obtain an interpenetrated system comprising a Cu <sup>2+</sup> imprinted poly(acrylic acid) hydrogel and a poly( <i>N</i> -isopropylacrylamide) temperature-sensitive hydrogel. (Reproduced from Yamashita, K. et al., 2003. With permission from the Society of Polymer Science of Japan). ....	28
Figure 2.11. The consumption pattern of cadmium in its various end use applications. ....	32
Figure 2.12. Schematic of a dispersive IR absorption spectrometer. ....	33
Figure 2.13. Basic features of the SEM. ....	36
Figure 2.14. Principles of EDS. ....	37
Figure 2.15. Schematic construction of a double beam AAS. ....	38
Figure 3.1. Digital photographs of Cd(II) imprinted p(NIPA-MAC) hydrogels at the end of the polymerization (a) at room temperature, (b) after incubating at 50°C for 30 min, (c) and (d) after taken out from the glass tubes. ....	43
Figure 4.1. The chemical structures of monomers used and schematic preparation of the non-imprinted or Cd <sup>2+</sup> imprinted p(NIPA-MAC) hydrogels. ....	49

Figure 4.2. Effect of NIPA/MAC feed ratio on the temperature dependence of equilibrium swelling ratios of p(NIPA-MAC) hydrogels.....	51
Figure 4.3. Temperature dependence of swelling ratio for p(NIPA-MAC) hydrogel with different amount of cross-linker (wt %)......	52
Figure 4.4. Temperature dependence of swelling ratio for the p(NIPA), non-imprinted p(NIPA-MAC) and template removed Cd(II)-imprinted p(NIPA-MAC) hydrogels. ....	53
Figure 4.5. Swelling kinetics of the pNIPA, p(NIPA-MAC), and Cd <sup>2+</sup> imprinted p(NIPA-MAC) hydrogels at 22°C.....	56
Figure 4.6. FT-IR spectrums of the pNIPA, non-imprinted p(NIPA-MAC), and Cd <sup>2+</sup> imprinted p(NIPA-MAC) hydrogels.....	58
Figure 4.7. SEM images of freeze dried pNIPA, non-imprinted p(NIPA-MAC), and Cd(II) imprinted p(NIPA-MAC) hydrogels swollen at 20°C (at the left side) and shrunken at 50°C (at right side). The size of the bar is 20µm and the samples are viewed at magnification of 1.00 K X.....	60
Figure 4.8. EDS spectrums of non-imprinted p(NIPA-MAC) and Cd <sup>2+</sup> imprinted p(NIPA-MAC) hydrogels.....	62
Figure 4.9. Time dependent adsorption of Cd(II) ions on the pNIPA, non-imprinted and template removed Cd(II) imprinted p(NIPA-MAC) hydrogels. Adsorption conditions: 50 mL, 10 ppm Cd(II) solution; pH:4.5; temperature 20°C.....	63
Figure 4.10. Effect of pH on the adsorption amount of pNIPA, p(NIPA-MAC), and template removed Cd(II) imprinted p(NIPA-MAC) hydrogels for Cd(II) ions. ....	65
Figure 4.11. Effect of initial Cd(II) ion concentration on the adsorption amount of pNIPA, p(NIPA-MAC), and template removed Cd(II) imprinted p(NIPA-MAC) hydrogels.....	66
Figure 4.12. Effect of temperature on the adsorption amount for Cd(II) ions of the non-imprinted and Cd <sup>2+</sup> imprinted p(NIPA-MAC) hydrogels.....	69

Figure 4.13. The amount of  $\text{Cd}^{2+}$ ,  $\text{Cu}^{2+}$ , and  $\text{Pb}^{2+}$  ions adsorbed by using pNIPA, non-imprinted p(NIPA-MAC) and Cd(II) imprinted p(NIPA-MAC) hydrogels (a) from each metal ion solution (noncompetitive) (b) from the mixtures of these metal ions (competitive). ..... 71

Figure 4.14. The amount of  $\text{Cd}^{2+}$ ,  $\text{Cr}^{3+}$ , and  $\text{Fe}^{3+}$  ions adsorbed by using pNIPA, non-imprinted p(NIPA-MAC) and Cd(II) imprinted p(NIPA-MAC) hydrogels (a) from each metal ion solution (noncompetitive) (b) from the mixtures of these metal ions (competitive). ..... 72

Figure 4.15. Desorption of Cd(II) ions from the non-imprinted and imprinted p(NIPA-MAC) hydrogels by raising the temperature above LCST, at  $50^{\circ}\text{C}$ , after the adsorption was carried out at  $22^{\circ}\text{C}$ . ..... 74

## LIST OF TABLES

Table 3.1. Preparation conditions of Cd(II) imprinted poly(NIPA-MAC) gels. ....	42
Table 3.2. Working conditions for metal ions in AAS. ....	46
Table 4.1. Feed compositions of pNIPA hydrogels. ....	51
Table 4.2. Elemental analysis of the hydrogels. ....	57
Table 4.3. Reusability of the imprinted and non-imprinted hydrogels; adsorption-desorption of Cd(II) ions from the hydrogels. ....	75
Table 4.4. The content of the certified water sample, NWTMDA-52.3. ....	75
Table 4.5. Results for determination of Cd(II) ions in certified water sample. ....	76

## **1. INTRODUCTION**

Environmental stimuli-responsive polymers are getting more and more attention from both technological and scientific aspects, because of their promising application potentials in the fields of controlled drug delivery (A.S. Hoffman, 2001), enzyme immobilization (Zhu et al., 1998; Lee et al., 2004), chemical separation (Vassilev and Turmanova, 2008; Ishida, 2007), catalysis (Suzuki and Kawaguchi, 2006), sensor (Yeghiazarian et al., 2005), and so on. Environmental stimuli-responsive polymers are also called smart or intelligent polymers or environmentally sensitive polymers. Intelligent polymers are soluble, surface coated or cross-linked polymeric systems that exhibit relatively large and sharp physical or chemical changes in response to small physical or chemical external stimuli such as temperature or pH (Hoffman, 1995). Polymeric hydrogels are one such class of intelligent or smart material; they respond to the specific environmental stimuli by changing their size.

Environmentally sensitive hydrogels have the ability to sense changes of pH, temperature, solvent, additives, and ionic strength etc., and release their load as a result of such a change. As a representative thermal-sensitive hydrogel, poly(*N*-isopropylacrylamide), pNIPA, has been studied extensively, especially in applications such as controlled drug release because of their biocompatibility with the human body and also because of they resemble natural living tissue more than any other class of synthetic biomaterials. This is due to their high water content and soft consistency that is similar to natural tissue (Geever et al., 2007).

Covalently cross-linked pNIPA hydrogels display temperature-induced phase transitions or lower critical solution temperature (LCST) in response to the change of the surrounding temperature. At a temperature lower than 32°C, the pNIPA gel swells well in water due to the formation of hydrogen bonds between water molecules and the hydrophilic –CONH– groups in the polymer side chains. When the temperature is increased to above LCST, the gel network disrupted; the hydrophobic groups in the polymer side chains become naked and hydrophobic interaction plays the key role (Zhang et al., 2004), consequently the hydrogel loses a great amount of water and changes its volume dramatically.

## *Introduction*

In literature to date, limited number of study reported novel adsorbents using thermosensitive hydrogels for trapping heavy metal ions (Kanazawa et al., 2004;Tokuyama et al., 2005; Ju et al., 2009) where pNIPA was used as a thermosensitive backbone polymer. A chelating group, which interacts with heavy metal ions, was introduced into pNIPA with a molecular imprinting technique (Wulff et al., 1998) using a specific metals as the template. The molecularly imprinted adsorbents reconstruct multi-point adsorption sites at a specific temperature and disrupt them through swelling/deswelling deformation at another specific temeperature. Such adsorbents, therefore, are suitable for the control of adsorption and desorption of a specific heavy metal ion with the change in temperature. Using the adsorbents described here provides an energy saving and environmentally friendly process for the separation of both undesirable and valuable metals in aquatic environment, industrial effluents etc.

Heavy metals are natural components of the Earth's crust. They can not be degraded or destroyed. To a small extent they enter our bodies via food, drinking water and air. As trace elements, some heavy metals (e.g. copper, selenium, zinc) are essential to maintain the metabolism of the human body. However, at higher concentrations they can lead to poisoning. Heavy metal poisoning could result, for instance, from drinking water contamination, high ambient air concentrations near emission sources, or intake via the food chain. Heavy metals can enter a water supply by industrial and consumer waste, or even from acidic rain breaking down soils and releasing heavy metals into streams, lakes, rivers, and ground water. The three most pollutant heavy metals are Lead, Cadmium, and Mercury.

The toxicities of heavy metals may be caused by the following mechanism: blocking the essential functional groups of biomolecules; displacing essential metal ions from biomolecules; modifying the active conformation of biomolecules; disrupting the integrity of biomembranes and modifying some other biologically active agents (Stokinger, 1981). Toxic metals are absorbed through the air passages and alimentary canal with food and drinking water. They disturb the economy of endogenous metals and biochemical equilibrium. They have an etiological effect on hypertension, cancer, decrease the ventila of the lungs and



other lung diseases. Toxic metal ions are the source of degeneration, reduction of pancreatic, efficiency and disfunction of kidneys (Frieberg and Elinder, 1985).

The most significant use of cadmium is nickel/cadmium batteries, as rechargeable or secondary power sources exhibiting high output, long life, low maintenance and high tolerance to physical and electrical stress. Cadmium coatings provide good corrosion resistance, particularly in high stress environments such as marine and aerospace applications where high safety or reliability is required (Morrow and Keating, 1997). Other uses of cadmium are as pigments, stabilizers for PVC, in alloys and electronic compounds (Cook, 1994). Cadmium is also present as an impurity in several products, including phosphate fertilizers, detergents and refined petroleum products. In the general, non-smoking population the major exposure pathway is through food, via the addition of cadmium to agricultural soil from various sources (atmospheric deposition and fertiliser application) and uptake by food and fodder crops. Additional exposure to humans arises through cadmium in ambient air and drinking water.

In this thesis, ion-imprinted p(NIPA-MAC), poly(N-isopropylacrylamide-co-methacryloylamidocysteine), thermosensitive hydrogels were prepared with the aim of reversibly adsorb and release Cd(II) ions, for the selective removal of Cd(II) ions from aqueous media.

The present work was organized in two main parts. During the first part of the study, Cd(II) imprinted p(NIPA-MAC) hydrogel was synthesized by free radical polymerization technique. The effects of amount of the cross-linker and the amount of MAC monomer used in the synthesis of the hydrogel were investigated in order to improve the swelling/deswelling behavior of the hydrogel. For comparison, pNIPA and non-imprinted p(NIPA-MAC) hydrogels were also prepared. The characterization of the prepared thermosensitive hydrogels was carried out by using swelling test, Fourier Transform Infrared Spectroscopy (FTIR), elemental analysis, SEM images, and energy dispersive x-ray (EDX) techniques. In the second part of the study, adsorption and desorption of Cd(II) ions from aqueous solutions onto the template removed Cd(II) imprinted p(NIPA-co-MAC), non-imprinted p(NIPA-MAC), and pNIPA hydrogels was investigated in batch processes. The effect of the initial Cd(II) concentration and pH of the

## *Introduction*

medium on the adsorption rate and adsorption capacity were studied both on the p(NIPA-MAC) and Cd(II)-imprinted p(NIPA-MAC) hydrogels. Selectivity studies of Cd(II) ions versus other interfering metal ion mixture  $\text{Pb}^{2+}$ ,  $\text{Cu}^{2+}$ ,  $\text{Cr}^{3+}$ , and  $\text{Fe}^{3+}$ , was reported. Repeated use of the Cd(II)-imprinted p(NIPA-MAC) particles from aqueous solutions and the recovery of Cd(II) ions from a certified water sample was also studied.

## 2. THEORETICAL INFORMATION

### 2.1. Smart Polymers

Polymers with reversible solubility are combined under the names “smart polymers,” “intelligent polymers,” or “stimuli-responsive” polymers. The characteristic feature that actually makes them “smart” is their ability to respond to very slight changes in the surrounding environment. The uniqueness of these materials lies not only in the fast macroscopic changes occurring in their structure but also these transitions being reversible. The responses are manifested as changes in one or more of the following—shape, surface characteristics, solubility, formation of an intricate molecular assembly, a sol-to-gel transition and others. The environmental trigger behind these transitions can be either change in temperature (Okano et al., 1993a) or pH shift (Twaittes et al., 2004), increase in ionic strength (Twaittes et al., 2004), presence of certain metabolic chemicals (Lomadze et al., 2005), addition of an oppositely charged polymer (Kabanov et al., 1994) and polycation–polyanion complex formation (Leclercq et al., 2003). More recently, changes in electric (Filipcsei et al., 2000) and magnetic field (Zrinyi et al., 2000), light or radiation forces (Juodkazis et al., 2000) have also been reported as stimuli for these polymers. The physical stimuli, such as temperature, electric or magnetic fields, and mechanical stress, will affect the level of various energy sources and alter molecular interactions at critical onset points (Figure 2.1).

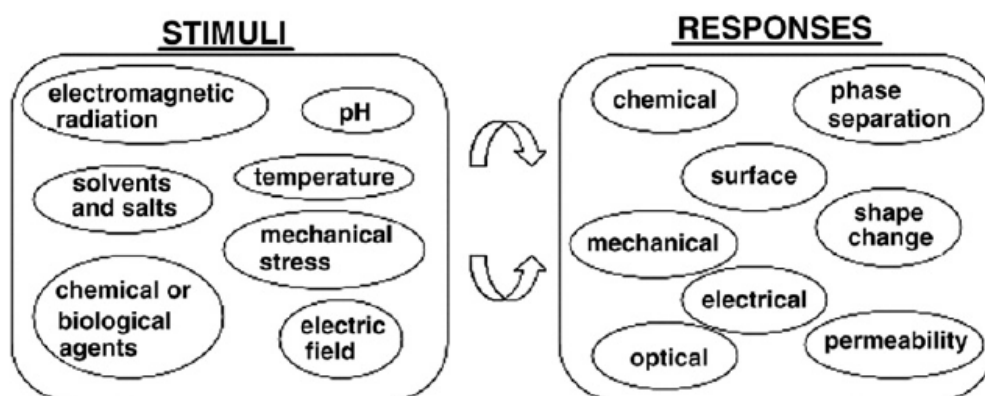


Figure 2.1. Potential stimuli and responses of synthetic polymers.

They undergo fast, reversible changes in microstructure from a hydrophilic to a hydrophobic state (Galaev et al., 1996). These changes are apparent at the macroscopic level as precipitate formation from a solution or order-of-magnitude changes in the size and water content of stimuli-responsive hydrogels (Taylor et al., 1975). An appropriate proportion of hydrophobicity and hydrophilicity in the molecular structure of the polymer is believed to be required for the phase transition to occur. With respect to water soluble smart polymers and their hydrogels, this definition can be formulated as follows. Smart polymers undergo fast and reversible changes in microstructure triggered by small property changes in the medium (pH, temperature, ionic strength, presence of specific chemicals, light, electric or magnetic field). These microscopic changes of polymer microstructure manifest themselves at the macroscopic level as the formation of a precipitate in a solution or as the manifold decrease/increase of the hydrogel size and hence of water content. Macroscopic changes in a system with smart polymers/hydrogels are reversible, and the system returns back to its initial state if the conditions in the medium are brought back to their original state. In most cases, the polymers need only one type of parameter change in the medium (pH, temperature, etc.) to induce phase separation, but in some cases it may be advantageous to use more than one mode to induce precipitation (Guogiang et al., 1995; Galaev and Mattiasson, 1999). An ideal polymer for affinity precipitation must:

- Contain reactive groups for ligand coupling
- Not interact strongly with the ligand or impurities, thereby making the ligand available for interaction with the target protein and preventing nonspecific coprecipitation of impurities
- Give complete phase separation of the polymer upon a change of property in the medium; in this respect, synthetic polymers are superior to natural polymers, which have a broader molecular weight distribution and thereby a less-well-characterized transition
- Form polymer precipitates that are compact, thereby allowing easy separation and avoiding the trapping of impurities within a gel structure
- Be easily solubilized after the precipitate is formed; the precipitation/solubilization cycle must be repeatable many times with good recovery

- Be available and cheap

In general, all smart polymer/hydrogel systems can be divided into three groups (Galaev et al., 1996; Galaev and Mattiasson, 2002):

1. pH-responsive smart polymers
2. Thermoresponsive smart polymers
3. Reversibly cross-linked polymer networks

### **2.1.1. pH-Responsive Smart Polymers**

This group consists of the polymers for which poor solvent conditions are created by decreasing the net charge of the polymer/hydrogel. In a typical pH-sensitive polymer, protonation/deprotonation events occur and impart the charge over the molecule (generally on carboxyl or amino groups). The net charge can be decreased by changing pH to neutralize the charges on the macromolecule, hence reducing the hydrophilicity (increasing the hydrophobicity) of the macromolecule and the repulsion between polymer segments (Figure 2.2). For instance, copolymers of methylmethacrylate (hydrophobic part) and methacrylic acid (hydrophilic at high pH when carboxy groups are deprotonated, but more hydrophobic when carboxy groups are protonated) precipitate from aqueous solutions upon acidification to pH around 5, while copolymers of methyl methacrylate (hydrophobic part) with dimethylaminethyl methacrylate (hydrophilic at low pH when amino groups are protonated, but more hydrophobic when amino groups are deprotonated) are soluble at low pH but precipitate at slightly alkaline conditions. The pH induced precipitation of smart polymers is very sharp and typically requires a change in pH of not more than 0.5 units. Increasing the hydrophobicity of the pH-sensitive polymer through copolymerization with more-hydrophobic monomers results in transitions at higher pH. There are ranges of different proteins/enzymes that have been purified successfully by affinity precipitation using pH-responsive polymers. In general, a specific ligand is chemically coupled to the polymer backbone, which later binds to the target protein in solution, and the protein–polymer complex is precipitated by a change of pH, as it renders the polymer backbone insoluble. But in some cases the polymer itself has the affinity for the target protein, and the polymer acts as a

microligand. pH-responsive smart polymers have been used successfully in affinity precipitation of many proteins, but the charged character of the polymer, which shows some nonspecific interactions with other proteins, has been limiting factor in the use of these polymers.

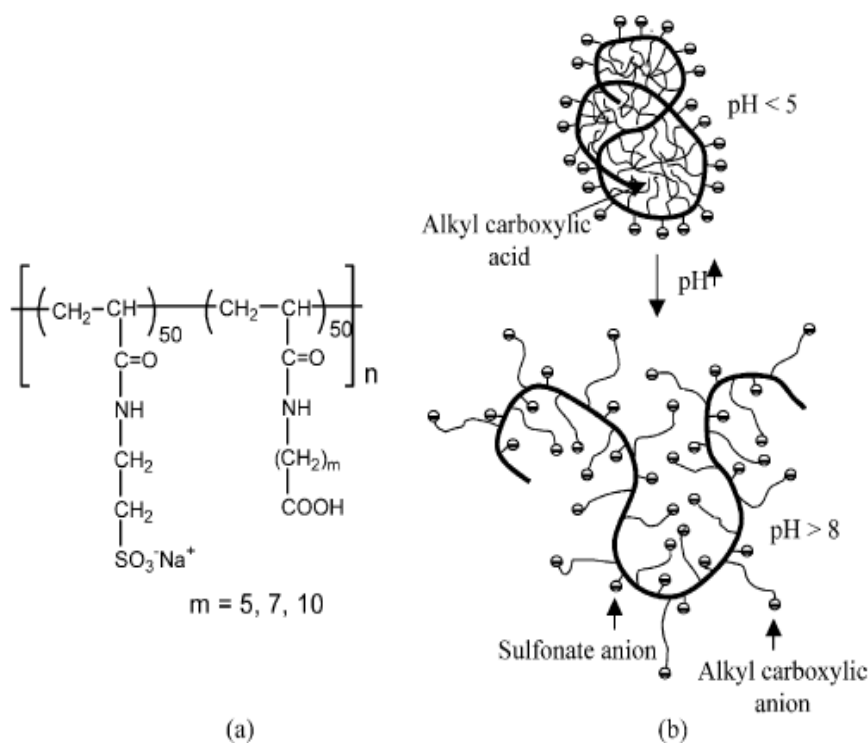


Figure 2.2. (a) Copolymer of sodium 2-(acrylamido)-2-methylpropanesulfonate (NaAMPS) with a series of monomers bearing long chain alkyl carboxyl pendants. (b) Schematic illustration of pH responsive unimer micelle (Yusa et al., 2002).

### 2.1.2. Thermoresponsive Smart Polymers

This is the most important group of smart polymers and has shown tremendous potential in developing affinity-precipitation methods for protein purification. This group of smart polymers consists of uncharged polymers soluble in water due to the hydrogen bonding with water molecules. Changes in hydrophobic–hydrophilic balance are induced by increasing temperature or ionic strength. The efficiency of hydrogen bonding is reduced upon raising temperature. There is a critical temperature for some polymers at which the efficiency of hydrogen bonding becomes insufficient for continued solubility of the macromolecule, and the phase separation of polymer takes place. When the temperature of an aqueous solution of a smart polymer is raised to a point higher than its critical temperature (lower

critical solution temperature [LCST] or “cloud point”), the solution separates into two phases; (i) a polymer-enriched phase and an aqueous phase containing practically no polymer (ii) that can be easily separated (Figure 2.3).

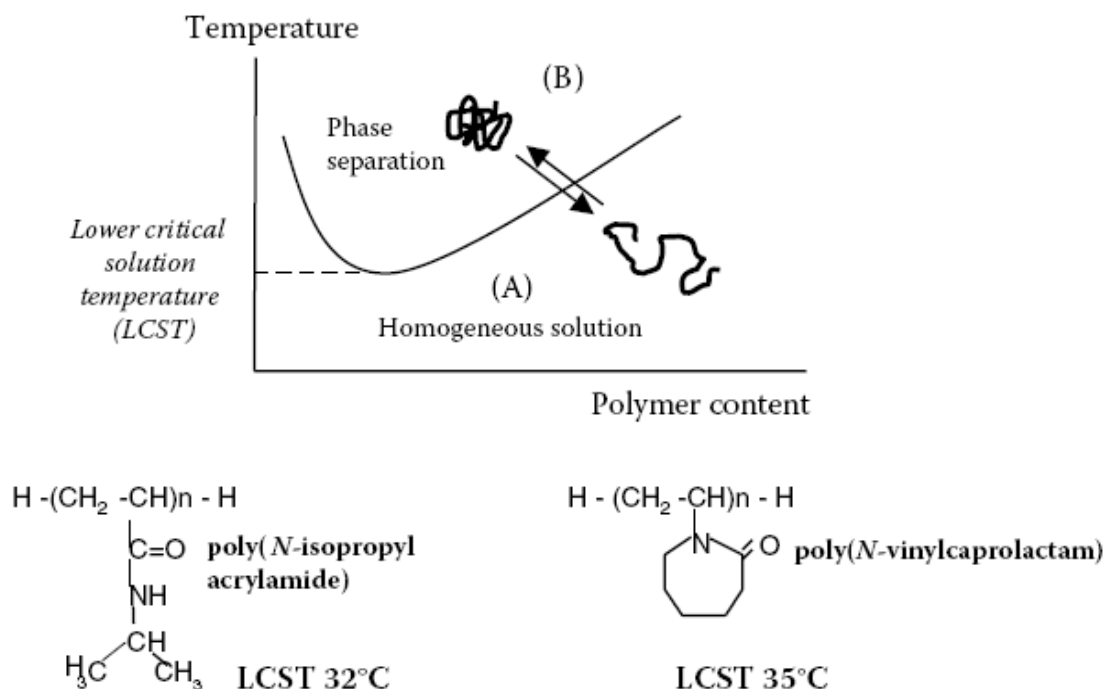


Figure 2.3. Temperature response for thermosensitive polymers: (a) soluble phase (below LCST); (b) insoluble phase (above LCST).

This phase separation is completely reversible, and the smart polymer dissolves in water upon cooling. In aqueous solution, several *N*-substituted poly(acrylamides) undergo a thermally induced, reversible phase transition. The LCSTs of such homopolymers as p(*N*-isopropylacrylamide), p(*N,N*-diethylacrylamide), p(*N*-cyclopropylacrylamide), and p(*N*-ethylacrylamide) in distilled H<sub>2</sub>O have been reported to be 32, 33, 58, and 74°C, respectively (Figure 2.4) (Galaev and Mattiasson, 1993). With present-day advanced synthetic polymer chemistry, it has been possible to design polymers with different transition temperatures ranging from 4 to 5°C for poly(*N*-vinyl piperidine) to 100°C for poly(ethylene glycol). Among these homopolymers, poly(*N*-isopropylacrylamide) (PNIPAM) has received special attention because of its sharp phase-transition temperature at 32°C (Schild, 1992), and various strategies for synthesizing the hydrogel and its derivatives have been described. Efforts

have been directed toward altering the swelling/shrinking behavior and preparing copolymers that also respond to other stimuli. Critical insight into the deswelling mechanism was obtained through the work of Hoffman et al. on PNIPAM (Park and Hoffman, 1994).

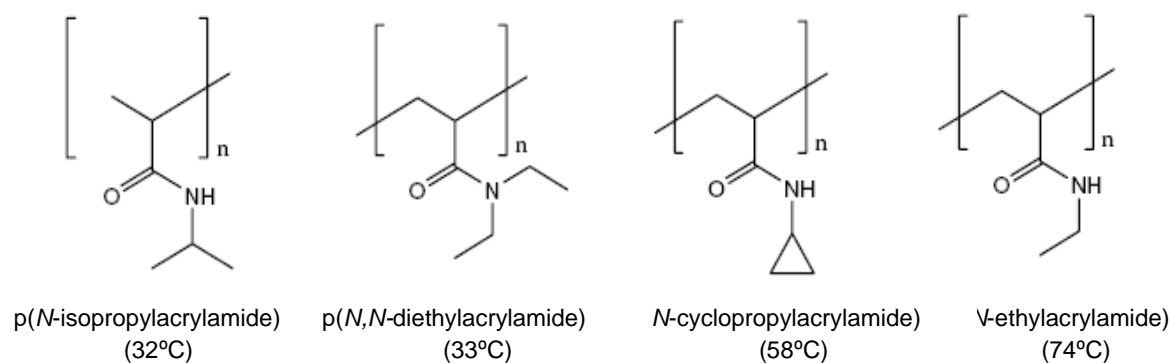


Figure 2.4. Structures of thermoresponsive homopolymers.

In contrast to pH-sensitive smart polymers, which contain carboxy or amino groups that can be used for the covalent coupling of ligands, the thermosensitive polymers do not have inherent reactive groups. Thus copolymers containing reactive groups should be synthesized. *N*-hydroxyacrylsuccinimide (Liu et al., 1995) or glycidyl methacrylate (Mori et al., 1994) are commonly used as active co-monomers in copolymerization with NIPAM, allowing further coupling of amino-group-containing ligands to the synthesized copolymers. Other co-monomers (along with NIPAM) that have been assessed include acrylic acid, methacrylic acid, 2-methyl-2-acrylamidopropane sulfonic acid, trimethyl-acrylamidopropane sulfonic acid, trimethyl-acrylamidopropyl ammonium 3-methyl-1-vinylimidazolium iodide, sodium acrylate, sodium methacrylate, and 1-(3-sulfopropyl)-2-vinylpyridinium betaine (Xue and Hamley, 2002; Solpan et al., 2002). An alternative strategy is to modify the ligand with an acryloyl group and then copolymerize the modified ligand with NIPAM. The use of methacrylic acid, along with NIPAM, not only changes the LCST, but also makes the hydrogels responsive to both temperature and pH (Lee and Shieh, 1999).



### **2.1.3. Reversibly Cross-Linked Polymer Networks**

The third group of smart polymers combines systems with reversible noncovalent cross-linking of separate polymer molecules into insoluble polymer networks. The most common systems of this group are alginate, chitosan, and *k*-carrageenan, which behave as reversibly soluble–insoluble polymers by responding to  $\text{Ca}^{2+}$ , pH, and  $\text{K}^+$ , respectively (Charles et al., 1974; Linne Larsson et al., 1992). Others include boric acid polyols or boric acid polysaccharides (Bradshaw and Sturgeon, 1990, *Biotechnol. Technol.*). These types of polymers have found limited application as carriers in affinity precipitation, but they are more promising for the development of “smart” drug-delivery systems capable of releasing drugs in response to a signal, e.g., release of insulin when glucose concentration is increasing (Lee and Park, 1996). A polymer sensitive to pH and temperature has recently been prepared by genetic engineering (Nagarsekar et al., 2003). Such materials are block copolymers containing repeating sequences from silk (GAGAGS) and elastin (GVGVP), where, in some cases, valine has been replaced by glutamic acid. By varying the extent of this change, the sensitivity to pH, temperature, and ionic strength can be controlled fairly precisely. Recombinant methods have also been used to design multidomain assemblies in which leucine zipper domains flank a central flexible polyelectrolyte (Petka et al., 1998). Changes in pH/temperature stimuli trigger a sol–gel transition.

## **2.2. Hydrogels**

Hydrophilic gels, also called “hydrogels,” are hydrophilic polymer networks swollen in water. Water inside the hydrogel allows free diffusion of some solute molecules, while the polymer serves as a matrix to hold water together. Hydrogels are mainly prepared by free-radical cross-linking copolymerization of acrylamide-based monomers with a divinyl monomer (cross-linker) in aqueous solutions. To increase their swelling capacity, an ionic co-monomer is also included in the monomer mixture. The desired properties of hydrogels (increased swelling capacity, modulus of elasticity, and degree of heterogeneity) are obtained by adjusting both the concentration and the composition of the initial monomer mixture. Hydrogels are able to absorb 10 to 1000 times their dry volume of water without dissolving. They also exhibit drastic volume changes in response to specific external stimuli,

such as the temperature, solvent quality, pH, electric field, etc (Shibayama and Tanaka, 1993). Depending on the design of the hydrogel matrices, this volume change can occur continuously over a range of stimulus level or discontinuously at a critical stimulus level. These properties of hydrogels have received considerable interest over the last three decades. Today, these soft and smart materials belong to the most important class of functional polymers in modern biotechnology. They are useful materials for drug-delivery systems, artificial organs, separation operations in biotechnology, processing of agricultural products, on-off switches, sensors, and actuators. Despite this fact and considerable research in this field, the design and control of hydrogel based devices still present some problems, since a number of network properties are inversely coupled. For example, decreasing the degree of crosslinking of hydrogels to increase their mesh size (“molecular porosity”) results in their accelerated chemical degradation. Further, loosely cross-linked hydrogels are soft materials when handled in the swollen state; typically, they exhibit moduli of elasticity on the order of kilopascals. The poor mechanical performance of highly swollen hydrogels limits their technological applications.

A fast response of hydrogels to the external stimuli is also a requirement in many application areas of these materials. However, the kinetics of hydrogel volume change involves absorbing or desorbing solvent by the polymer network, which is a diffusive process. This process is slow and even slower near the critical point. Increasing the response rates of hydrogels has been one of the challenging problems in the last 25 years. Several techniques have been proposed to increase their response rates. The simplest technique is to reduce the size of the hydrogel particles (Oh et al., 1998). Since the rate of response is inversely proportional to the square of the size of the gel (Tanaka and Fillmore, 1979), small hydrogel particles respond to the external stimuli more quickly than bulk gels. However, this approach has the drawback that, with a reduction of the gel size to submicrometer range, separation of gel particles from the surrounding liquid medium requires additional efforts. Attachment of linear polymer chains on the gel particles is another approach to increase the response rates of hydrogels.

Another technique to obtain fast-responsive hydrogels is to create voids (pores) inside the hydrogel matrix, so that the response rate becomes a function of the microstructure rather than the size or the shape of the gel samples. For a polymer network having an interconnected pore structure, absorption or desorption of water occurs through the pores by convection, which is much faster than the diffusion process that dominates the nonporous hydrogels. Macroporous hydrogels contain nanometer- to micron-size liquid channels separated by cross-linked polymer regions, which provide sufficient mechanical stability. It should be noted that the term “macroporous” does not mention the size of the pores in these materials; it is used to distinguish these gels from those exhibiting a swollen-state porosity, i.e., a molecular porosity due to the space between the network chains in their swollen states. Thus the term “macroporous hydrogel” refers to materials exhibiting a porosity in their dry state, which is characterized by a lower density of the network due to the voids than that of the matrix polymer. In contrast to inorganic porous gels such as silica gel carriers, macroporous gels offer flexibility, ductility, and the ability to react with a large number of organic molecules. The technique to obtain cross-linked polymers with a macroporous structure was discovered at the end of 1950s. Since then, the procedures to make such gels have greatly improved. The basic technique to produce macroporous hydrogels involves the free radical cross-linking copolymerization of the monomer-cross-linker mixture in the presence of an inert substance (the diluents), which is soluble in the monomer mixture. To obtain macroporous structures, a phase separation must occur during the course of the network formation process so that the two-phase structure formed is fixed by the formation of additional cross-links. After the polymerization, the diluent is removed from the network, leaving a porous structure within the highly cross-linked polymer network. Thus, the inert diluent acts as a pore-forming agent and plays an important role in the design of the pore structure of cross-linked materials. Today, the formation of macroporous polymers by the phase-separation technique is qualitatively understood, and several reviews have been published covering the developments in this area (O. Okay, 2000, *Prog. Polym. Sci.*).

Another technique to create a macroporous network structure is the use of inert templates in the preparation of hydrogels. In this technique, the polymer-formation

reactions are carried out in the presence of templates; a macroporous structure in the final hydrogel matrix appears after extraction of the template materials. For example, by the cryogelation technique, the polymer-formation reactions are carried out below the bulk freezing temperature of the reaction system. Thus, the essential feature of such reaction systems is that the monomers and the initiator are concentrated in the unfrozen microzones of the apparently frozen system. The polymerization and cross-linking reactions proceed in the unfrozen microzones of the reaction system. A macroporous structure in the final material appears due to the existence of ice crystals acting as a template for the formation of the pores. Macroporous hydrogels can also be prepared by foaming techniques, making use of gaseous pore-forming agents. These can be generated by evaporation of solvents or produced by chemical reactions (Omidian et al., 2005).

### **2.2.1. Fundamental Interactions**

The volume transition of polymer gels results from the competition between attractive and repulsive interactions within the polymer network that arise, depending of the chemical composition of the gel, from the combination of four fundamental interactions: Van der Waals, hydrophobic, electrostatic and hydrogen bonding (Shibayama and Tanaka 1993). Figure 2.5 shows a schematic representation of the intermolecular interactions acting in different polymer–solvent systems. The variables triggering the volume transition influences these forces causing a change in the net balance that governs the network swelling; when the net interaction becomes attractive the gel shrinks whereas the opposite is true when the repulsive interactions dominate.

#### **2.2.1.1. Van der Waals**

These forces result from the correlations in the fluctuating polarizations of nearby molecules and include three major contributions: i) interaction between permanent dipoles, ii) permanent dipole induced dipole, often referred as induction forces, and iii) instantaneous dipole-induced dipole, usually called dispersion forces. Nevertheless, some texts use the term Van der Waals to refer simply to dispersion forces. Induction and dispersion forces are always attractive while the interaction among permanent dipoles depends upon the relative orientation of the molecules

and can, therefore, be attractive or repulsive. Van der Waals interactions are always present and its range spans from typical interatomic distances to nanometers, playing an important role in the structure of macromolecules such as polymer or proteins. Since they are based on interactions between dipoles, they are expected to be more relevant in non-polar solvents. In fact, the first volume transition was observed in a partially hydrolyzed acrylamide gel immersed in acetone–water mixtures .

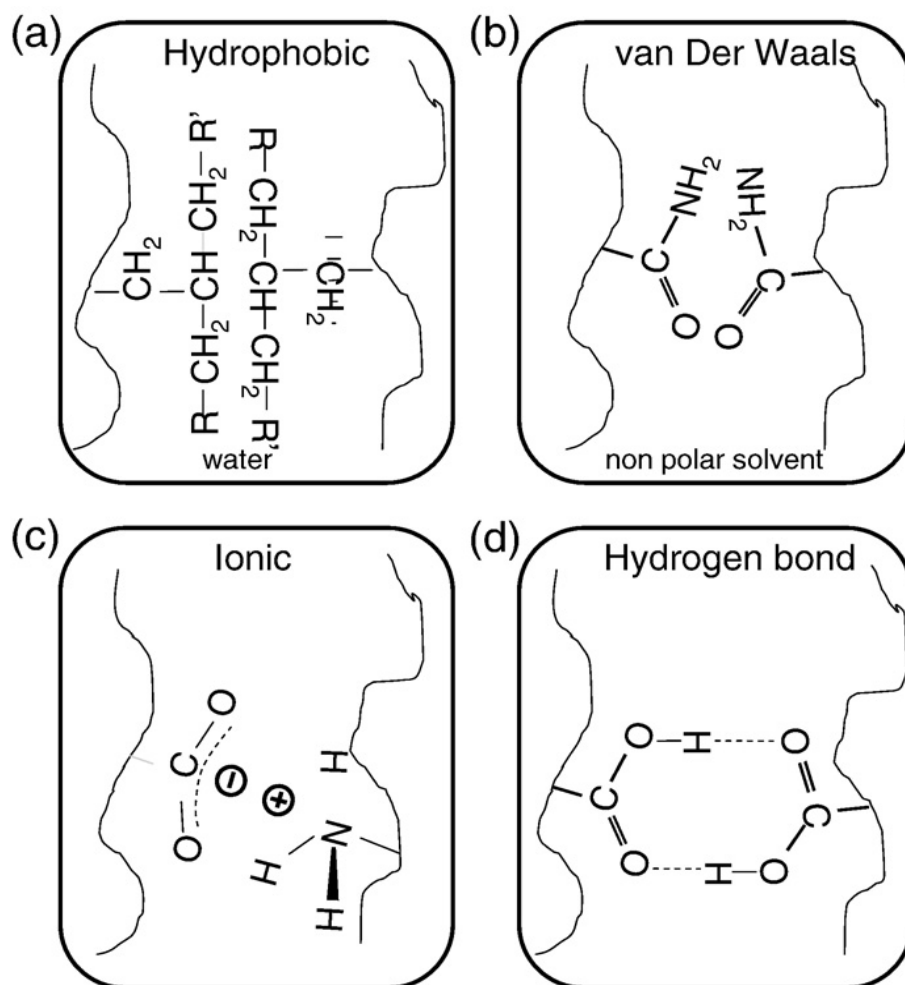


Figure 2.5. Fundamental interactions in polymer gels. a) For polar solvents, hydrophobic interaction use to dominate, b) while in the case of non polar solvent Van der Waals is specially relevant. The other two interaction usually present in polymer gels are c) electrostatic and d) hydrogen bonds. Change of the interaction balance by specific external modifications makes these systems suitable for a great deal of applications.

The addition of a nonpolar solvent as acetone increased the attractive Van der Waals interaction between polymer chains leading to the network collapse (Tanaka, 1979; Ilavsky, 1982).

#### **2.2.1.2. Hydrophobic**

This interaction describes the unusual strong attraction occurring between hydrophobic molecules immersed in water. It has an entropic origin that physically arises from the rearrangement of water molecules in the overlapping hydration zone when the molecules approach. As a result, the water molecules become more ordered than in pure water forming ice-like structures with the consequent loss of local entropy (Meyer et al., 2006). In order to maximize the entropy the chains are forced to aggregate. The hydrophobic force is relevant in the configuration and self-assembly of many biopolymer systems. In the case of synthetic gels, such interaction can be induced by changing the side group of the polymer chains. One of the best examples is the poly(N-isopropylacrylamide) gel, PNIPAM, which shows a thermally induced volume transition; the effect is stronger at higher temperatures, so hydrophobic gels tend to collapse when heated. The hydrophobic effect can be also enhanced upon the addition of organic solvents such as alcohols because the hydrocarbon molecules can encapsulate the neighbouring water molecules in a more ordered structure (Reed and Westacot, 2008).

#### **2.2.1.3. Hydrogen bonding**

The hydrogen bonding is an attractive interaction that appears when a hydrogen atom is located between two closely separated atoms with high electronegativity, e.g., O, N and F. It is required an adequate orientation of the involved groups to form the bounds. In the case of gels the flexibility of the polymer chains allows the formation of intra-chain and inter-chain bounding, both cases contributing to the network collapse since the force is always attractive. Hydrogen bounding is particularly important for the properties of biological assemblies such as membranes, proteins, nucleic acids, etc. For the case of synthetic polymers, this interaction appears mainly in systems bearing carboxyl groups. For instance, it is responsible for the volume transition occurring in interpenetrating polymer network

of poly(acrylic acid), and poly (acrylamide) (Ilmain et al., 1991). More recently, Hellweg et al. found a two-step volume phase transition for PNIPAM–Acrylic gels in which the hydrogen bonding has to be considered to explain the second deswelling process (Kratz and Hellweg, 2000).

#### **2.2.1.4. Electrostatic**

The electrostatic interaction is a long-range force that appears between charged molecules or ions. It is the strongest of the intermolecular interaction exposed here and play an important role in the volume transition of ionic gels through two distinct mechanisms, i) direct Coulombian interactions, which can be repulsive or attractive depending of the charge sign, and ii) the effect of the counterions that establish an osmotic pressure, as consequence of the ion redistribution, attempting to swell the gel. When the network carries a net charge, positive or negative, the Coulomb repulsion is usually screened by water and the dominant mechanism is the osmotic pressure of counterions. This has been observed experimentally in charged vinylpyridine gels (Fernandez-Nieves et al., 2000). On the other hand, for the case of polyampholyte gels bearing cationic and anionic groups attached to the network the polymer chains exert long-range electrostatic attractions while repel each other over short ranges (Neyret and Vincent, 1997).

### **2.3. Approaches to Molecular Imprinting**

The concept of molecular imprinting was first applied to organic polymers in the 1970s, when covalent imprinting in vinyl polymers was first reported (Grosberg and Khokhlov, 1997; Wulff, 1995). The noncovalent imprinting was introduced a decade later (Sellergren, 2001). Both approaches are aimed at creating tailor-made cavities shaped with a high specificity and affinity for a target molecule inside or at the surface of highly cross-linked polymer networks. To carry out the process, the template is added to the monomers and cross-linker solution before polymerization, which allows some of the monomers (called “functional” monomers) to be arranged in a configuration complementary to the template. The functional monomers are arranged in position through either covalent bonds or noncovalent interactions, such as hydrogen bond or ionic, hydrophobic, or charge-transfer interactions (Figure 2.6). In the first case, the template is covalently bound

to the monomers prior to polymerization; after synthesis of the network, the bonds are reversibly broken for removal of the template molecules and formation of the imprinted cavities. In the noncovalent or *self-assembly* approach, the template molecules and functional monomers are arranged prior to polymerization to form stable and soluble complexes of appropriate stoichiometry by noncovalent or metal coordination interactions. In this case, multiple-point interactions between the template molecule and various functional monomers are required to form strong complexes in which both species are bound as strongly as in the case of a covalent bond. The noncovalent imprinting protocol allows more versatile combinations of templates and monomers, and provides faster bond association and dissociation kinetics than the covalent imprinting approach (Ansell, 2004). By any of these approaches, copolymerization of functional monomer–template complexes with high proportions of cross-linking agents, and subsequent removal of the template, provides recognition cavities complementary in shape and functionality (Figure 2.7). These vacant cavities are then available for rebinding of the template or structurally related analogues. Excellent reviews about the protocols to create rigid imprinted networks can be found in the literature (Yan and Ramstrom, 2005; Mayes and Whitcombe, 2005).

Nowadays, molecular imprinting is a well-developed tool in the analytical field, mainly for separating and quantifying a wide range of substances contained in complex matrices (Andersson, 2000). Additionally, there has been a progressive increase in the number of papers and patents devoted to the application of molecularly imprinted polymers (MIPs) in the design of new drug-delivery systems and of devices useful in closely related fields, such as diagnostic sensors or chemical traps to remove undesirable substances from the body (Piletsky and Turner, 2002; Hillberg et al., 2005). To obtain functional imprinted cavities, several factors must be taken into account. It is essential to ensure that the template,

\*Does not bear any polymerizable group that could attach itself irreversibly to the polymer network

\*Does not interfere in the polymerization process

\*Remains stable at moderately elevated temperatures or upon exposure to UV irradiation



Other key issues are related to the nature and proportion of the monomers and to the synthesis conditions (solvent, temperature, etc.). The cavities should have a structure stable enough to maintain their conformation in the absence of the template and, at the same time, be sufficiently flexible to facilitate the attainment of a fast equilibrium between the release and reuptake of the template in the cavity. The conformation and the stability of the imprinted cavities are related to the mechanical properties of the network and depend to a great extent on the cross-linker proportion. Most imprinted systems require 50 to 90% of cross-linker to prevent the polymer network from changing the conformation adopted during synthesis (Sibrian-Vazquez and Spivak, 2003). Consequently, the chances to modulate the affinity for the template are very limited, and it is not foreseeable that the network will have regulatory or switching capabilities.

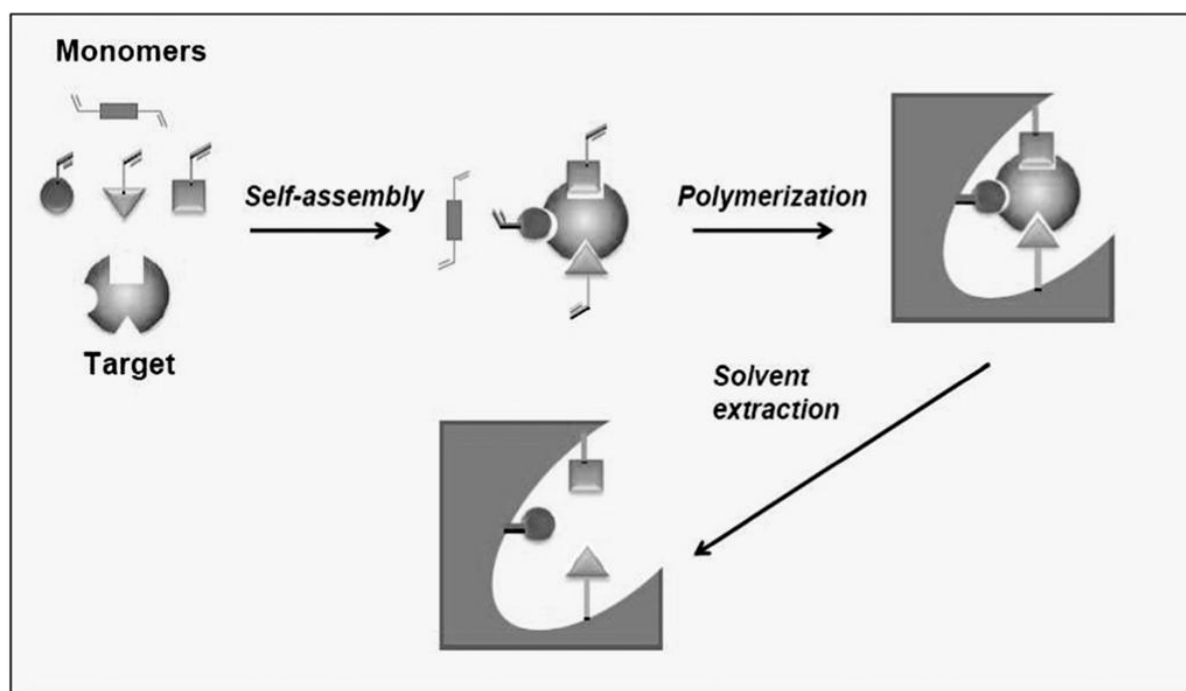


Figure 2.6. Schematic representation of the molecular imprinting process in synthetic polymers. Pre-assembly of functional monomers is achieved by virtue of their interaction with the template molecule. Polymerization in the presence of a high concentration of crosslinking agent “freezes” the bound groups, thus effectively forming a well defined cavity of molecular recognition. Removal of the template molecule either by solvent extraction, chemical or enzymatic scission generates binding sites with the capacity for specific recognition of the original template molecule.

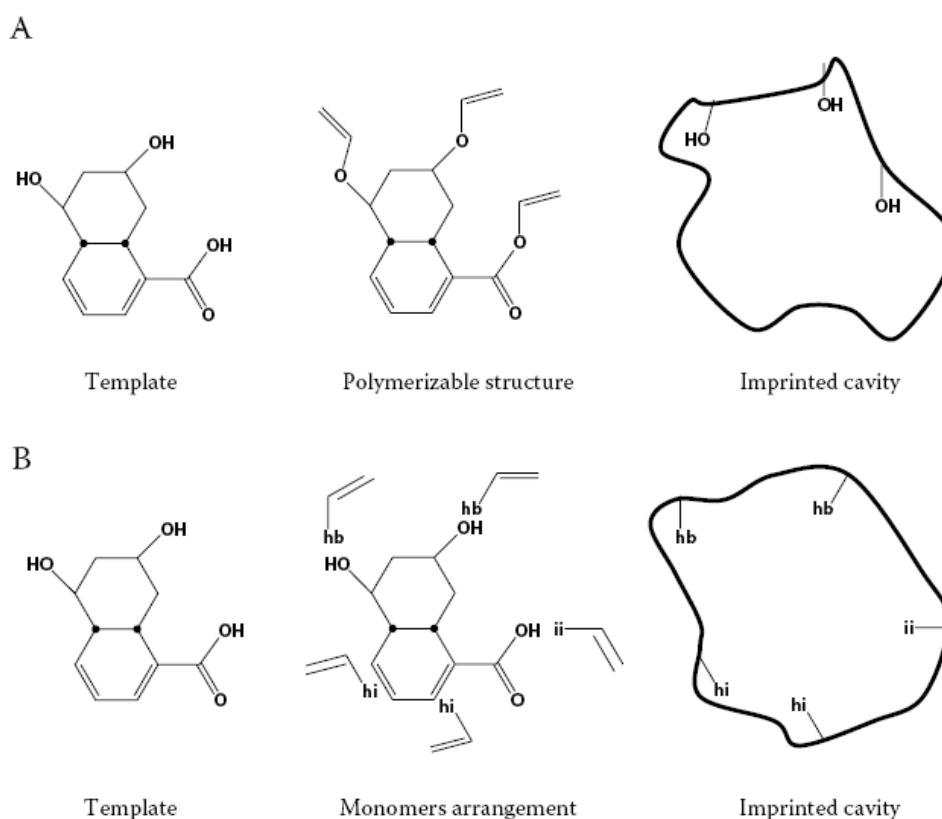


Figure 2.7. Schematic view of the imprinting process: (a) covalent approach, in which the template is covalently bound to polymerizable binding groups that are reversibly broken after polymerization; and (b) noncovalent approach, in which the template interacts with functional monomers through noncovalent interactions (e.g., ionic interaction, ii; hydrophobic interaction, hi; or hydrogen bond, hb) before and during polymerization.

The lack of response to changes in the physicochemical properties of the medium within the biological range or to the presence of a specific substance notably limits their utility in the biomedical field. A high crosslinker proportion also considerably increases the stiffness of the network, making it difficult to adapt its shape to a specific device or to living tissues.

### 2.3.1. Imprinting in Hydrogels

A further step in the imprinting technology is the development of stimuli sensitive imprinted hydrogels. The low-cross-linked proportion required to achieve adequate viscoelastic properties can compromise the stability of the imprinted cavities in the hydrogel structure, resulting in some sacrifice of both affinity and selectivity. Strong efforts are being made to adapt the molecular imprinting

technology to materials that are more flexible and thus more biocompatible, such as hydrogels for use in the biomedical field (Enoki et al., 2000; Miyata et al., 2002; Alvarez-Lorenzo and Concheiro, 2006). To produce low-cross-linked hydrogel networks capable of undergoing stimuli-sensitive phase transitions, the synthesis is carried out in the presence of template molecules, each able to establish multiple contact points with functional monomers (Alvarez-Lorenzo, 2001; D'Oleo et al., 2001; Moritani and Alvarez-Lorenzo, 2001; Stancil et al., 2005). Multiple contacts are the key for strong adsorption of the template molecules because of the larger energy decrease upon adsorption as well as the higher sensitivity due to the greater information provided for recognition. As in the classical noncovalent approach, the monomers and the template molecules are allowed to move freely and settle themselves into a configuration of thermodynamic equilibrium. The monomers are then polymerized in this equilibrium conformation at the collapsed state. As the hydrogel is made from the equilibrium system by freezing the chemical bonds forming the sequence of monomers, we might expect such a hydrogel to be able to return to its original conformation, at least to some degree of accuracy, upon swelling–collapse cycles in which the polymerized sequence remains unchanged (Figure 2.8). If the memory of the monomer assembly at the template adsorption sites is maintained, truly imprinted hydrogels will result. The combination of stimuli sensitivity and imprinting can have considerable practical advantages: the imprinting provides a high loading capacity of specific molecules, while the ability to respond to external stimuli modulates the affinity of the network for the target molecules, providing regulatory or switching capability of the loading/release processes.

### **2.3.2. The Tanaka Equation**

Tanaka and coworkers were pioneers in proposing the creation of stimuli-sensitive gels with the ability to recognize and capture target molecules using polymer networks consisting of at least two species of monomers, each having a different role. One forms a complex with the template (i.e., the functional or absorbing monomers capable of interacting ionically with a target molecule), and the other allows the polymers to swell and shrink reversibly in response to environmental changes (i.e., a smart component such as *N*-isopropylacrylamide, NIPA) (Figure

2.9). The gel is synthesized in the collapsed state and, after polymerization, is washed in a swelling medium.

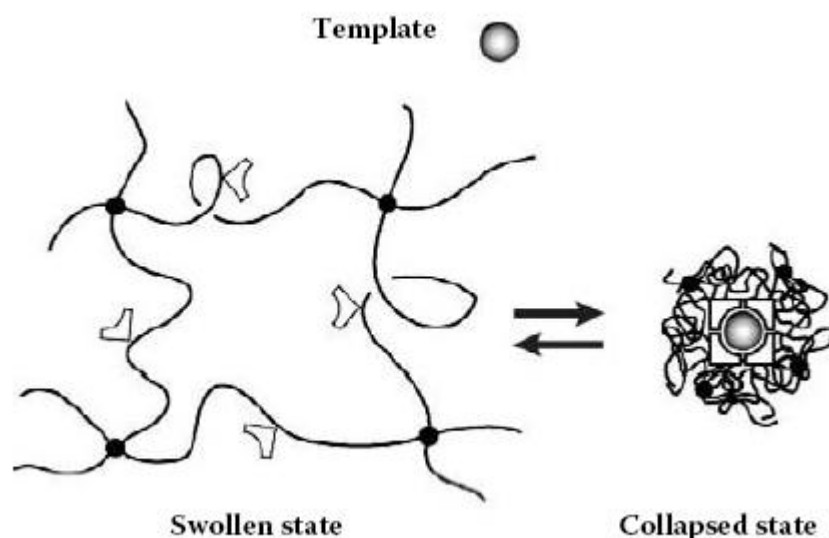


Figure 2.8. The volume phase transition of the hydrogel (induced by external stimuli such as a change in pH, temperature, or electrical field) modifies the relative distance of the functional groups inside the imprinted cavities. This alters their affinity for the template. The affinity is recalled when the stimulus reverses and the gel returns to its original conformation.

The imprinted cavities develop affinity for the template molecules when the functional monomers come into proximity, but when they are separated, the affinity diminishes. The proximity is controlled by the reversible phase transition that consequently controls the adsorption/release of the template (Figure 3.4). A systematic study of the effects of the functional monomer concentration and the cross-linker proportion of the hydrogels (for both imprinted and nonimprinted gels) and of the ionic strength of the medium on the affinity of the hydrogels for different templates led to the development of an equation, called the Tanaka equation in memory of the late Professor Toyochi Tanaka(1946–2000) (Ito et al., 2003).

### 2.3.3. Temperature-Sensitive Imprinted Hydrogels

Like proteins, a heteropolymer gel can exist in four thermodynamic phases:

1. Swollen and fluctuating

2. Shrunken and fluctuating
3. Shrunken and frozen in a degenerate conformation
4. Shrunken and frozen in the global minimum energy conformation

The order parameter that describes the phase transition between the first and the second phases is the polymer density or, equivalently, the swelling ratio of the gel. The third and fourth phases are distinguished by another order parameter: the overlap between the frozen conformation and the minimum energy conformation. In the third phase, the frozen conformation is random (Tanaka and Annaka, 1993).

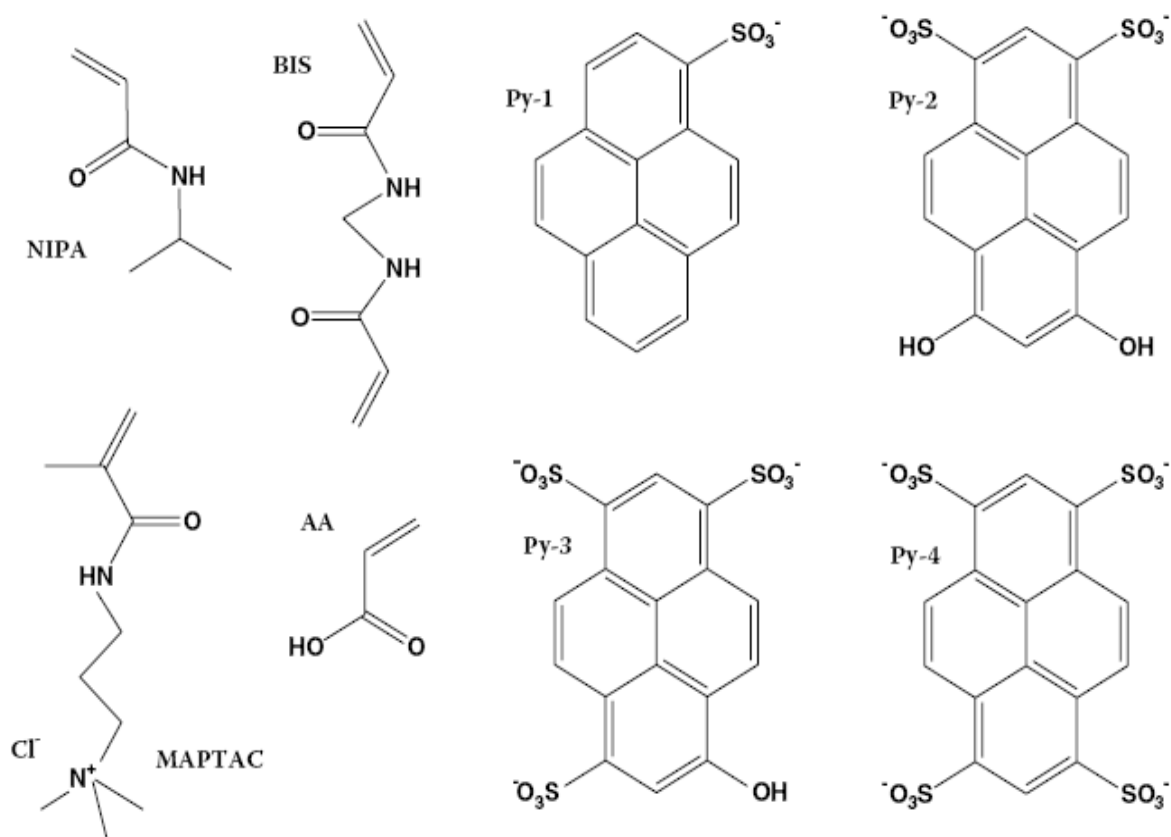


Figure 2.9. Chemical structures of some monomers used to create imprinted smart gels: *N*-isopropylacrylamide (NIPA, temperature-sensitive), *N,N'*-methylene-bisacrylamide (BIS, cross-linker), methacrylamidopropyl trimethylammonium chloride (MAPTAC, cationic adsorber), and acrylic acid (AA, anionic adsorber). Structures of some ionically charged derivatives of pyranine used as targets are also shown.

In the fourth phase, the frozen conformation is equivalent to that of the global energy minimum. Proteins in this fourth phase take on a specific conformation, which may be capable of performing catalysis, molecular recognition, or many other activities. Tanaka and colleagues strove to recreate such a fourth phase in gels by designing a low-energy conformation and then testing whether the gel could be made to reversibly collapse into this “memorized” conformation. According to developments in the statistical mechanics of polymers, to achieve the memory of conformation by flexible polymer chains, several requisites must be satisfied (Pande et al., 2000).

1. The polymer must be a heteropolymer, i.e., there should be more than one monomer species, so that some conformations are energetically more favorable than others.
2. There must be frustrations that hinder a typical polymer sequence from being able to freeze to its lowest energy conformation (as considered in absence of the frustration). Such frustrations may be due to the interplay of chain connectivity and excluded volume, or they may be created by cross-links. For example, a cross-linked polymer chain will not freeze into the same conformation as the noncross-linked polymer chain, at least for most polymer sequences.
3. The sequence of monomers must be selected so as to minimize these frustrations, i.e., a particular polymer sequence should be designed such that the frustrating constraints do not hinder the polymer from reaching its lowest energy conformation (Bryngelson and Wolynes, 1987).

These three conditions allow the polymer to have a global free-energy minimum at one designed conformation.

The nonimprinted gels satisfy the first two conditions, and can be engineered to satisfy the third. The adsorber and the main-component monomers provide heterogeneity in interaction energies, since adsorber interactions are favorably mediated by the target molecules (Tanaka et al., 1998). Frustrations to the achievement of the global energy minimum exist due to the cross-links in the gel as well as chain connectivity. To meet the third condition, the minimization of the frustration, the molecular imprinting technique can be particularly useful. In this section, we discuss the early experimental successes of the imprinting method

and the application of the Tanaka equation to imprinted gels. Two approaches were investigated to achieve elements of conformational memory in gels:

1. Cross-linking of a polymer dispersion or preformed gel in the presence of the target molecule (two-step imprinting or post-imprinted)
2. Simultaneous polymerization and cross-linking of the monomer solution (one-step imprinting)

The first approach was studied in heteropolymer gels consisting of NIPA as the major component sensitive to stimuli and MAPTAC as the charged monomer able to capture pyranine target molecules (Enoki et al., 2000). The polymer networks were randomly copolymerized, in the absence of pyranines, with a small quantity of permanent cross-links and thiol groups ( $-SH$ ). The gels were then further cross-linked by connecting thiol group pairs into disulfide bonds ( $-S-S-$ ). The process was carried out directly (nonimprinted gels) or after the gels were immersed in a solution of pyranines and had all charged groups forming complexes with the target molecules (postimprinting). These post-cross-links were still in very low concentrations, in the range 0.1 to 3 mol%, and therefore the gels could freely swell and shrink to undergo the volume phase transition. The postimprinted gels showed higher affinity for the target than those that were randomly post-cross-linked. However, this post-cross-linking approach has a fundamental drawback. Before the post-cross-linking, the sequence of the components has already been determined and randomly quenched. The minimization of the frustration is allowed only in the freedom of finding best partners among  $-SH$  groups. For this reason, the imprinting using a post cross-linking technique can give only a partial success. Ideally, the entire sequence of all monomers should be chosen so that the system will be in its global energy minimum. The complete minimization of the frustration can be achieved by polymerizing monomers while they selforganize in space at a low-energy spatial arrangement (Alvarez-Lorenzo et al., 2000; Stancil et al., 2005). This second approach controls the sequence formation, allowing the monomers to equilibrate in the presence of a target molecule. These monomers are then polymerized with a cross-linker. It is hoped that, upon removal of the template species, binding sites with the spatial features and binding preferences for the template are formed in the polymer matrix. The choice of functional monomers and the achievement of an adequate spatial arrangement of functional

groups are two of the main factors responsible for specificity and reversibility of molecular recognition.

The first experiments carried out by Alvarez-Lorenzo et al. used gels prepared by polymerization of NIPA, small amounts of methacrylic acid (MAA), and BIS in the absence (nonimprinted) or the presence of divalent cations. MAA was used as the functional monomer able to form complexes in the ratio 2:1 with divalent ions. The effect of temperature on the adsorption capacity of the imprinted copolymers prepared with different template ions and in different organic solvents was compared with that of the nonimprinted ones. Successful imprinting was obtained using calcium or lead ions as template. After removing the template and swelling in water at room temperature, the affinity for divalent ions notably decreased. When the gels were shrunken by an increase in temperature, the affinity was recovered. The measurements of the affinity suggested that multipoint adsorption occurs for both imprinted and nonimprinted gels in the collapsed state, but that in the imprinted gel, the multipoint adsorption is due to memorized binding sites. After recollapsing, two-point adsorption is recovered in the random gels, while the imprinted gels showed a stronger affinity. This is because the adsorbers are ordered such that they already form sites with their unique partners. Furthermore, the affinity of the imprinted gels does not change at all with an increase of the cross-linking density, while the affinity decreases for random gels. For random gels, it was difficult to pair randomly distributed MAA, and their affinity for divalent ions decreased exponentially as a function of cross-linker concentration. In contrast, in the imprinted gels, the local concentration of MAA in the binding site is very high, i.e., the members of each pair are closely fixed by the template during polymerization. If the gel did not memorize such pairs after washing the template out, swelling, and reshinking, an MAA would have to look for a new partner nearby, and such a probability would be the same as that in a nonimprinted gel. Therefore, it can be concluded that the greater adsorption capacity of the imprinted gels comes from the successfully memorized MAA pairs (Alvarez-Lorenzo et al., 2001; Stancil et al., 2005).

Güney et al. followed a similar procedure to prepare temperature sensitive gels that specifically recognize and adsorb heavy metal ions from aqueous media in an



effort to develop chemosensors (Guney et al., 2002). Kanazawa et al. used another functional monomer *N*-(4-vinyl) benzyl ethylenediamine) (Vb-EDA) that contains two nitrogen groups that can specifically form coordination bonds with one copper ion; each copper ion requires two functional monomers to complete its bonding capacity (Kanazawa et al., 2004). This occurs when the gel is formed at the shrunken state. At the swollen state, the bonds are broken and the affinity for the ions disappears. These gels showed a high specificity for  $\text{Cu}^{2+}$  compared with  $\text{Ni}^{2+}$ ,  $\text{Zn}^{2+}$ , or  $\text{Mn}^{2+}$ . The different coordination structure (square planar for  $\text{Cu}^{2+}$  and  $\text{Ni}^{2+}$ , tetrahedral for  $\text{Zn}^{2+}$ , and octahedral for  $\text{Mn}^{2+}$ ) together with the differences in ion radii explains this specificity, which was not observed in the nonimprinted gels. The amphiphilic character of the functional monomer Vb EDA made it possible to develop an emulsion polymerization procedure to prepare imprinted microgels. The main advantage of these microgels is that they can adsorb and release the copper ions faster because of their quick volume phase transitions (Kanazawa et al., 2004).

Detailed calorimetric studies of the thermal volume transition of polyNIPA hydrogels and the influence of ligand binding on the relative stability of subchain conformations have been carried out by Grinberg and coworkers (Grinberg et al., 2000). The dependence of the critical temperature of PNIPA hydrogels on the proportion of ionic comonomers is an obstacle to obtaining devices with a high loading capability while still maintaining the PNIPA temperature-sensitive range. This can be overcome by synthesizing interpenetrated polymer networks (IPN) of PNIPA with ionizable hydrophilic polymers. Although only a few papers have been devoted to this topic, the results obtained in those studies have shown the great potential of IPNs (Alvarez-Lorenzo et al., 2005; Yamashita et al., 2003). A two-step approach to imprint interpenetrated gels with metal ions was identified by Yamashita et al. It basically consists in (a) polymerization of AA monomers to have a loosely cross-linked (1 mol%) polyAA network; (b) immersion of polyAA in copper solution to enable the ions to act as junction points between different chains; and (c) transfer of polyAA-copper ion complexes to a NIPA solution containing cross-linker (9.1 or 16.7 mol%) and synthesis of the NIPA network in the collapsed state (Figure 2.10). The nonimprinted IPNs (i.e., prepared in the absence of copper ions) showed a similar affinity for  $\text{Cu}^{2+}$  and for  $\text{Zn}^{2+}$ . In contrast,

the imprinted IPNs in the collapsed state could discriminate between the square planar structure of  $\text{Cu}^{2+}$  and the tetrahedral structure of  $\text{Zn}^{2+}$ . NIPA-based imprinted hydrogels have also been prepared using organic molecules as templates. Watanabe et al. observed that NIPA (16 mmol)/ acrylic acid (4 mmol) cross-linked (1 mmol) polymers synthesized in dioxane and in the presence of norephedrine (2 mmol) or adrenaline (2 mmol) showed, after template removal, an increase in the swelling ratio in the collapsed state as the target molecule concentration in water increases completely, which leads to a reduction of the number of free binding sites and template bleeding during the assays (Watanabe et al., 1998). Recent efforts showed the possibilities of using adsorbing monomers directly bonded to each other prior to polymerization, which avoids the use of the template polymerization technique (D'Oleo et al., 2001; Moritani and Alvarez-Lorenzo, 2001). Each adsorbing monomer can be broken after polymerization to obtain pairs of ionic groups with the same charge.

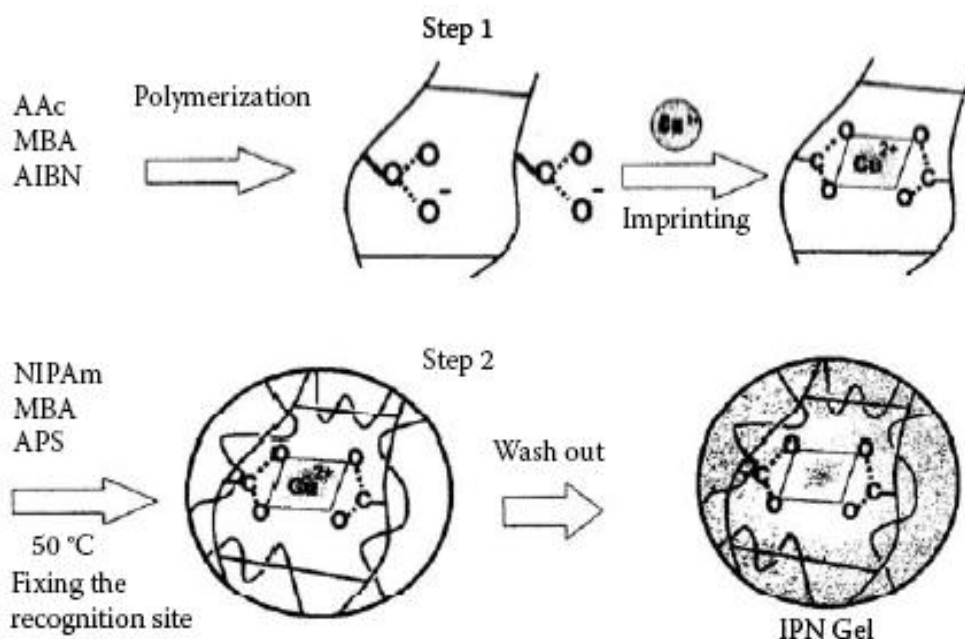


Figure 2.10. Two-step procedure to obtain an interpenetrated system comprising a  $\text{Cu}^{2+}$  imprinted poly(acrylic acid) hydrogel and a poly(*N*-isopropylacrylamide) temperature-sensitive hydrogel. (Reproduced from Yamashita, K. et al., 2003. With permission from the Society of Polymer Science of Japan).

Since the members of each pair are close together, they can capture target molecules through multipoint ionic interactions (Figure 2.10). The adsorption process was found to be independent of the cross-linking density, and the entropic frustrations were completely resolved. Divalent ions or molecules with two ionic groups in their structures can be loaded in a greater amount and with higher affinity by these “imprinted” hydrogels (Moritani and Alvarez-Lorenzo., 2001). Furthermore, the hydrogels prepared with PNIPA and imprinters were gifted with a new ability not observed in common stimuli-sensitive gels: they can re-adsorb, at the shrunken state, a significantly high amount of the templates previously released at the swollen state. Common (nonimprinted) temperature-sensitive PNIPA hydrogels have a pulsate release behavior that allows a substance entrapped in the polymer network to diffuse out of the hydrogel in the swollen state, but then stops the release when the temperature increases and the network collapses (Qiu and Park, 2001; Kikuchi and Okano, 2002). In contrast, a change from the swollen to the shrunken state of the imprinted PNIPA hydrogels not only stops the release, but also promotes a re-adsorption process. This process occurs quickly and in a way that can be reproduced after several temperature cycles. At 37°C, the high affinity for the template provokes a stop in the release when an equilibrium concentration between the surrounding solution and the hydrogel is reached. This type of hydrogel has a great potential for development of drug-delivery devices capable of maintaining stationary drug levels in their environment. The gel would stop the release while the released drug has not yet been absorbed or distributed but remains near the hydrogel.

#### **2.4. Toxicities of Heavy Metals**

In small quantities, certain heavy metals are nutritionally essential for a healthy life. Some of these are referred to as the trace elements (e.g., iron, copper, manganese, and zinc). Other heavy metals such as mercury, cadmium, and lead are toxic metals that have no known vital or beneficial effect on organisms, and their accumulation over time in the bodies can cause serious illness. The symptoms of the toxic effects of heavy metals may vary widely at the physiological level, but the basic toxicity mechanisms at the molecular level may be limited. The toxicities of heavy metals may be caused by the following mechanisms:

(1) Blocking the essential functional groups of biomolecules such as enzymes: Specific amino acid residues, such as serine-OH, cysteine-SH and histidine-N often constitute the active sites of enzymes. Hg(II), for example, binds strongly to cysteine-SH's, blocking an enzymatic activity.

(2) Displacing essential metal ions from biomolecules: A metal ion may displace a native ion, if its affinity to the binding site is stronger than that of the native one. Often a biomolecule with a foreign metal ion loses its activity.

(3) Modifying the active conformation of biomolecules, especially enzymes and perhaps polynucleotides: A coordination of a cation may change the conformation of a protein, rendering it non-functional.

(4) Disrupting the integrity of biomembranes: A metal cation binds the negatively charged head(s) of phospholipids and the integral protein residues of the membrane.

(5) Modifying some other biologically active agents: For example Cd(II) and Pb(II) appear to potentiate the endotoxins produced by bacteria. This might be due to their effect to block some enzymes, which degrade to endotoxin.

(6) Binding with bioanions, resulting in a decreased level of essential bioanions, especially  $\text{PO}_4^{3-}$  or a displacement of an essential cation from biominerals: For example, Pb(II) having a size similar to that of Ca(II), could replace Ca(II) on a bone mineral. As a result the mechanical strength of the bone may be affected. The size and the electrical charge would be an important factor in these effects. One of the basic toxic effects of Pb(II) is considered to be binding of  $\text{PO}_4^{3-}$ , rendering its cytoplasmic level very low.

These toxicity mechanisms are all based on the strong binding abilities of these metallic ions. And as in the case of selectivity in uptake mechanism, substitution of a metallic ion by another is relatively simple. This is so except for substitution-inert metals. In practice, however, any metal cation bound to a large, somewhat rigid biomolecule is kinetically difficult to displace, though not necessarily substitution-inert. This does not necessarily apply to the case of proteins of a rather flexible conformation. What happens often is that a replacement takes place when an apo-protein binds a cation. A wrong cation can be incorporated in this step, if present there.

Cd(II) and Hg(II), for example, can replace the native Zn(II) ion from many proteins and enzymes to a degree that depends on their affinities. Cu(I), Ag(I) and Au(I) also have similar characters to Zn(II), Cd(II) and Hg(II) because of their isoelectronicity. It would be needless to point out that the cations such as Cu(II), Ni(II), etc., also displace a native cation such as Zn(II) from enzymes and proteins. For example, the carcinogenicity of Ni(II) is considered to be due to its replacement of Zn(II) and/or Mg(II), the essential cations in DNA polymerase. Because of its different size, Ni(II) seems to increase the chance of binding wrong nucleotides, thus resulting in the formation of DNA of a wrong sequence (Loeb et al., 1980).

## **2.5. Cadmium, An Overview**

Cadmium is a toxic transition heavy metal of continuing occupational and environmental concern with a wide variety of adverse effects. Cadmium has an extremely long biological half-life that essentially makes it a cumulative toxin. To date there are no proven effective treatments for chronic cadmium intoxication. Cadmium has been designated a human carcinogen by the International Agency for Research on Cancer and the US National Toxicology Program and is clearly a potent, multi-tissue animal carcinogen.

Cadmium derives its toxicological properties from its chemical similarity to zinc an essential micronutrient for plants, animals and humans. In humans, long-term exposure is associated with renal dysfunction. High exposure can lead to obstructive lung disease and has been linked to lung cancer, although data concerning the latter are difficult to interpret due to compounding factors (Goering, 1994). Cadmium may also produce bone defects (osteomalacia, osteoporosis) in humans and animals. In addition, the metal can be linked to increased blood pressure and effects on the myocardium in animals, although most human data do not support these findings.

The average daily intake for humans is estimated as 0.15 $\mu$ g from air and 1 $\mu$ g from water. Smoking a packet of 20 cigarettes can lead to the inhalation of around 2-4 $\mu$ g of cadmium, but levels may vary widely.

Cadmium is produced as an inevitable by-product of zinc (or occasionally lead) refining, since these metals occur naturally within the raw ore. However, once collected the cadmium is relatively easy to recycle.

The most significant use of cadmium is in nickel/cadmium batteries, as rechargeable or secondary power sources exhibiting high output, long life, low maintenance and high tolerance to physical and electrical stress (Figure 2.11). Cadmium coatings provide good corrosion resistance, particularly in high stress environments such as marine and aerospace applications where high safety or reliability is required; the coating is preferentially corroded if damaged. Other uses of cadmium are as pigments, stabilisers for PVC, in alloys and electronic compounds. Cadmium is also present as an impurity in several products, including phosphate fertilisers, detergents and refined petroleum products (Cook and Morrow, 1995).

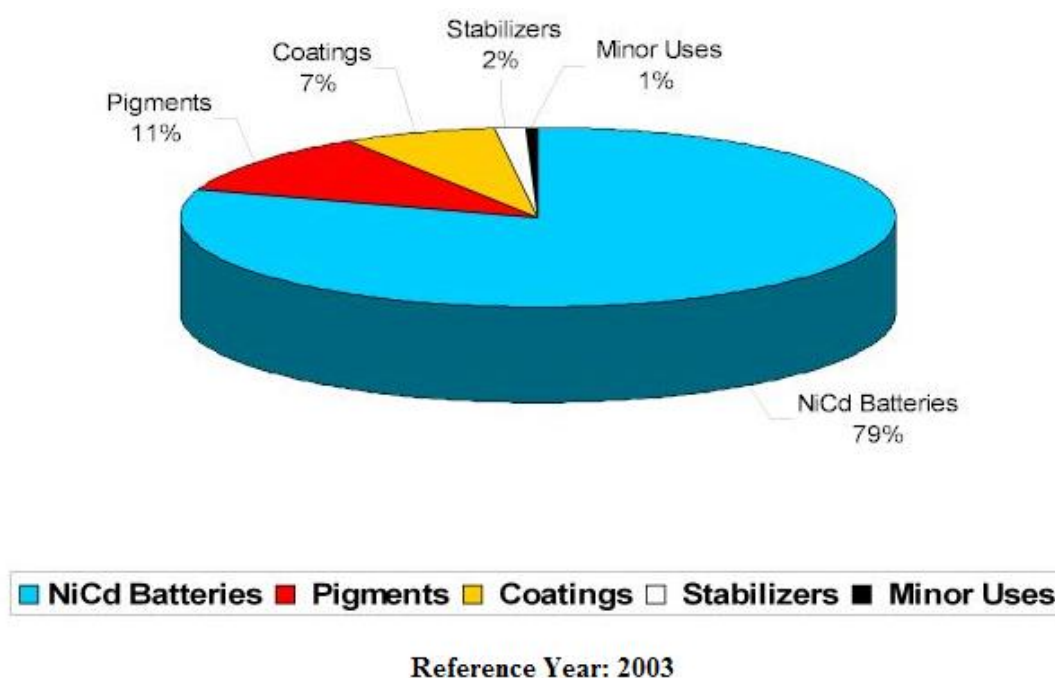


Figure 2.11. The consumption pattern of cadmium in its various end use applications.

In the general, non-smoking population the major exposure pathway is through food, via the addition of cadmium to agricultural soil from various sources

(atmospheric deposition and fertiliser application) and uptake by food and fodder crops. Additional exposure to humans arises through cadmium in ambient air and drinking water.

## 2.6. Analytical Techniques

### 2.6.1. Fourier Transform Infrared Spectroscopy (FTIR)

Infrared (IR) spectroscopy is one of the most common spectroscopic techniques used by organic and inorganic chemists. Simply, it is the absorption measurement of different IR frequencies by a sample positioned in the path of an IR beam (Figure 2.12). The main goal of IR spectroscopic analysis is to determine the chemical functional groups in the sample. Different functional groups absorb characteristic frequencies of IR radiation. Using various sampling accessories, IR spectrometers can accept a wide range of sample types such as gases, liquids, and solids. Thus, IR spectroscopy is an important and popular tool for structural elucidation and compound identification. With the advent of Fourier transform infrared spectroscopy (FTIR) the range of applications and the materials amenable to study has increased enormously, owing to its increased sensitivity, speed, wavenumber accuracy and stability. Conventional infrared spectroscopy relies on the dispersion of an infrared beam via a grating into its monochromatic components, and slowly scanning through the entire spectral region of interest. When a sample is placed in the beam, various wavelengths of infrared radiation are absorbed by the sample as the beam is scanned, and the result recorded as the infrared spectrum of the sample.

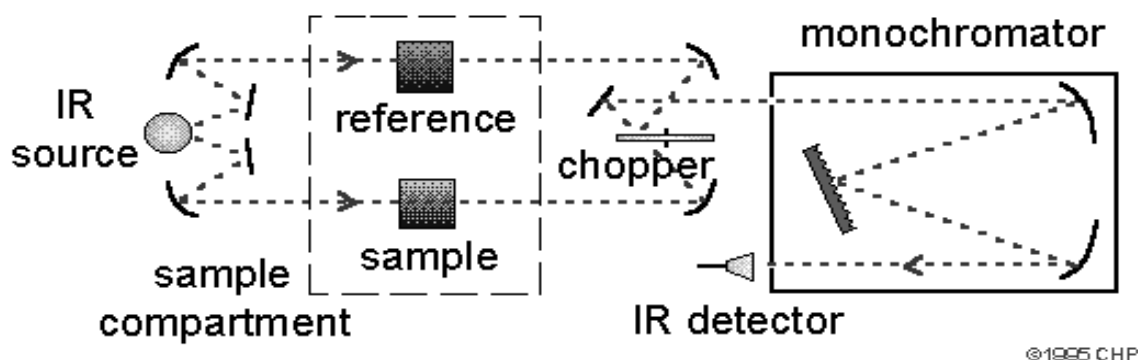


Figure 2.12. Schematic of a dispersive IR absorption spectrometer.

Over most of the mid-infrared spectral range, Fourier transform instruments appear to have signal-to-noise ratios that are better than those of a good-quality dispersive instrument by more than an order of magnitude. The enhanced signal-to-noise ratio can, of course, be traded for rapid scanning, with good spectra being attainable in a few seconds in most cases. A theoretical advantage of Fourier transform instruments is that their optics provide a much larger energy throughput (one or two orders of magnitude) than do dispersive instruments, which are limited in throughput by the necessity of narrow slit widths. The potential gain here, however, may be partially offset by the lower sensitivity of the fast-response detector required for the interferometric measurements. Finally, it should be noted that the interferometer is free from the problem of stray radiation because each IR frequency is, in effect, modulated at a different frequency.

The areas of chemistry where the extra performance of interferometric instruments appears to be particularly relevant include: (1) very-high resolution work, which is encountered with gaseous mixtures having complex spectra resulting from the superposition of vibrational and rotational bands, (2) the study of samples with high absorbances, (3) the study of substances with weak absorption bands, (4) investigations requiring fast scanning such as kinetic studies or detection of chromatographic effluents, (5) collecting infrared data from very small samples, and (6) infrared emission studies (Skoog and Leary, 1992).

### **2.6.2. Scanning Electron Microscopy (SEM)**

In many fields of chemistry, material science, geology, and biology detailed knowledge of the physical nature and chemical composition of the surfaces of solids on a submicrometer scale is becoming of greater and greater importance (Skoog and Leary, 1992). By far the most important on surface structure, at least in the first stage of examination of a sample, comes from the techniques that provide images of structural differentiation in the surface layers. The simplest and most accessible of these techniques is scanning electron microscopy (SEM).

SEM is a type of electron microscope that images the sample surface by scanning it with a high-energy beam of electrons in a raster scan pattern. The electrons interact with the atoms that make up the sample producing signals that contain



information about the sample's surface topography, composition and other properties such as electrical conductivity. Secondary electron images can be obtained on all materials identifying surface features, on most instruments, to a limit of  $\sim 100$  nm. Despite the considerable depth of penetration of the incident primary electron beam (e.g.  $0.5\text{-}5\ \mu\text{m}$ ), the re-emitted electrons (as secondary and backscattered electrons) come from mean depths of  $50\ \text{nm}\text{-}0.5\ \mu\text{m}$  depending on the density of the material. Hence, the technique is sensitive to the near-surface region. Scanning (or rastering) the beam over the surface minimizes surface damage and surface charging. The surface features in this range include extensive faceting, phase separation, morphology of crystals, the structure of fracture faces, precipitates, pores, distribution of materials in composites, bonding at interfaces and preferential reaction at different sites on the surface. Backscattered electron images can give contrast based on the average atomic number of the region or phase examined. Topographic images, obtained by combining different backscattered electron images, can reveal detail of pits and protusions, precipitates and altered regions on the surface. The SEM is relatively easy to use requiring straightforward specimen preparation and conventional vacuum. The essential elements of an SEM are shown schematically in Figure 2.13. The electron gun, fitted by a W,  $\text{LaB}_6$  or Field Emission (FE) gun operates typically over the range  $0.1\text{-}30$  kV accelerating voltage. A condenser lens produces a demagnified image of the electron source, which in turn is imaged by the probe forming lens (often called the objective lens) onto the specimen. The electron path and sample chamber are evacuated. Scanning coils deflect the probe over a rectangular raster, the size of which, relative to the display screen, determines the magnification. Detectors collect the emitted electron signals, which after suitable amplification can be used to modulate the intensity of a TV-like image tube, which is rastered in synchronism with the probe (Connor et al., 2003).

### **2.6.3. Energy Dispersive X-Ray Spectroscopy**

Energy Dispersive X-Ray Spectroscopy (EDS or EDX) is a chemical microanalysis technique used in conjunction with scanning electron microscopy (SEM). The EDS technique detects x-rays emitted from the sample during bombardment by an electron beam to characterize the elemental composition of the analyzed volume.

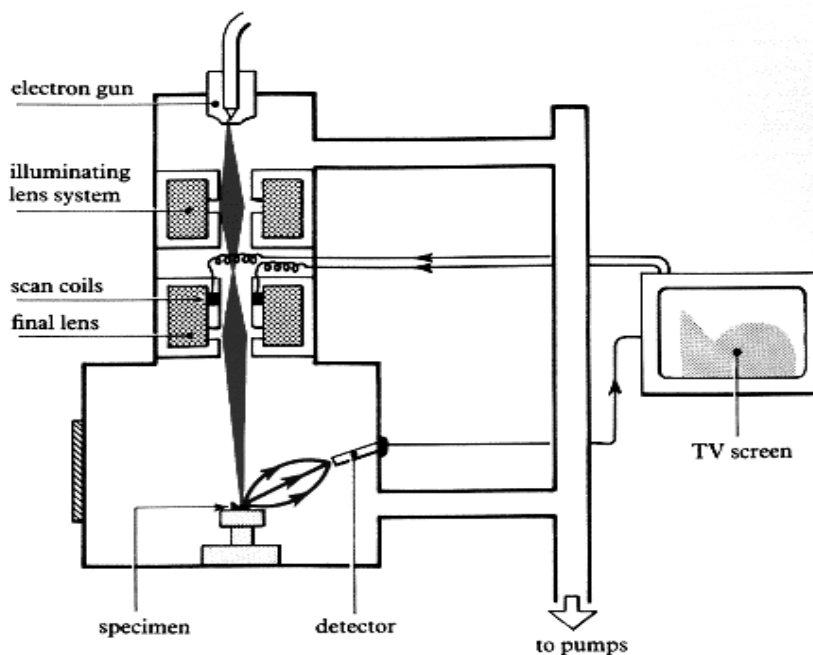


Figure 2.13. Basic features of the SEM.

Features or phases as small as 1  $\mu\text{m}$  or less can be analyzed. When the sample is bombarded by the SEM's electron beam, electrons are ejected from the atoms comprising the sample's surface. The resulting electron vacancies are filled by electrons from a higher state, and an x-ray is emitted to balance the energy difference between the two electrons' states. The x-ray energy is characteristic of the element from which it was emitted (Figure 2.14). The EDS x-ray detector measures the relative abundance of emitted x-rays versus their energy. The detector is typically a lithium-drifted silicon, solid-state device. When an incident x-ray strikes the detector, it creates a charge pulse that is proportional to the energy of the x-ray. The charge pulse is converted to a voltage pulse (which remains proportional to the x-ray energy) by a charge-sensitive preamplifier. The signal is then sent to a multichannel analyzer where the pulses are sorted by voltage. The energy, as determined from the voltage measurement, for each incident x-ray is sent to a computer for display and further data evaluation. The spectrum of x-ray energy versus counts is evaluated to determine the elemental composition of the sampled volume.

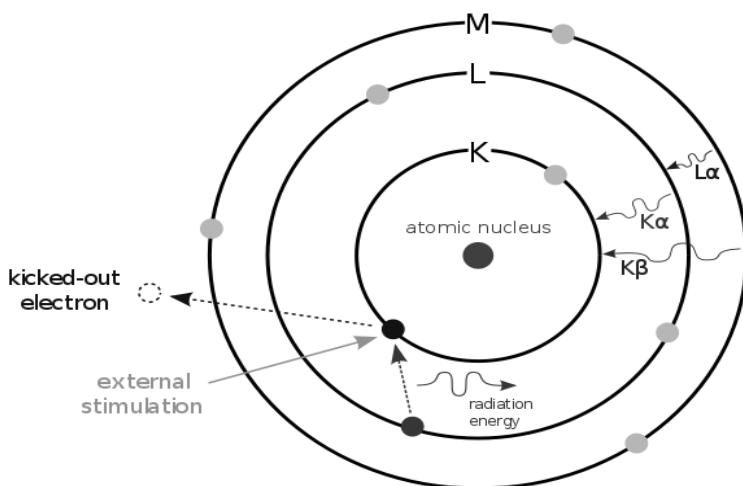


Figure 2.14. Principles of EDS.

The sample x-ray energy values from the EDS spectrum are compared with known characteristic x-ray energy values to determine the presence of an element in the sample. Elements with atomic numbers ranging from that of beryllium to uranium can be detected. The minimum detection limits vary from approximately 0.1 to a few atom percent, depending on the element and the sample matrix.

Quantitative results can be obtained from the relative x-ray counts at the characteristic energy levels for the sample constituents. Semi-quantitative results are readily available without standards by using mathematical corrections based on the analysis parameters and the sample composition. The accuracy of standardless analysis depends on the sample composition. Greater accuracy is obtained using known standards with similar structure and composition to that of the unknown sample.

#### 2.6.4. Elemental Analysis (EA)

Elemental analysis on carbon, hydrogen and nitrogen is the most essential, and in many cases the only, investigation performed to characterize and/or prove the elemental composition of an organic sample. Elemental analysis or "EA" almost always refers to CHNX analysis, the determination of the percentage weights of carbon, hydrogen, nitrogen, and heteroatoms (X) (halogens, sulfur) of a sample.

The most common form of elemental analysis, CHNX analysis, is accomplished by combustion analysis. In this technique, a sample is burned in an excess of

oxygen, and various traps collect the combustion products; carbon dioxide, water, nitric oxide, sulfur dioxide, and hydrohalogenides. The weights of these combustion products can be used to calculate the composition of the unknown sample ([http://www.univie.ac.at/Mikrolabor/chn\\_eng.htm](http://www.univie.ac.at/Mikrolabor/chn_eng.htm)).

### 2.6.5. Atomic Absorption Spectroscopy (AAS)

Atomic Absorption Spectrometry (AAS) is the measurement of the absorption of optical radiation by atoms in the gaseous state. The original equipment was developed by Walsh in 1955. AAS is one of the most important instrumental techniques for both quantitative and qualitative analysis of metallic and some of the nonmetallic elements in inorganic or organic materials.

The general construction of an atomic absorption spectrophotometer is simple and is shown schematically in Figure 2.15. The most important components are a radiation source, which emits the spectrum of the analyte element; an atomizer, such as a flame, in which the atoms of the sample to be analyzed are formed; a monochromator for the spectral dispersion of the radiation with an exit slit for selection of the resonance line; a detector permitting measurement of radiation intensity, followed by an amplifier and a readout device that presents a reading.

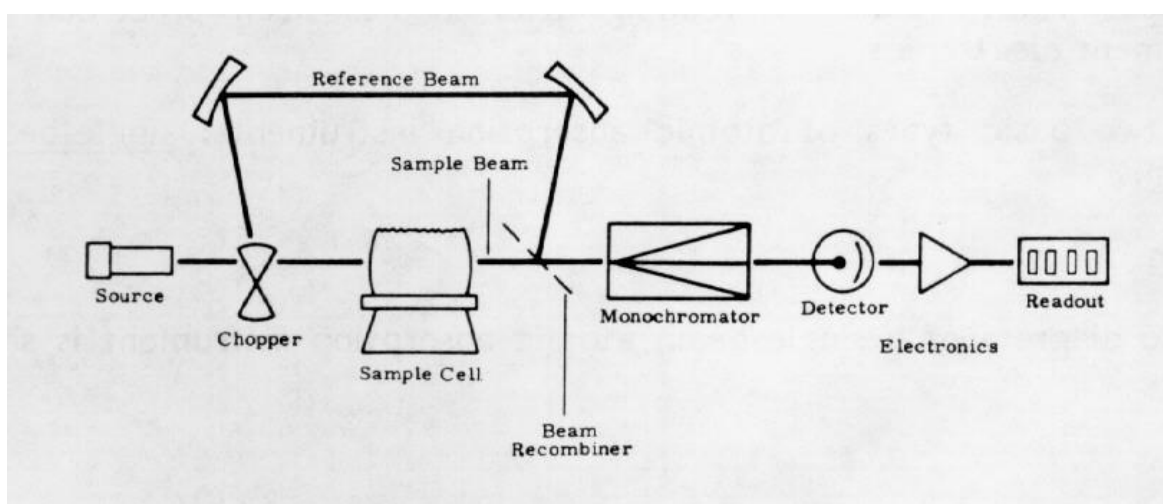


Figure 2.15. Schematic construction of a double beam AAS.

Since atoms are only able to absorb radiation within a very narrow frequency interval, certain demands must be placed upon the radiation source. Although

continuum radiation sources afford a high total illumination intensity, the illumination intensity in the interval of interest about 0.0005 nm to 0.005 nm is nevertheless too weak. For this reason the radiation source used for absorption measurements should emit the spectrum of the element to be determined. The most common sources for atomic absorption measurements are hollow cathode lamp and electrodeless discharge lamps.

The emission spectrum of the analyte element emitted from the radiation source is passed through an "absorption cell" in which a portion of the incident radiation is absorbed by atoms produced by thermal dissociation. Accordingly, the most important function of this absorption cell is to produce analyte atoms in the ground state from the ions or molecules present in the sample. This is without doubt the most difficult and critical process within the whole atomic absorption procedure. The success or failure of a determination is virtually dependent upon the effectiveness of the atomization; the sensitivity of the determination is directly proportional to the degree of atomization of the analyte element in the sample.

The presence of other constituents accompanying the analyte element in the sample cell can lead to interferences, which can cause systematic errors in the determination. The influence of the atomizing medium, such as the flame, graphite material, or quartz cell, or of the solvent is not regarded as interference since sample and reference solutions are affected to equal degrees. An interference will cause an error in the analytical result only if the interference is not adequately accounted for in the evaluation procedure. In spectrochemical analysis, interferences are generally divided into two classes: Spectral interferences and non-spectral interferences.

Spectral interferences are caused by the incomplete isolation of the radiation absorbed by the analyte element from other radiation or radiation absorption due to, or affected by, the interferent. Several methods have been developed for correcting the interferences; (a) the two line correction method (b) the continuous source correction method (c) background correction based on the Zeeman effect (d) background correction based on source self-reversal.

Non-spectral or chemical interferences result from various chemical processes occurring during atomization that the analyte signal is affected directly. Perhaps the most common type of interference is by anion, which form compounds of low volatility with the analyte and thus reduce the rate at which it is atomized. Interference due to formation of species of low volatility can often be eliminated or moderated with the use of higher temperatures. Alternatively, releasing agent, which are cations that react preferentially with the interference and prevents its interaction with the analyte, can be employed. Protective agents prevent interference by forming stable but volatile species with the analyte. An ionization buffer is added to suppress ionization. By adding an easily ionized element, such as cesium or potassium, the concentration of the free electrons in the absorption volume is increased substantially, thereby suppressing and stabilizing ionization of the analyte (Welz, 1985).

### 3. EXPERIMENTAL

#### 3.1. Preparation of Polymeric Hydrogels

##### 3.1.1. Materials

*N*-isopropylacrylamide (NIPA), the crosslinker *N,N*-methylenebis(acrylamide) (MBAA), the initiator ammonium peroxodisulfate (APS), the accelerator *N,N,N',N'*-tetramethylethylenediamine (TEMED) were obtained from Aldrich Chem. Co. (USA) and used as supplied without further purification. Cadmium nitrate salt,  $\text{Cd}(\text{NO}_3)_2 \cdot 4(\text{H}_2\text{O})$ , cysteine,  $\text{HSCH}_2\text{CH}(\text{NH}_2)\text{COOH} \cdot \text{HCl}$ , and methacryloyl chloride,  $\text{H}_2\text{C}=\text{C}(\text{CH}_3)\text{COCl}$ , were of reagent grade and were purchased from Merck AG (Darmstadt, Germany) and Sigma (St Louis, USA), respectively. Deionized water of 18.2  $\mu\text{S}$  specific conductivity obtained from a Milli-Q water purification system (Millipore) served for hydrogel synthesis and preparation of all solutions.

##### 3.1.2. Synthesis of 2-methacryloylamidocysteine (MAC) Chelating Monomer and the Complex with Cd(II) Ions

The chelating monomer, MAC, was prepared according to the method developed by Denizli et al. (2003). Briefly, the following experimental procedure was applied for the synthesis of MAC monomer: 5.0 g of cysteine and 0.2 g of  $\text{NaNO}_2$  were dissolved in 30 mL of  $\text{K}_2\text{CO}_3$  aqueous solution (5%, v/v). This solution was cooled to 0°C. 4.0 mL of methacryloyl chloride was poured slowly into this solution under nitrogen atmosphere and then the solution was stirred magnetically at room temperature for 2 h. At the end of this period, the pH of this solution was adjusted to 7.0 and then was extracted with ethylacetate. The aqueous phase was evaporated in a rotary evaporator. The residue (i.e., MAC) was crystallized in ethanol and ethylacetate. In order to prepare MAC- $\text{Cd}^{2+}$  complex, solid 2-methacryloylamidocysteine (MAC) (0.120g) was added slowly into 10 mL of deionized water, which was then treated with cadmium nitrate (0.090 g) at room temperature by stirring with a magnetic stirrer for 3 h. Then, the aqueous metal-monomer complex was used in the hydrogel synthesis without any further treatment.

### 3.1.3. Preparation of Cd(II)-imprinted p(NIPA-MAC) Hydrogels

Cd(II)-imprinted p(NIPA-MAC) hydrogels were synthesized by free radical crosslinking copolymerization of NIPA (main polymer constituent) and MAC-Cd(II) complex in aqueous solutions. *N,N*-methylenebis(acrylamide), (MBAA), was used as a cross-linker agent. APS and TEMED were used as the redox initiator system. First, MAC-Cd(II) complex was prepared in 10 mL deionized water and then NIPA was added slowly onto it while stirring the solution magnetically at 300 rpm. After stirring for 2 h, APS was added and stirred for 1h. Then, the crosslinker was added to the polymer solution and stirred for one more hour. After that the solution was purged with nitrogen gas for 10 minutes. Finally TEMED was added and the polymer solution was placed in glass tubes of 6 mm inner diameter and 4 cm long. The glass tubes were sealed and the polymerization was carried out at room temperature for 24 h. After gelation was completed, all the gels were taken out of the glass tubes and washed consecutively with deionized water by incubating the gels in cold water (swollen form) and hot water (shrunken form) alternatively to remove the residual monomers and the initiator. The hydrogels were dried in a lyophilizator (Christ Freeze Dryer Alpha LD 1-2 plus, German). The hydrogel synthesis conditions are summarized in Table 3.1 and some photographs of the prepared imprinted hydrogels at different stages are shown in Figure 3.1.

Table 3.1. Preparation conditions of Cd(II) imprinted poly(NIPA-MAC) gels.

		<u>Amount</u>
Monomer:	NIPA	0.850 g
Chelating Monomer:	MAC-Cd(II) complex	0.120 g
Cross-linker:	MBAA	0.02 g
Accelerator:	TEMED	10 $\mu$ L
Initiator:	APS	0.01 g



## Experimental

The nonimprinted p(NIPA-MAC) gel and pNIPA gel were also prepared. In the preparation of nonimprinted gel, the chelating monomer (0.110g of MAC) which has no complex with Cd(II) ions was used. pNIPA gel was prepared without the chelating monomer.

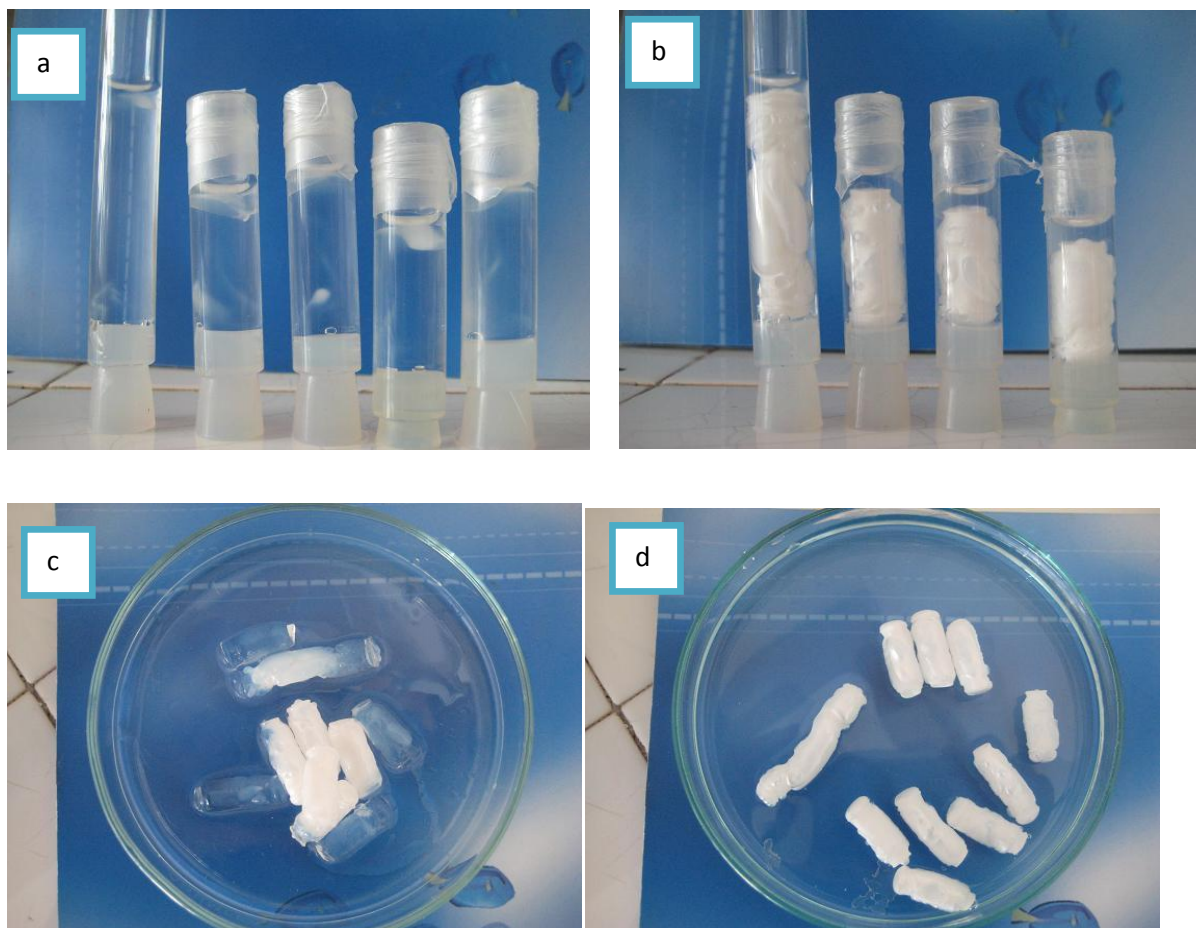


Figure 3.1. Digital photographs of Cd(II) imprinted p(NIPA-MAC) hydrogels at the end of the polymerization (a) at room temperature, (b) after incubating at 50°C for 30 min, (c) and (d) after taken out from the glass tubes.

### 3.1.4. Removal of the Template Cd(II) ions

In order to remove the template Cd(II) ions, freeze-dried Cd(II) imprinted p(NIPA-MAC) gels were immersed into 50 mL of the 0.1 M HNO<sub>3</sub> solution for 6 h at room temperature. This procedure was repeated several times until all the Cd(II) ions were removed from the hydrogels. After that the template free polymers were dried in a lyophilizator.

## 3.2. Characterization of the Hydrogels

### 3.2.1. Temperature Dependence of Swelling Ratios

For the study of temperature-dependent swelling, hydrogel samples were equilibrated in an excess amount of deionized water at a temperature ranging from 5 (below LCST) to 60°C (above LCST). The samples were allowed to swell in deionized water for at least 24 h at each predetermined temperature controlled up  $\pm 0.1$  °C by a thermostated water bath with a cooling unit (Julabo, F34, Germany). After 24 h immersion in deionized water at a predetermined temperature, the hydrogels were taken out from water and blotted with a moistened filter paper to remove excess water on the hydrogel surface and then weighed until a constant weight was reached. After this weight measurement, hydrogels were re-equilibrated in deionized water at another predetermined temperature and their wet weight was determined thereafter. The dry weight of each sample was determined after drying the hydrogels in a vacuum oven at 40°C for 3 days. Because measuring the weight of a swelling hydrogel is much easier than the measuring the volume, the swelling ratio of hydrogels is usually expressed based on weights. The average values among three measurements were taken for each sample, and swelling ratio (SR) was calculated as follows,

$$\text{SR} = \frac{W_s}{W_d} \quad (3.1)$$

where,  $W_s$  is the weight of swollen hydrogel at a certain temperature and  $W_d$  is the dry weight of hydrogel. The LCST of the hydrogel samples was determined as the abscissa of the inflection point of the swelling ratio vs. temperature curves.

### 3.2.2. Swelling kinetics

The kinetics of swelling of the hydrogels was measured gravimetrically at 22°C. The dried hydrogel samples were immersed in deionized water at 22°C to record the weight when swelling at regular time intervals. Water uptake was calculated as follows,

$$\frac{-}{-} \quad (3.2)$$

where  $W_t$  is the weight of the swollen hydrogel after wiping off the excess water of the hydrogel at time  $t$  and  $22^\circ\text{C}$ ,  $W_d$  is the dry weight of hydrogel, and  $W_e$  is the weight of the hydrogel at equilibrated swelling at  $22^\circ\text{C}$ .

### 3.2.3. FTIR Characterization

The chemical structures of pNIPA, p(NIPA-MAC), and Cd(II) ion imprinted p(NIPA-MAC) hydrogels were characterized using a Fourier Transform Infrared Spectrometer (FTIR 8000 Series, Shimadzu, Japan) in the wavenumber range of  $4000\text{-}400\text{ cm}^{-1}$  with the KBr disc technique. Dried hydrogel specimens were prepared using a freeze-drying method.

### 3.2.4. Elemental Analysis

Carbon, nitrogen, hydrogen, and sulfur contents in pNIPA, p(NIPA-MAC), and template removed Cd(II) imprinted p(NIPA-MAC) hydrogels were obtained by elemental analysis (EA, 1106, Carlo Erba Co., Italy) to evaluate the MAC incorporation of the gels.

### 3.2.5. Morphologies of Hydrogels

The pNIPA, p(NIPA-MAC), and Cd(II) imprinted p(NIPA-MAC) hydrogel samples were first equilibrated in 50 mL deionized water at both  $20^\circ\text{C}$  and  $50^\circ\text{C}$ , separately, to reach an equilibrium state. The equilibrated hydrogel samples were quickly frozen in liquid nitrogen and further freeze-dried under vacuum at  $-45^\circ\text{C}$  for 2 days until the solvent was sublimed. The freeze-dried samples were then fractured carefully and their interior morphology was studied by using a Scanning Electron Microscope (Quanta 400-ESEM, FEI). Before SEM observation, hydrogel specimens were fixed on aluminum stubs and coated with gold.

### 3.2.6. Energy Dispersive X-Ray Analysis

The presence of cadmium ions in Cd(II) imprinted p(NIPA-MAC) hydrogels was investigated by using an energy dispersive x-ray spectrometer (EDX) in

conjunction with SEM. Thus the same hydrogel sample used for the SEM observation was analyzed. The non imprinted p(NIPA-MAC) sample, which served as a reference, was also investigated for its cadmium free content.

### 3.3. Adsorption and Desorption Studies

#### 3.3.1. Reagents and Apparatus

All chemicals were of analytical-reagent grade. Standard solutions of 1000 mg/L Cd(II), 1000 mg/L Pb(II), 1000 mg/L Cu(II), 1000 mg/L Cr(III), and 1000 mg/L Fe(III) were prepared from  $\text{Cd}(\text{NO}_3)_2 \cdot 4\text{H}_2\text{O}$  (Merck),  $\text{Pb}(\text{NO}_3)_2$  (Aldrich),  $\text{Cu}(\text{NO}_3)_2 \cdot 3\text{H}_2\text{O}$  (Merck),  $\text{Cr}(\text{NO}_3)_3 \cdot 9\text{H}_2\text{O}$  (Merck), and  $\text{Fe}(\text{NO}_3)_3 \cdot 9\text{H}_2\text{O}$  (Merck) in deionized water, respectively. From these solutions, other dilute standard solutions were prepared daily. Deionized water of 18.2  $\mu\text{S}$  specific conductivity obtained from a Milli-Q water purification system (Millipore) served for preparation of all solutions. Nitric acid (65%, Merck) and pure sodium hydroxide pellets (Merck) were used to adjust the sample pH.

A thermostatic water bath (Clifton 13210 Model, England) was used to control the temperature of the experiments.

A Perkin Elmer Model AAnalyst 200 (USA) Atomic Absorption Spectrophotometer equipped with deuterium lamp background correction was employed to determine the metal ion concentration. The working conditions are given in Table 3.2.

Table 3.2. Working conditions for metal ions in AAS.

Element	$\lambda$ , nm	Slit, mm	HCL current	Flame Composition		Calibration standard (max.)
				Acetylene	Air	
Cd(II)	228.8	2.7/1.35	8 mA	2.5 L/min	10 L/min	1.0 ppm
Pb(II)	283.3	2.7/1.05	8 mA	2.5 L/min	10 L/min	10.0 ppm
Cu(II)	324.8	2.7/0.8	15 mA	2.5 L/min	10 L/min	4.0 ppm
Cr(III)	357.9	2.7/0.8	25 mA	3.3 L/min	10 L/min	4.0 ppm
Fe(III)	248.3	1.8/1.35	30 mA	2.5 L/min	10 L/min	5.0 ppm

### 3.3.2. Temperature-Dependent Adsorption Studies

The adsorption abilities of the Cd(II) imprinted p(NIPA-MAC) hydrogel adsorbent for Cd(II) were determined batch wise. Pieces of cylindrical gels of dry weight of 0.200 g of the hydrogel were added into a beaker containing 50 mL of aqueous solution of Cd(NO<sub>3</sub>)<sub>2</sub>.4H<sub>2</sub>O of various concentrations ranging from 0.100 mg/L to 100 mg/L, and at different pH values (in the range of 2.5 - 7.5) and then the beaker was sealed up and placed on a magnetic stirrer at a speed of 300 rpm at room temperature for 24 h. For the adsorption studies at 50°C, the sealed beaker was placed in a thermostatic water bath shaker and operated under 300 rpm at designed temperature for 24 h. The desired pH was adjusted by the addition of small quantities of HNO<sub>3</sub>(aq) and NaOH(aq). After the desired treatment periods, the concentration of the Cd(II) ions in the aqueous phase was measured by using a Perkin-Elmer AAnalyst 200 atomic absorption spectrophotometer. The amount of Cd(II) adsorption of the Cd<sup>2+</sup> imprinted p(NIPA-MAC) hydrogels was evaluated by using the following expression:

$$Q = \frac{(C_0 - C)V}{m} \quad (3.3)$$

Here, Q is the amount Cd(II) ions adsorbed onto unit mass of the gels (mg/g); C<sub>0</sub> and C are the concentrations of the Cd(II) ions in the initial solution and in the aqueous phase after treatment for certain period of time, respectively (mg/L); V is the volume of the solution (L); and m is the mass of the hydrogels used (g).

For comparison, similar adsorption experiments were also carried out with pNIPA and non imprinted p(NIPA-MAC) hydrogels.

### 3.3.3. Desorption and Reusability Studies

To take out the Cd(II) ions from the Cd(II)-imprinted p(NIPA-MAC) hydrogel-adsorbent the gels were squeezed. For this purpose, first the Cd(II) ions adsorption of the hydrogel was realized as described in detail in previous section at 20°C. After the adsorption was completed, adsorption medium was placed in a thermostatic water bath at 50°C for 24 h. At the end of this period, aqueous phase was removed from the hydrogels and its Cd(II) ion content was measured by using AAS.

## *Experimental*

The Cd(II) ions bound on the hydrogels were completely desorbed from the hydrogels by means of acid treatment. The metal ions adsorbed hydrogel samples were immersed in 50 mL of 0.1 M HNO<sub>3</sub> solution and stirred continuously (at a stirring rate of 300 rpm) for 3 h at room temperature. The concentration of the Cd(II) ions in desorption medium was measured by atomic absorption spectrophotometer. Desorption ratio was calculated from the amount of Cd(II) ions adsorbed on the gels and the final Cd(II) ions concentration in the desorption medium by the following equation;

---

(3.4)

In order to test the reusability of the Cd(II) imprinted poly(NIPA-MAC) hydrogels, Cd(II) ions adsorption-desorption procedure was repeated three times by using the same hydrogels in each cycle. In order to regenerate, after desorption, the gels were washed with 50 mM NaOH solution.

### **3.3.4. Selectivity Experiments**

In order to show the ion-recognition behavior of the Cd(II) imprinted poly(NIPA-MAC) hydrogels, competitive adsorptions were also studied. The Pb(II), Cu(II), Cr(III), and Fe(III) ions in addition to Cd(II) ion were selected for the measurements of selectivity. The adsorption experiments were carried out with 10.0 mg/L aqueous solutions of each metal ion and the mixture of these ions in the similar manner as described previously. Experiments were performed at a constant pH=6.0 and at 20°C. The measurements of the concentrations of these metal ions were also performed with AAS.

## 4. RESULTS AND DISCUSSION

### 4.1. Preparation of Hydrogels

Polymerization of water soluble monomers in the presence of crosslinking agents leads to the formation of chemically crosslinked hydrogels. In literature to date, most biomedical or environmental hydrogels were synthesized by free radical polymerization. The three monomers, NIPA, MAC, and MAC-Cd(II) complex were selected in our study for the following reasons. NIPA is the most often used monomer in the preparation of thermosensitive gels, and its homopolymer has a LCST at moderate temperature ( $\sim 32^\circ\text{C}$ ). MAC is a monomer used to improve the adsorbent ability of the pNIPA hydrogel by providing the functional sites binding for metal ions. MAC-Cd complex was used as a monomer to give an ion-recognition behavior to the hydrogel for obtaining an adsorbent which is specific for a certain metal ion. MBAA was employed as a crosslinker to provide rigidity and impart mechanical stability to the gels. Initiator APS was used because it is soluble in water at room temperature. The chemical structures and schematic preparation of  $\text{Cd}^{2+}$  imprinted p(NIPA-MAC) hydrogels are shown in Figure 4.1.

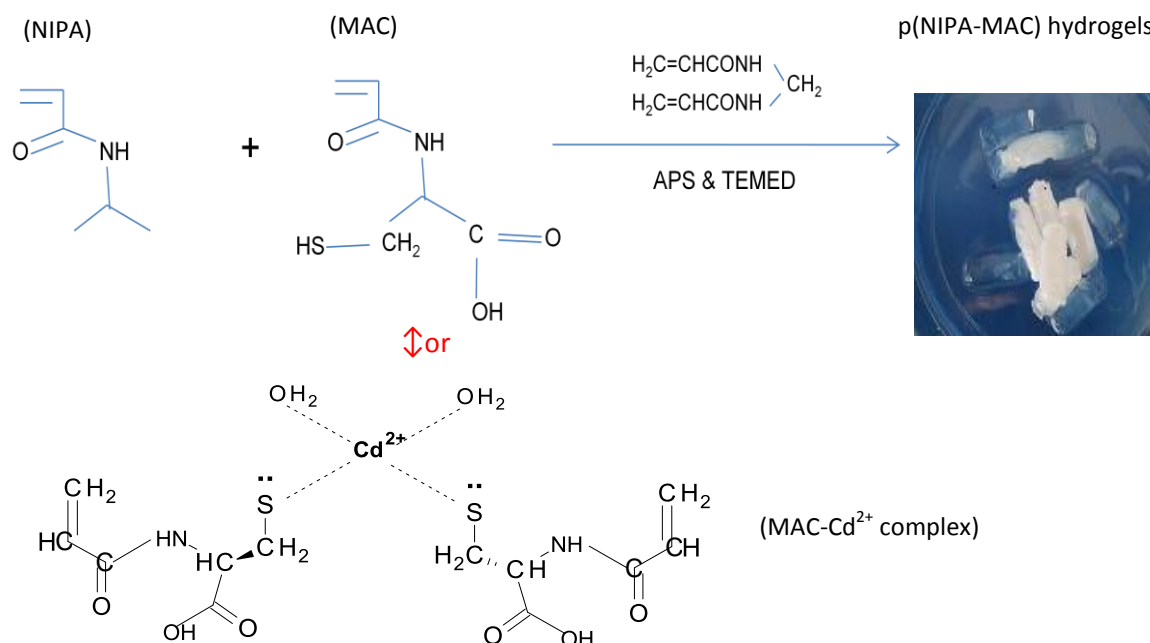


Figure 4.1. The chemical structures of monomers used and schematic preparation of the non-imprinted or Cd(II) imprinted p(NIPA-MAC) hydrogels.

## 4.2. Characterization of Cd<sup>2+</sup> Imprinted p(NIPA-MAC) Hydrogels

### 4.2.1. Temperature Dependence of Swelling Ratio of the Hydrogels

Figure 4.2. shows the effect of NIPA/MAC feed ratio on swelling ratios of p(NIPA-MAC) hydrogels over a temperature range from 5 to 60°C. The feed composition of hydrogels is summarized in Table 4.1. The data in Figure 4.2 show that the swelling ratio of hydrogels increased with MAC contents from 0 to 120 mg. This increase in swelling ratio with MAC contents in hydrogels was attributed to the hydrophilic nature of MAC in hydrogel network. It is known that a hydrophilic/hydrophobic balance exists in the pNIPA network (because of its hydrophilic and hydrophobic segments) as well as many intermolecular and intramolecular interactions, such as hydrogen bonds and polymer polymer interactions (Bae et al. 1990). As additional hydrophilic MAC segments were introduced into the backbone of the pNIPA hydrogel, the hydrophilic/hydrophobic balance of the resulting hydrogel network was shifted toward more hydrophilic nature, leading to an increase in water content at temperatures below LCST. In the literature, the volume phase transition temperature or LCST of these types of hydrogels is defined as the temperature at which the swelling ratio has decreased to a half of its value at the initial temperature or room temperature (Wu et al.1992). The hydrogel's LCST is also regarded as the temperature at which phase-separation degree (changes of the swelling ratio vs. temperature changes around the transition temperature,  $\Delta SR/\Delta T$ ) is greatest or the temperature at which the swelling ratio of hydrogel decreased most dramatically (Zhang et al., 1999; Zhang et al., 2000). Figure 4.2 also shows the LCSTs of p(NIPA-MAC) hydrogels. The LCST data also show that an increase in the content of MAC in the hydrogel led to an increasing LCST of the copolymer hydrogels. The LCST of pNIPA was around 32 °C. Introducing MAC monomer into the polymer structure, the LCST temperature increased from 32 °C to 34 °C.

For further studies, p(NIPA-MAC) hydrogels with NIPA/MAC molar ratio of 92/8 was used (because of its higher metal ion adsorption capacity compared to other hydrogels with lower MAC content).



Table 4.1. Feed compositions of pNIPA hydrogels.

	NIPA/MAC molar ratios			
	100/0	98/2	96/4	92/8
NIPA (mg)	850	850	850	850
MAC (mg)	0	25	60	120
MBAA (mg)	20	20	20	20
H <sub>2</sub> O (mL)	10	10	10	10
APS (mg)	10	10	10	10
TEMED (mL)	0.01	0.01	0.01	0.01

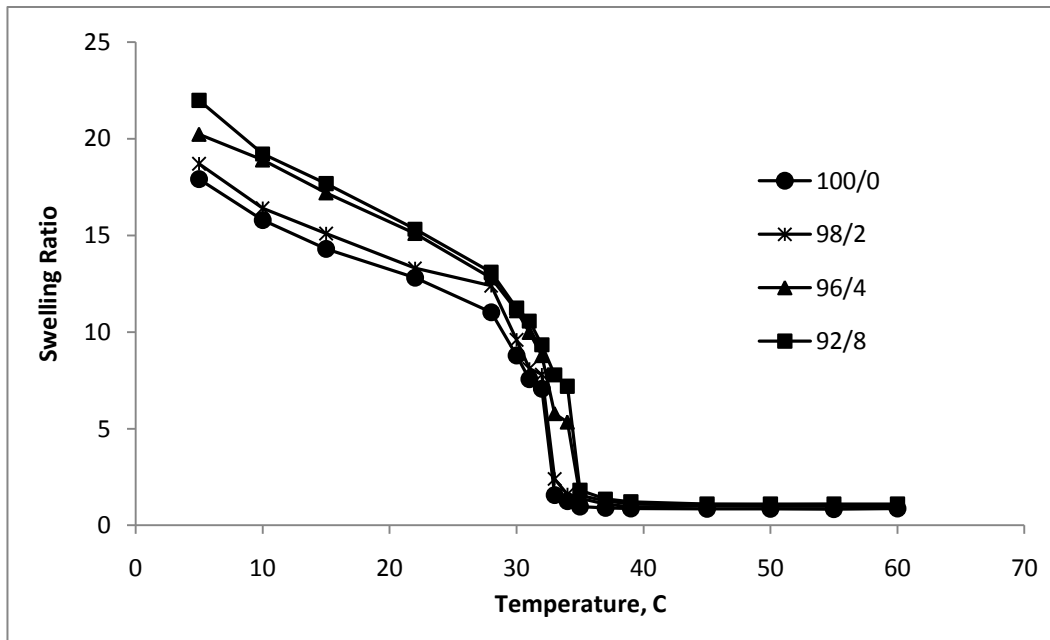


Figure 4.2. Effect of NIPA/MAC feed ratio on the temperature dependence of equilibrium swelling ratios of p(NIPA-MAC) hydrogels.

In order to investigate the effect of cross-linking density on the swelling ratio for hydrogels with the same NIPA/MAC monomer molar ratio of 92/8 and different amount of the MBAA cross linker was also investigated. As can be seen in Figure 4.3, the hydrogels had the same LCST, 34 °C, with different amounts of the MBAA (1.0 – 4.0 wt%, based on total monomer). So the amount of the cross linker did not influence the LCST and phase separation behavior of hydrogels evidently in the range of 1.0 - 4.0 wt%. As the cross-linking density within the hydrogel

increased, swelling ratio difference was not change significantly at temperatures above LCST. At 10°C or 20°C (below LCST), however, for the hydrogels with higher crosslinking density, lower swelling ratio was observed, compared to hydrogels with lower cross-linking density. This result indicated that high cross-linking density made the structure collapse more tightly than in the other samples. It decreases the diffusion of chains and thus reduces the dilatation of three dimensional net structures of hydrogels. Hydrogel with cross-linking density of 2.0 wt% was chosen for further investigations, because of easy handling of it in swollen form, compared to 4.0 wt% one.

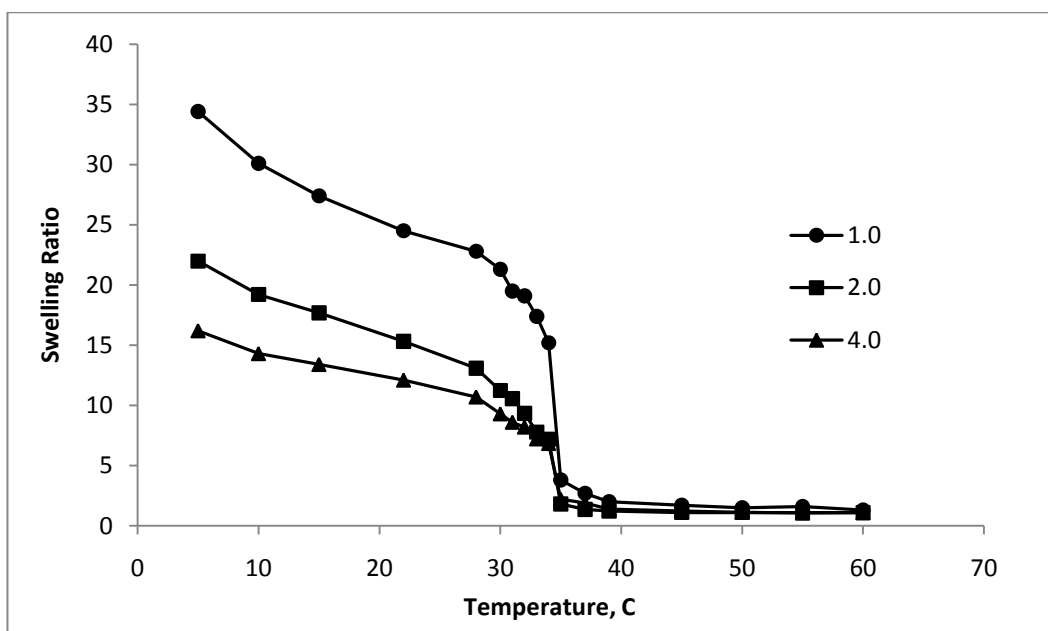


Figure 4.3. Temperature dependence of swelling ratio for p(NIPA-MAC) hydrogel with different amount of cross-linker (wt %).

Figure 4.4 shows the temperature dependence of the swelling ratio and LCST of the poly(NIPA), non-imprinted poly(NIPA-MAC) and template removed Cd<sup>2+</sup>-imprinted poly(NIPA-MAC) hydrogels when the temperature increased from 5 to 60°C. The amounts of NIPA, MBAA, and MAC used to prepare the hydrogels were given in Table 4.1, and were constant for all hydrogels. As shown in Figure 4.4, p(NIPA), non-imprinted p(NIPA-MAC) and template removed Cd(II)-imprinted p(NIPA-MAC) hydrogels exhibit a negative temperature sensitivity, which is

swelling at lower temperature and shrinking at higher temperature. Under equilibrium swelling conditions, all gels showed increasing swelling ratio at lower temperatures, but they deswelled at high temperatures because of the aggregation of the network chains. The highest LCST value was observed at 34°C for p(NIPA-MAC) gels, followed by template removed Cd<sup>2+</sup>-imprinted p(NIPA-MAC) and pNIPA hydrogels with the LCST of 33 and 32°C, respectively.

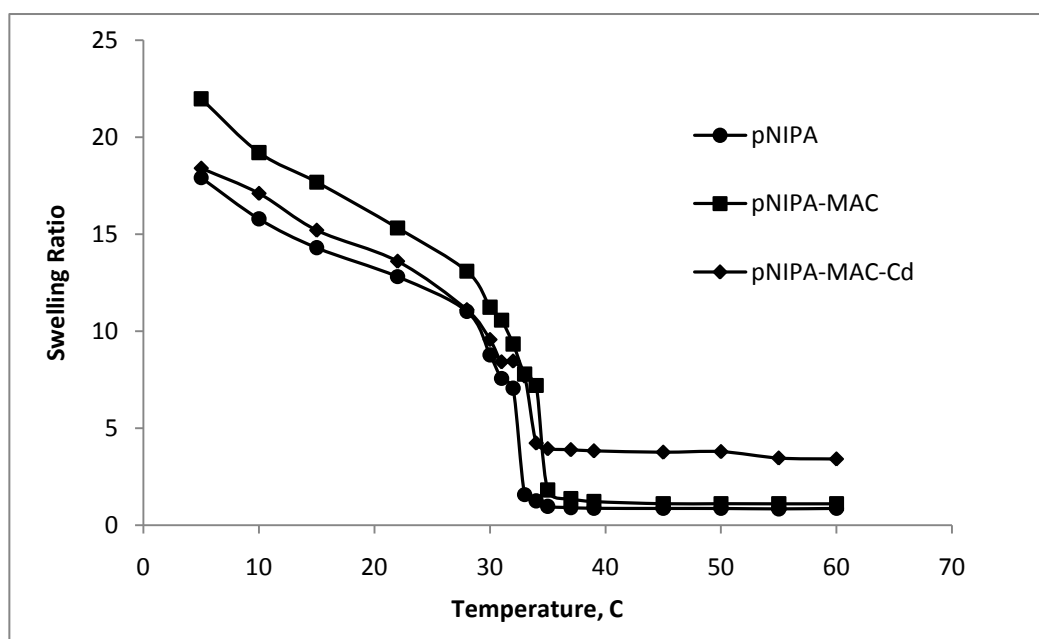


Figure 4.4. Temperature dependence of swelling ratio for the p(NIPA), non-imprinted p(NIPA-MAC) and template removed Cd(II)-imprinted p(NIPA-MAC) hydrogels.

Although the swelling ratio of template removed Cd<sup>2+</sup>-imprinted p(NIPA-MAC) is somewhat lower than that of p(NIPA-MAC), it is still higher than that of pNIPA at temperatures below LCST, as can be seen in Figure 4.4. As described above, incorporation of more hydrophilic monomer (MAC or MAC-Cd complex) to pNIPA hydrogels increases the LCST value because the ionized  $-\text{COO}^-$  groups are sufficiently soluble to counteract the aggregation of the hydrophobic temperature sensitive units. Also, the repulsion of the  $-\text{COO}^-$  groups or the formation of hydrogen bonds between the amide groups in NIPA and the  $-\text{COO}^-$  groups in MAC may impede the collapse induced by the NIPA components, increasing the LCST (Yu et al., 2008). At temperatures above LCST, a notable result for the

template removed  $\text{Cd}^{2+}$ -imprinted p(NIPA-MAC) gel was observed. The data in Figure 4.4 show that all the hydrogels exhibited a temperature-induced reduction in swelling ratio, a classical characteristic of pNIPA-based material; but the incorporation of the MAC-Cd complex monomer into pNIPA backbone decreased the magnitude of the thermo-induced shrinkage. The swelling ratio of template removed  $\text{Cd}^{2+}$ -imprinted p(NIPA-MAC) hydrogel reduced from 17.1 to 3.4, as temperature changed from 10 to 60°C, with a  $\Delta$  swelling ratio of 13.7 ( $\text{SR}_{10^\circ\text{C}} - \text{SR}_{60^\circ\text{C}}$ ). Over the same temperature range,  $\Delta$  swelling ratios of pNIPA and p(NIPA-MAC) were 14.9 and 18.1, respectively. The decrease in the magnitude of  $\Delta$  swelling ratio observed for template removed  $\text{Cd}^{2+}$ -imprinted p(NIPA-MAC) hydrogel can be attributed to the structure of the MAC-Cd complex influenced changes in the hydrophilic/hydrophobic nature and morphology of the polymer that prevented collapsing of the hydrogel above the LCST.

In the literature, a wide variety of thermosensitive pNIPA-based hydrogels prepared by using various cross-linkers and comonomers have been reported. Gotoh et al. investigated the effect of synthesis temperature on swelling degree of the pNIPA hydrogels prepared by using MBAA as crosslinking agent, TEMED and APS as the polymerization accelerator and initiator, respectively. They showed the swelling degree of the pNIPA gels scarcely depended on the synthesis temperature (Gotoh et al., 1997). Lee and Lin studied the effect of different crosslinkers on swelling behavior of NIPAAm/PEGMEA (poly(ethylene glycol) methylether acrylate) copolymeric hydrogels. They synthesized the copolymeric hydrogels by free radical polymerization with MBAA, tetraethylene glycol diacrylate (TEGDA), and ethylene glycol dimethacrylate (EGDMA) as three different crosslinkers and APS and TEMED as initiator and accelerator, respectively. They reported that the swelling ratios for the present copolymeric gels decrease with increase in temperature. In addition, their results also showed that the higher swelling ratios for the present gels prepared from TEGDA were obtained due to larger space between the gel networks (Lee and Lin, 2006). Yu et al. investigated the effect of different amount of the crosslinker on swelling behavior for the p(NIPA-co-AAc) hydrogels prepared with N-acrylchitosan as crosslinker. They reported that as the cross-linking density within the hydrogel increased, the water content difference was not statistically significant at 25°C.

However, at 37°C, for the hydrogels with higher cross-linking density, they reported lower water content compared to hydrogels with lower cross-linking density (Yu et al., 2007).

#### **4.2.2. Swelling Kinetics of the Hydrogels**

The swelling kinetics of pNIPA, non-imprinted p(NIPA-MAC), and template removed Cd(II)-imprinted p(NIPA-MAC) hydrogels at room temperature (22°C) are shown in Figure 4.5. During the swelling in other words hydration process, water penetration is a crucial step to determine the swelling kinetics of hydrogels. The data in Figure 4.5 showed that the slope of the curve belonging to pNIPA is smaller than the others at the beginning of swelling process, which indicates that the hydration of pNIPA hydrogel was slower from the beginning of swelling process. In the case of pNIPA, about 8% of water was adsorbed within 15 min, about 18% within 60 min and 40% at the end of 240 min. However, non-imprinted p(NIPA-MAC) and template removed Cd(II) imprinted p(NIPA-MAC) hydrogels adsorbed about 13 and 10% water within 15 min, respectively, and about 52 and 44% within 240 min, respectively. This relationship suggests that water can diffuse into the hydrogel networks faster if the hydrogel had more hydrophilic (MAC monomer) contents.

Although the template removed Cd(II)-imprinted p(NIPA-MAC) hydrogel exhibits rather faster swelling rate with respect to pNIPA in Figure 4.5, it shows a slower swelling rate in comparison with non-imprinted p(NIPA-MAC). This can be indication of; incorporating the MAC-Cd complex into the hydrogel changed the systematic distribution of the hydrophilic monomer during the polymerization of the hydrogel when compared in the case of plain MAC used, so decrease of intramolecular interactions (hydrogen bonds) between MAC segments and NIPA groups would lead to a reduction in the rate of water absorption.

Generally, three steps were suggested to control hydrogel swelling rate (Zhang et al., 2000; Yoshida et al., 1994): the diffusion of water molecules into hydrogel network, the subsequent relaxation of hydrated polymer chains, and the expansion of polymer network into surrounding aqueous solution.

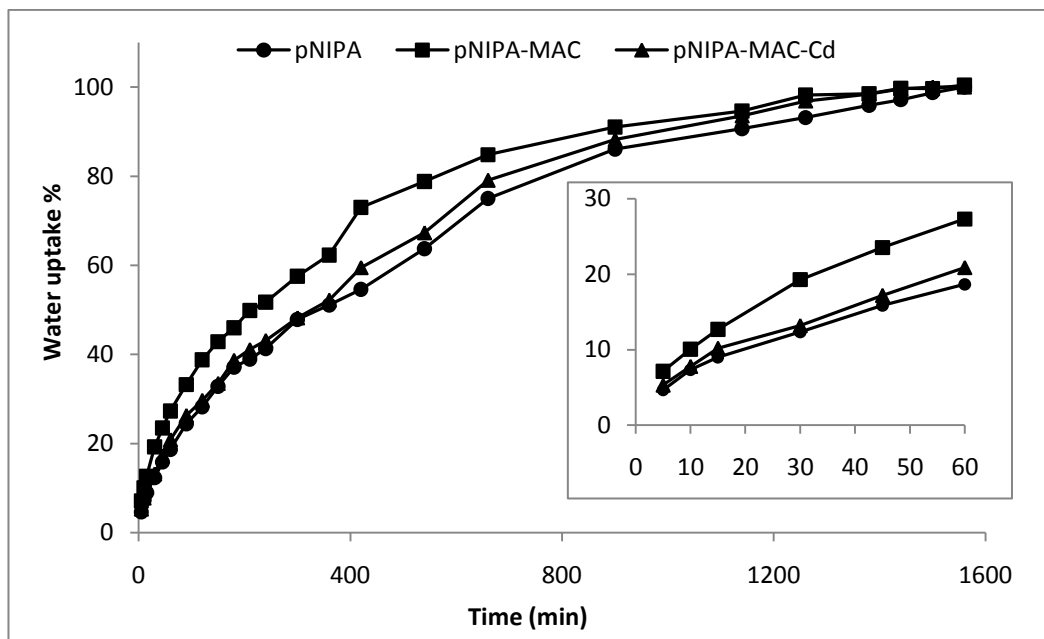


Figure 4.5. Swelling kinetics of the pNIPA, p(NIPA-MAC), and Cd(II) imprinted p(NIPA-MAC) hydrogels at 22°C.

Therefore, porous morphology and the nature of the pore cell wall are very important during the swelling process. This is because a porous morphology could increase the diffusion of water molecules into hydrogel network, while a thick and rigid pore cell wall would retard the relaxation of hydrated polymer chains. In fact, the swelling rate was the macroscopic observation resulted from the combination of these three steps. Based on the SEM observations in Figure 4.7, the non-imprinted p(NIPA-MAC) hydrogel would exhibit a faster swelling rate than the pNIPA or the imprinted one.

#### 4.2.3. Elemental Analysis

The incorporation of MAC and MAC-Cd complex into the hydrogels were evaluated by C, H, N, and S contents of these hydrogels measured by elemental analysis. Table 4.2 shows the elemental analysis results of the pNIPA, p(NIPA-MAC), and Cd(II) imprinted p(NIPA-MAC) gels. Because the NIPA and MBAA do not contain any sulfur, the sulfur amount determined by elemental analysis comes from incorporated MAC groups into the polymeric structure. Note that the initiator, APS, contains sulfur but its contribution was very low, so the increase in the

elemental S% in Table 4.2 supported to confirm the successful incorporation of MAC groups into pNIPA chains.

Table 4.2. Elemental analysis of the hydrogels.

Hydrogel	C%	N%	H%	S%
pNIPA	59.67	12.41	8.18	0.67
Non-imprinted p(NIPA-MAC)	59.04	12.56	7.82	2.36
Cd <sup>2+</sup> imprinted p(NIPA-MAC)	59.10	12.27	7.71	1.83

#### 4.2.4. FTIR Characterization

The FTIR spectra of the dried hydrogels are presented in Figure 4.6. From the given spectra we can find the amide I band ( $\sim 1653 \text{ cm}^{-1}$ ) ascribed to the C=O stretch of PNIPA and the amide II band ( $\sim 1546 \text{ cm}^{-1}$ ) due to the N-H bending vibration in every spectrum. The broad peak at the range from 3200 to 3600  $\text{cm}^{-1}$  belongs to the N-H or O-H stretching vibration. Furthermore, the characteristic double peaks at 1388 and 1366  $\text{cm}^{-1}$  for isopropyl group of NIPA appeared in all FTIR spectra of pNIPA, non-imprinted p(NIPA-MAC), and Cd(II) imprinted p(NIPA-MAC) hydrogels. Specifically, the appearance of the C-S stretching vibrations in the region 700-600  $\text{cm}^{-1}$  in both FTIR spectrum of p(NIPA-MAC) and Cd(II) imprinted p(NIPA-MAC) hydrogels denoted a successful incorporation of MAC groups into copolymeric hydrogels.

#### 4.2.5. SEM Observation of Synthesized Hydrogels

Morphology is a critical factor that determines response behaviors of pNIPA based hydrogels (Zhang and Chu, 2003). The interior morphology of swollen (at 20°C, below LCST) and shrunken (at 50°C, above LCST), and freeze dried hydrogels is shown in Figure 4.7. As illustrated in Figure 4.7, among all the hydrogels in swollen form at 20°C, the p(NIPA-MAC) hydrogel had the largest pore size with a  $>20 \mu\text{m}$  in diameter, and also exhibited more homogenous pore distribution like honey comb. The enlarged porous network of the p(NIPA-MAC) hydrogel was attributed to the ionic hydrophilic property of the incorporated MAC comonomer. When a pure pNIPA hydrogel swells in water at room temperature ( $< \text{LCST}$ ), there

## Results and Discussion

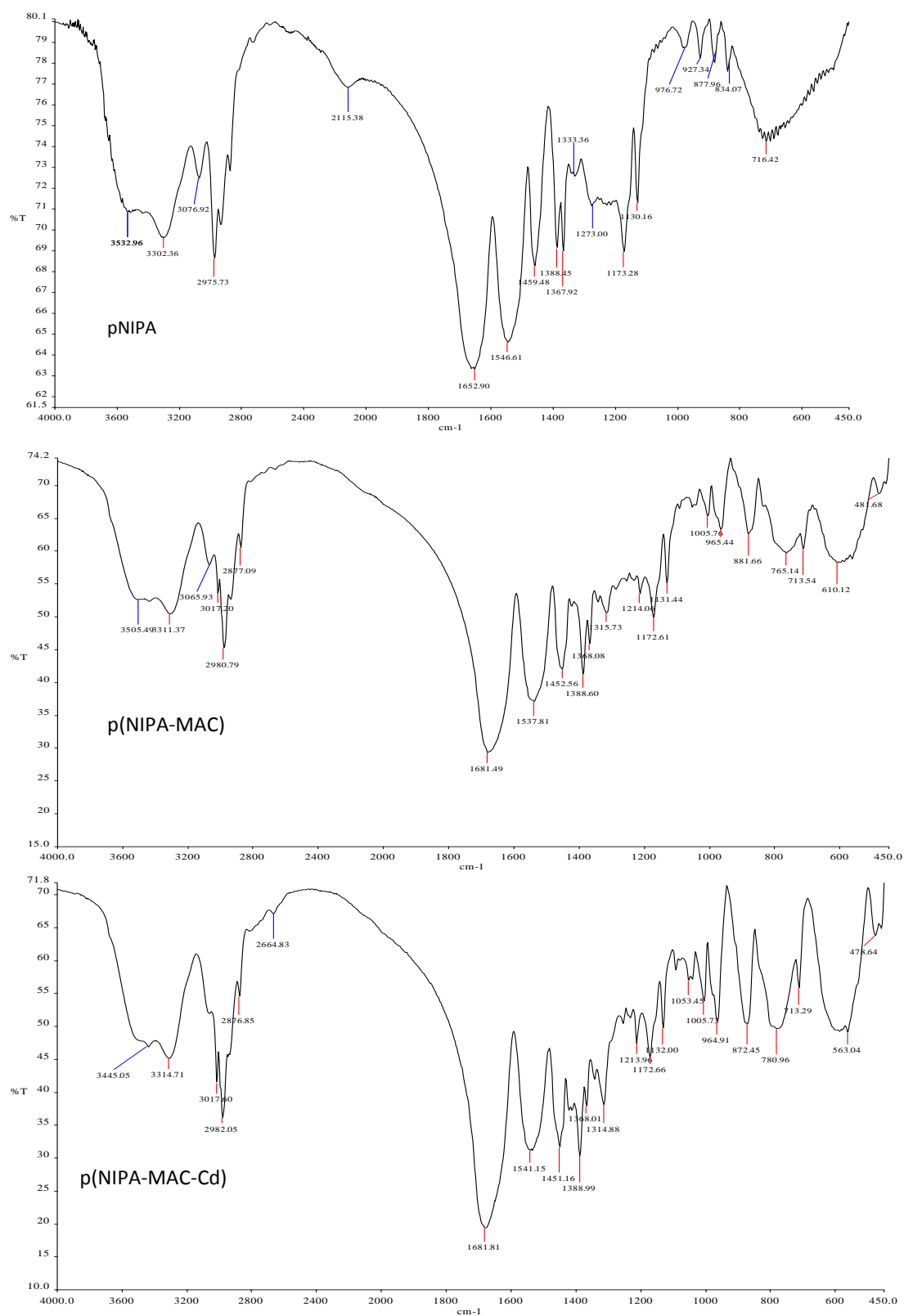


Figure 4.6. FT-IR spectra of the pNIPA, non-imprinted p(NIPA-MAC), and Cd(II) imprinted p(NIPA-MAC) hydrogels.



exist hydrogen bond interactions between amide groups of pNIPA chains and surrounding water (Zhang and Chu, 2007).

These interactions may lead to the formation of cage-like structures around hydrophobic groups, in other words, structured water molecules surround the hydrophobic groups, which results in swelling of pNIPA hydrogels in water (Tanaka et.al, 1984 and Otake et.al, 1990). With the introduction of MAC comonomer, p(NIPA-MAC) hydrogels might exhibit special network structure due to the formation of two types of hydrogen bonds that pure pNIPA does not have: hydrogen bond between  $\text{-COO}^-$  group and water and hydrogen bond between amide and  $\text{-COO}^-$  groups. Thus, due to a much higher ionization and stronger hydrophilic characteristic of the MAC segments, more water could be attracted and contained in p(NIPA-MAC) than pure pNIPA hydrogels, and the water attracted to the MAC segments might assemble into a better and more organized structure than those waters attracted to the amide group of pNIPA segments. Those results are agreed with the higher swelling ratio of the p(NIPA-MAC) hydrogel which was shown in Figure 4.4, previously.

According to the SEM images below LCST in Figure 4.7, moderately disorganized morphology and rather small pores observed for imprinted p(NIPA-MAC) hydrogel compared with the non-imprinted one may result from the molecular structure difference between the MAC molecule and the MAC-Cd(II) complex molecule. As can be seen in Figure 5.1, one mol of the MAC-Cd<sup>2+</sup> complex contains two moles of MAC groups. It can be suggested that, with the introduction of MAC-Cd<sup>2+</sup> complex during the polymerization, the propagation of pNIPA chains was assembled and/or crosslinked resulting in different orientations of the hydrophilic/hydrophobic groups ( $\text{-COO}^-$ ,  $\text{-NH}$ , and isopropyl groups) between the complex monomer and the NIPA monomer due to the two pieces of MAC segments in each unit of the complex when compared with plain MAC molecule. Finally, the resulting Cd(II) imprinted p(NIPA-MAC) hydrogel exhibited a heterogeneously distributed matrix with a rather small pores from its non-imprinted one. This observed morphological difference between the Cd(II) imprinted p(NIPA-MAC) and non-imprinted p(NIPA-MAC) hydrogels has disclosed the lower swelling ratio of the Cd(II) imprinted p(NIPA-MAC) compared to p(NIPA-MAC) hydrogel in

## Results and Discussion

Figure 4.4. Generally, as a result of reduced pore size, the free volume within the hydrogel network should be expected to be lower and hence lesser water should be accommodated; which means lower swelling ratio (Zhang and Chu, 2005).

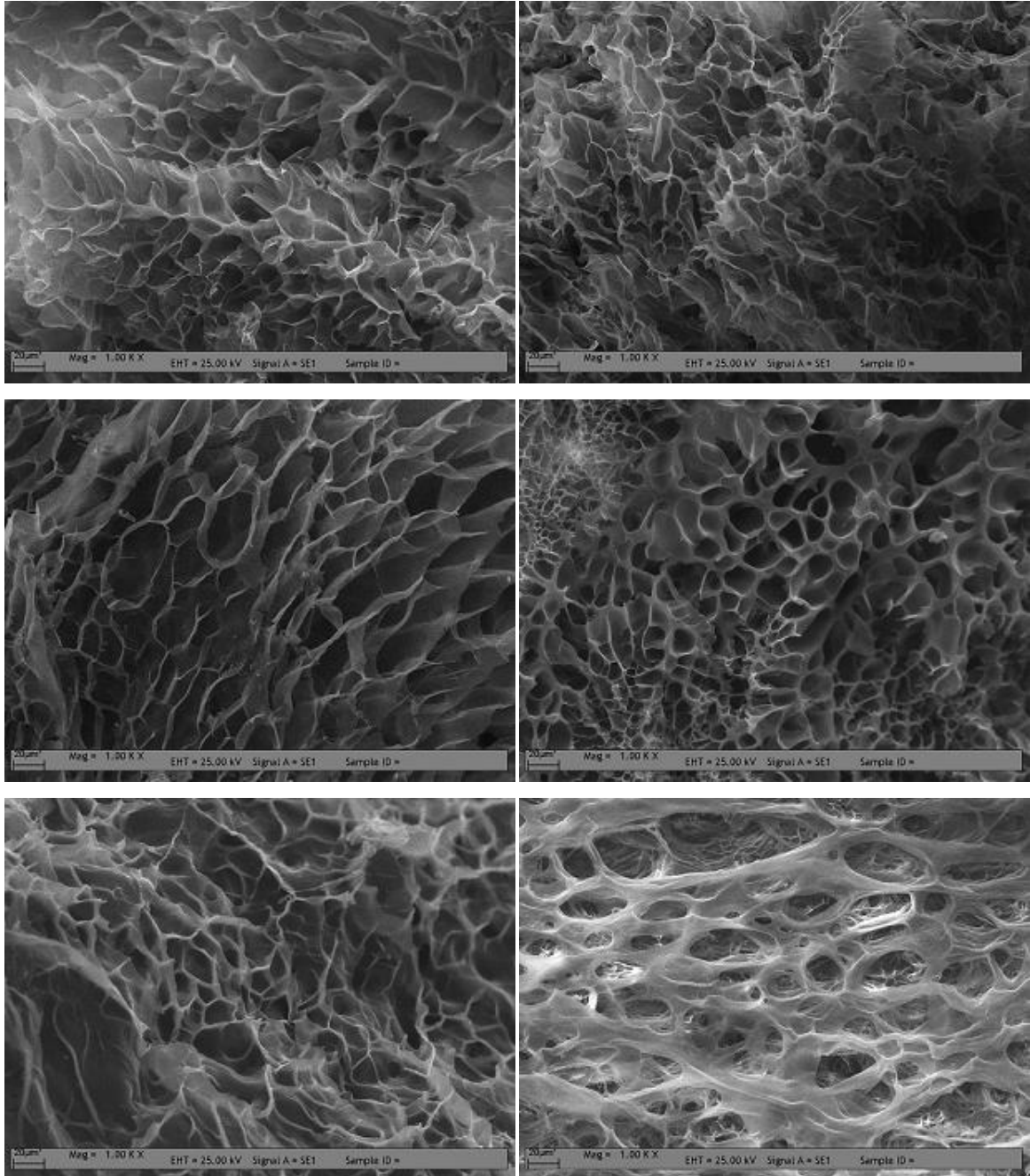


Figure 4.7. SEM images of freeze dried pNIPA, non-imprinted p(NIPA-MAC), and Cd(II) imprinted p(NIPA-MAC) hydrogels swollen at 20°C (at the left side) and shrunken at 50°C (at right side). The size of the bar is 20µm and the samples are viewed at magnification of 1.00 K X.

As can be seen in Figure 4.7, the SEM images above LCST show that the pNIPA and p(NIPA-MAC) hydrogels exhibited rather compact network structure with small pores when compared with their corresponding SEM images below LCST. However the Cd<sup>2+</sup> imprinted p(NIPA-MAC) hydrogel has dramatically changed porous matrix from an open hollow (channel like) pores to a round and shallow pores when the temperature changed from 20°C to 50°C. These results are consistent with the deswelling degree of the hydrogels observed in Figure 4.4. Zhang et al. reported that, for achieving quickly and timely diffusion of freed water during the shrinking at temperature above LCST, the hydrogel should have good release channels throughout the network (Zhang and Chu, 2005), besides of, these water release channels should be kept open for the freed water to transfer out quickly and mostly (completely) as Wu et al. reported (1992). Thus, the most possible reason that the Cd(II) imprinted p(NIPA-MAC) hydrogel exhibits lower deswelling at temperatures above LCST compared to the other hydrogels shown in Figure 4.4 was attributed to the altered water release channels throughout the network and hence the outward diffusion of entrapped water from the hydrogel interior restricted during the shrinking process.

#### **4.2.6. Energy Dispersive X-ray (EDS) Analysis**

EDS, when combined with SEM, provides elemental analysis on areas as small as nanometers in diameter. The impact of the electron beam on the sample produces x-rays that are characteristic of the elements found in the sample. EDS spectrums for non-imprinted p(NIPA-MAC) and Cd(II) imprinted p(NIPA-MAC) hydrogels are given in Figure 4.8. From comparative analysis of the EDS spectrums in Figure 4.8, the copolymerization of NIPA and MAC-Cd<sup>2+</sup> complex was confirmed due to the appearance of the Cd peaks in the range 3-4 keV in the EDS spectrum of Cd(II) imprinted p(NIPA-MAC) hydrogel but not in the spectrum of the non-imprinted p(NIPA-MAC) hydrogel. The feature peaks suggested a successful production of Cd<sup>2+</sup> imprinted p(NIPA-MAC) copolymeric hydrogel.

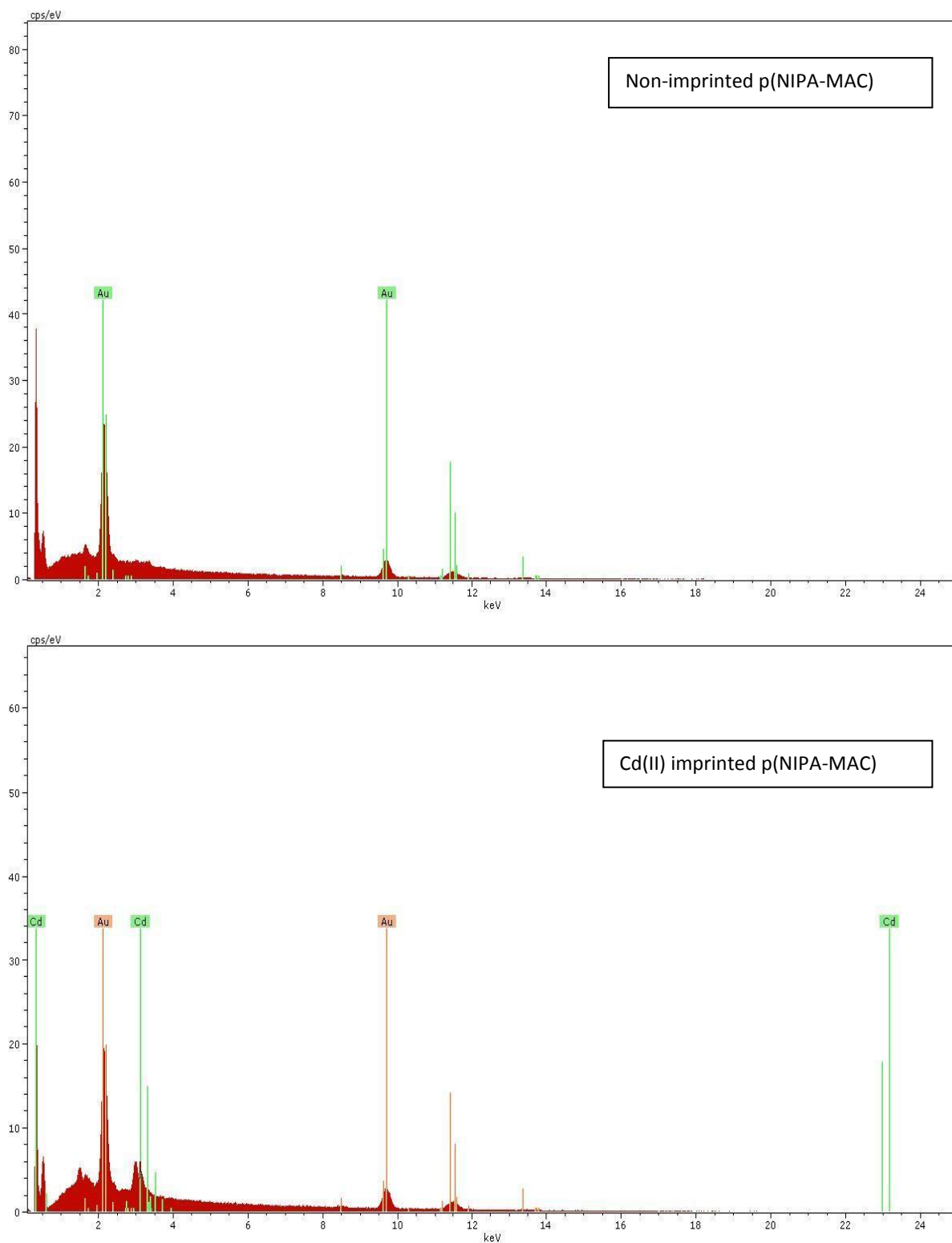


Figure 4.8. EDS spectra of non-imprinted p(NIPA-MAC) and Cd(II) imprinted p(NIPA-MAC) hydrogels.

### 4.3. Adsorption Studies

#### 4.3.1. Adsorption Rate

The variation of the Cd(II) ion adsorption amounts of the pNIPA, non-imprinted p(NIPA-MAC), and template removed Cd(II) imprinted p(NIPA-MAC) hydrogels as a function of time are presented in Figure 4.9, and the adsorption conditions are given in the figure legend. All the hydrogels were previously shrunken at 50°C, and then the adsorption was carried out at 20°C. The initial slopes of these curves reflect the adsorption rates. High adsorption rates are observed at the beginning, and then plateau values (i.e., adsorption equilibrium) are gradually reached within 240 min for both non-imprinted p(NIPA-MAC), and Cd<sup>2+</sup> imprinted p(NIPA-MAC) hydrogels.

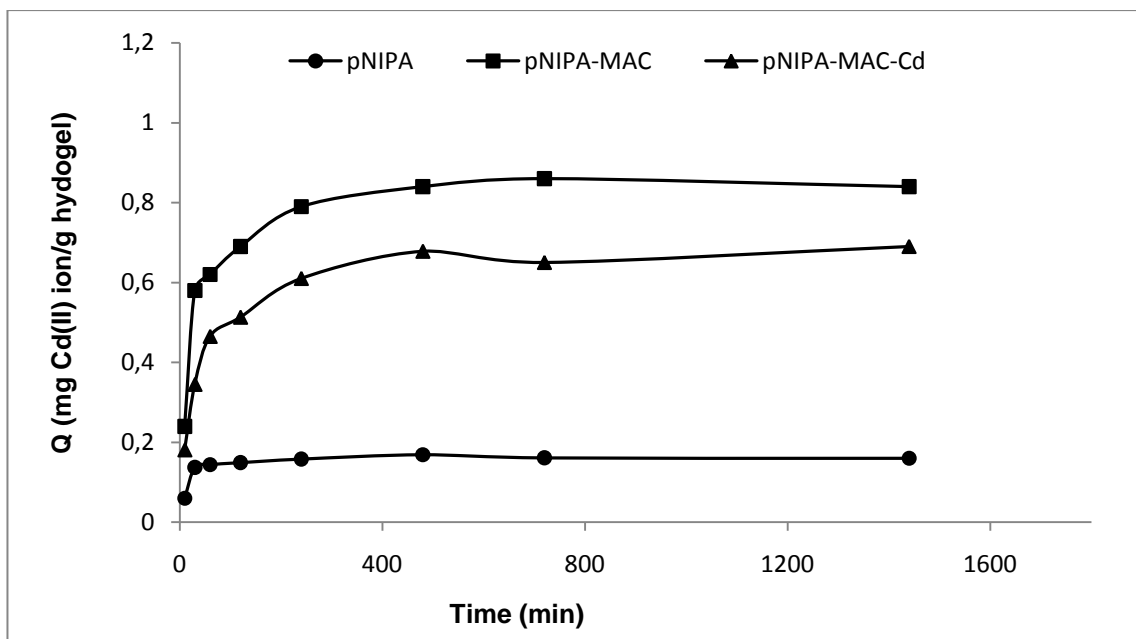


Figure 4.9. Time dependent adsorption of Cd(II) ions on the pNIPA, non-imprinted and template removed Cd(II) imprinted p(NIPA-MAC) hydrogels. Adsorption conditions: 50 mL, 10 ppm Cd(II) solution; pH:4.5; temperature 20°C.

The slow adsorption is considered due to the fact that the swelling of the thermosensitive gel network requires some time course for the formation of the expanded network structure. In the case of pNIPA, equilibrium adsorption rate is observed within 60 minutes which indicates that the Cd(II) ion adsorption is not

affected with the expanded network structure of the pNIPA hydrogel compared to MAC incorporated hydrogels, due to poorer binding ability for Cd(II) ions of amide group in the NIPA.

In literature to date, several experimental data on the adsorption of various ions by thermosensitive polymers have shown a wide range of adsorption rates. Kanazawa et.al have studied adsorption/desorption properties of heavy metals ions by using poly(*N*-isopropylacrylamide-co-*N*-(4-vinyl)benzyl ethylenediamine) [poly(NIPA-Vb-EDA)] thermosensitive gels and they have found that adsorption equilibrium is reached in 100 hours (Kanazawa et al., 2004). Tokuyama et.al, using the same polymer but having different amount of cross-linker, have found the adsorption time as 1100 min. Ju et al. studied the removal of lead (II) ions from aqueous solutions by using p(NIPAM-co-benzo-18-crown-6-acrylamide) [p(NIPAM-co-BCAm)] hydrogels. They reported that the equilibrium adsorption time was 3.5 hours. According to these results both the non-imprinted and the imprinted particles have shown fast adsorption rates and which are most probably due to high complexation of MAC monomer with Cd(II) ions and low diffusion barrier as a result of higher porous polymer network.

#### **4.3.2. Effect of pH**

It is well known that in most equilibria between metal ions and metal complexation ligands, the metal ions compete with protons for the binding sites on sorbents so that, as in almost all aqueous equilibria pH will be of dominant importance. The distribution of metal cations between free and bound states will depend on pH, and generally metal ion should bound under acidic conditions rather than at basic pH. Also, the extent of ionization of functional groups in sorbent is pH dependent, i.e., the carboxyl, hydroxyl, and sulfhydryl groups are protonated at low pH values. Conversely, at higher pH the deprotonated groups (e.g., negatively charged thiols or carboxylate) will be more nucleophilic than the protonated species, therefore can form ion pairs or complexes with the metal ions (Der-Chyan and Srinivasan, 1996). Therefore, in this study, in order to establish the effect of pH on adsorption of Cd(II) ions onto the pNIPA, non-imprinted p(NIPA-MAC), and template removed Cd<sup>2+</sup> imprinted p(NIPA-MAC) hydrogels, at pH values in the range 2.5-7.5 were investigated. For this purpose, 50 mL of 10 ppm Cd(II) solutions at different pH

values were interacted with 0.200 g of the gels for 24h, at temperature 20°C. The effect of pH on the Cd<sup>2+</sup> adsorption using the non-imprinted and the imprinted thermosensitive hydrogels is given in Figure 4.10.

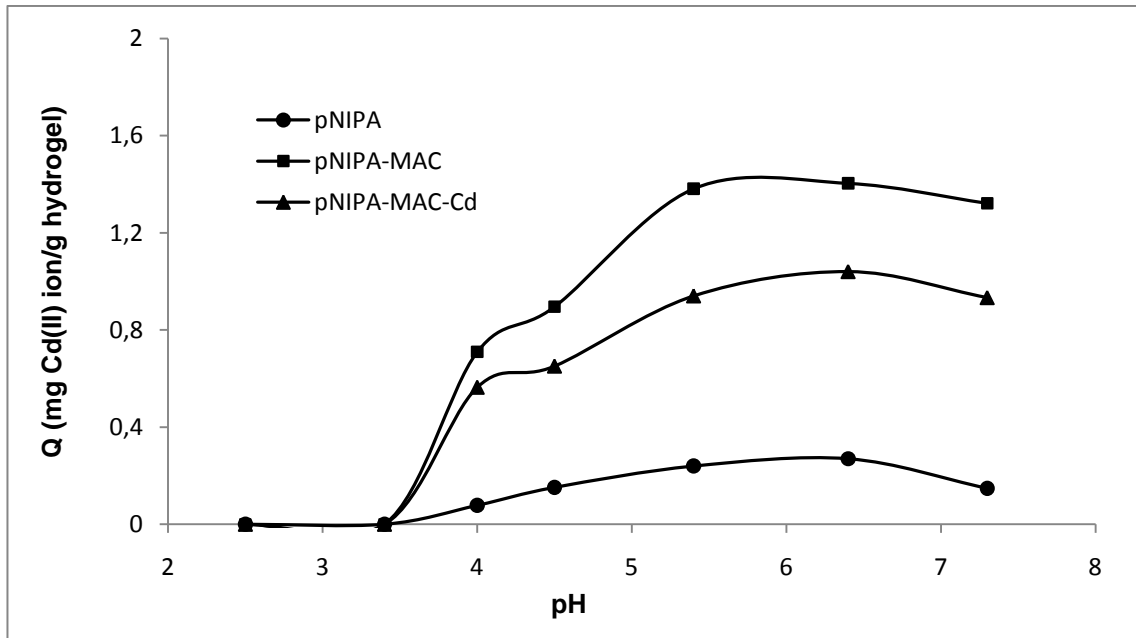


Figure 4.10. Effect of pH on the adsorption amount of pNIPA, p(NIPA-MAC), and template removed Cd(II) imprinted p(NIPA-MAC) hydrogels for Cd(II) ions.

Figure 4.10 shows that, in all of the cases, the adsorption amount increased with increasing pH, reaching a maximum value at around pH 5.5. However, at low pH values, i.e. below pH:4, the adsorption amount is lower which can be considered due to fact that in such a low pH range, the nitrogen, sulfur, and carboxyl ligands in MAC are strongly protonated.

#### 4.3.3. Adsorption Capacity

In order to investigate the adsorption capacity of the template removed Cd(II) imprinted p(NIPA-MAC) hydrogels, 50 mL of Cd(II) solution at different initial concentrations ranging from 0.1 to 100 ppm (pH ~ 5.5) were interacted with 0.200 g hydrogel for 24 h, at temperature 20°C. For comparison, adsorption capacity of the pNIPA and non-imprinted p(NIPA-MAC) were also studied by applying the

same adsorption conditions. The Cd(II) ion adsorption amounts of all the hydrogels are given as a function of the initial concentration of Cd(II) ions within the aqueous adsorption medium in Figure 4.11.

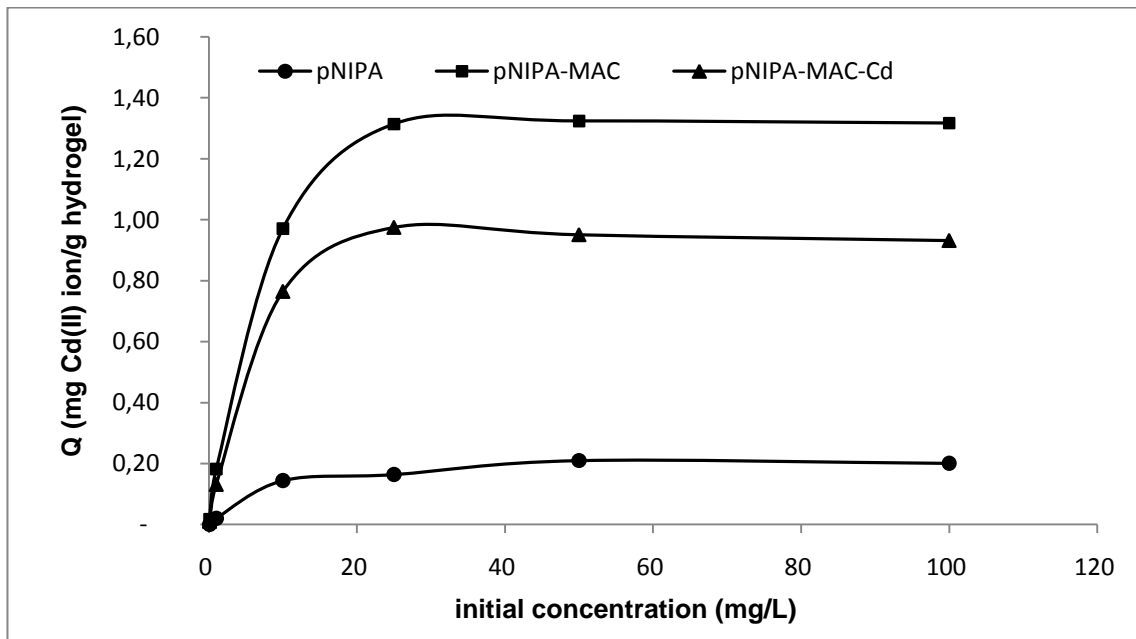


Figure 4.11. Effect of initial Cd(II) ion concentration on the adsorption amount of pNIPA, p(NIPA-MAC), and template removed Cd(II) imprinted p(NIPA-MAC) hydrogels.

As can be seen from this figure, the amount of Cd(II) ions adsorbed per unit mass of the hydrogels increased with the initial concentration of Cd(II) ions, as expected. The adsorption capacities, in other terms saturation of the active sites (which are available for specific interaction with metal ions) on the sorbent, of the imprinted and non-imprinted p(NIPA-MAC) hydrogels are 0.975 mg Cd(II)/g hydrogel and 1.324 mg Cd(II)/ g hydrogel, respectively. The higher adsorption capacity of the non-imprinted p(NIPA-MAC) hydrogels than the imprinted one can be attributed to the higher MAC content in non-imprinted p(NIPA-MAC) hydrogels. According to elemental analysis data, higher degree of incorporation of MAC into the non-imprinted p(NIPA-MAC) hydrogels was realized by using sulfur stoichiometry which was 2.36% for non-imprinted p(NIPA-MAC) and 1.83% for Cd<sup>2+</sup> imprinted p(NIPA-MAC) hydrogels. In the case of pNIPA, very low adsorption capacity was observed compared to MAC incorporated hydrogels. Lower adsorption capacity of the pNIPA hydrogels indicated that poorer binding ability of



the pNIPA (–N atom of the amide group in NIPA) than those of MAC groups towards Cd(II) ions. From the findings that we obtained in this study, we resulted that the new polymeric imprinted hydrogels presented in this communication are promising for the adsorption of Cd(II) ions from aqueous media.

In the literature, limited numbers of thermosensitive polymers with a wide range of adsorption capacities for heavy metal ions have been reported. Kanazawa et al. studied adsorption/desorption properties of heavy metal ions by using poly(*N*-isopropylacrylamide-co-*N*-(4-vinyl)benzyl ethylenediamine) [poly(NIPA-Vb-EDA)] thermosensitive gels and they reported adsorption capacity of 2.20 mg Cu/ g dry gel for Cu(II) imprinted poly(NIPA-Vb-EDA) at temperature 32.5°C (Kanazawa et al., 2004). Yamashita et al. examined the preparation of interpenetration network IPN-type stimuli-responsive heavy-metal-ion adsorbent gel. For this purpose they synthesized both NIPAm-co-NaAAc copolymer gel and IPN gel consisting of PNIPAm and PNaAAC and they reported that the NIPAm-co-NaAAc copolymer gel absorbed water and adsorbed Cu(II) ions sufficiently (0.8 mmol Cu(II)/g copoly gel) but did not exhibit the volume-phase transition behavior at all in the Cu(II) ion adsorption condition. On the other hand, the IPN gel exhibited the volume-phase transition behavior in the adsorption condition and adsorbed Cu(II) ions (0.2 mmol Cu(II)/g) below its LCST but not above the LCST (Yamashita et al., 2003). Ju et al. investigated the removal of lead (II) ions from aqueous solutions by using p(NIPAM-co-benzo-18-crown-6-acrylamide) [p(NIPAM-co-BCAm)] hydrogels. They reported that the adsorption capacity of 142 mg Pb(II)/g hydrogel at low temperature (23°C) (Ju et al., 2009). In such an adsorption process, there are several parameters which determine the adsorption capacity, such as sorbent structural properties (e.g. size, porosity, surface area), amount of sorbent, amount of functional monomer in the sorbent, metal ion properties (e.g. hydrated ionic radius, acid-base properties), pH, temperature, agitation rate, crosslinking degree, ,and of course, existing of other ions which may compete with the ions of interest for active adsorption sites; consequently it is not reasonable to make comparisons of the adsorption capacities reported.

#### **4.3.4. Temperature-Dependent Adsorption**

The amount of cadmium ions adsorbed as a function of temperature and non-imprinted and Cd<sup>2+</sup> imprinted p(NIPA-MAC) hydrogels at pH 5 are presented in Figure 4.12. The initial Cd(II) concentration was 10 ppm and the adsorption time was 24 hours. As shown in Figure 4.12, both non-imprinted and Cd<sup>2+</sup> imprinted p(NIPA-MAC) hydrogels show high adsorption amount for Cd(II) ions at low temperature, 22°C (below LCST), and the adsorbed amount of cadmium ions per unit mass of the hydrogels decreases with increasing the temperature (above LCST). The results indicated that the hydrophilic-to-hydrophobic transition of polymer networks triggered by the temperature increase affected the adsorption of Cd(II) ions. Thus, the higher adsorption capabilities of both non-imprinted and Cd<sup>2+</sup> imprinted p(NIPA-MAC) hydrogels towards Cd(II) ions below LCST can be attributed to fact that the adsorption of the hydrogels mainly depend on the complexation of Cd<sup>2+</sup> ions with MAC groups. The “swollen-shrunken” configuration change of p(NIPA-MAC) based hydrogel networks triggered by environmental temperature could influence the formation of MAC-Cd<sup>2+</sup> complexes. At temperatures lower than the LCST, the copolymer networks stretch, which makes it easier for the inner MAC groups to capture the Cd(II) ions, so that the hydrogels exhibit higher adsorption capacity. On the other hand, at temperatures above LCST, the p(NIPA-MAC) copolymer networks shrink and the inner MAC groups are close to each other. As a result, the electrostatic repulsions among the ions affect the formation of stable MAC-Cd<sup>2+</sup> complexes inside hydrogel, which leads to smaller adsorbed amount of Cd(II).

From a practical point of view, the results demonstrate that the available adsorption sites decrease with changes in hydrogel dimension produced by temperature variation.

#### **4.3.5. Selectivity Experiments**

In this group of experiments, competitive adsorption of Cd(II), Pb(II) and Cu(II) ions and Cd(II), Cr(III) and Fe(III) from their separate solutions containing the ions together was investigated. For this purpose, competitive adsorption studies performed in two ways. First, adsorption studies were done with separate

solutions of Cd(II), Pb(II), Cu(II), Cr(III), and Fe(III) ions with each solutions containing 10 ppm of each metal ions, at pH:5 with a stirring rate of 350 rpm for 24h at 22°C. Second, the mixture of Cd(II), Pb(II), and Cu(II) solution containing 10 ppm of each metal ion, and Cd(II), Cr(III), and Fe(III) solution which is also containing 10 ppm of each metal ions; other adsorption conditions were kept same as in the case of separate solutions of these metal ions. The measurements were carried out with the imprinted and non-imprinted hydrogels. Figure 4.13 (b) and Figure 4.14 (b) show the results of the selective adsorption of Cd(II) ions in competitive solutions. For comparison, noncompetitive adsorption results of each metal ion are given in Figure 4.13 (a) and over again in Figure 4.14 (a).

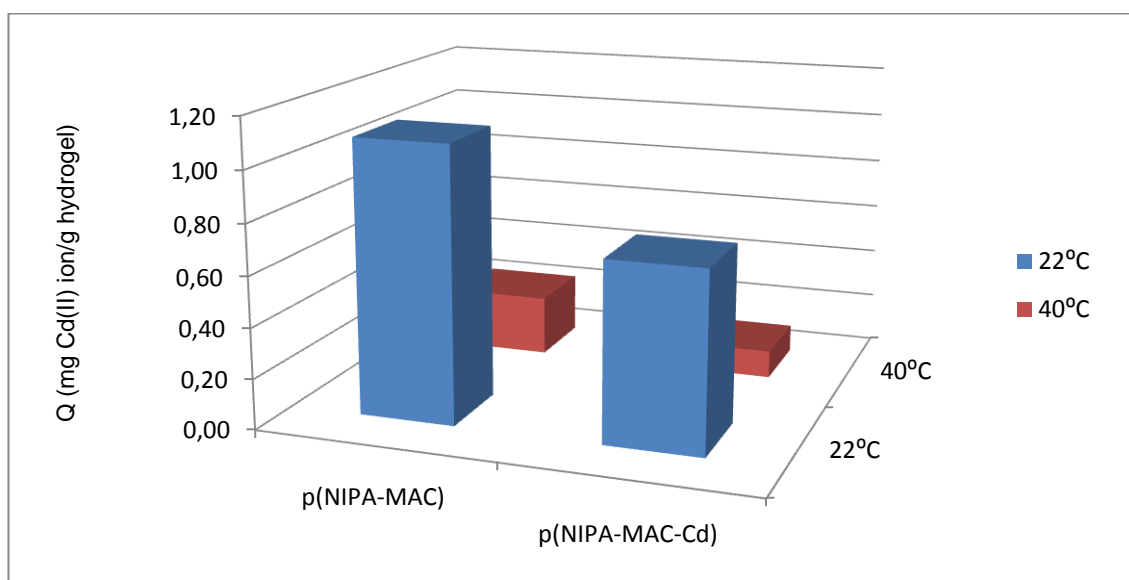


Figure 4.12. Effect of temperature on the adsorption amount for Cd(II) ions of the non-imprinted and Cd<sup>2+</sup> imprinted p(NIPA-MAC) hydrogels.

As can be seen from the data in Figure 4.13 (a), under noncompetitive conditions, the metal ion adsorption amount for the imprinted hydrogel increased in the order of Cd(II)>Pb(II)>Cu(II)>Fe(III)>Cr(III). On the other hand, in the case of the non-imprinted hydrogel the adsorption amount of Pb(II) ions (1.32 mg Pb<sup>2+</sup>/g hydrogel) was a little large compared with Cd(II) ions (1.28 mg Cd<sup>2+</sup>/g hydrogel). These results support the ion-recognition behavior of the Cd(II) imprinted p(NIPA-MAC) hydrogel. According to Pearson, complexation behavior of ligands and cations in terms of electron pair donating Lewis bases and electron pair accepting Lewis

acids, metal ions are termed hard, soft, and borderline. Hardness of metal ions (Lewis acids) will determine their preference to binding. Softer ions (e.g.,  $\text{Cd}^{2+}$ , low positive charge relative to large size, very polarizable) are expected to bind sulfur and nitrogen donor atoms of the ligand on the polymer, whereas hard metals (e.g.,  $\text{Cr}^{3+}$ , high charge to radius ratio, not very polarizable) coordinate to carboxylate groups, and borderline ions (e.g.,  $\text{Cu}^{2+}$  and  $\text{Pb}^{2+}$ ) would bind to any of the ligands according to conditions that may change the hardness of the ligand (R. Pearson, *Chemical Hardness*, 1997). On the other hand, under competitive conditions, less amount of all these ions adsorbed to the imprinted and non-imprinted p(NIPA-MAC) hydrogels because of competitions of these ions. However, the selective adsorption of the Cd(II) ion on the imprinted hydrogel was observed in the same manner as in Figure 4.13 (a). This can be concluded that, non-imprinted and imprinted p(NIPA-MAC) hydrogels show the following metal ion affinity in the order of  $\text{Cd}^{2+} > \text{Pb}^{2+} > \text{Cu}^{2+} > \text{Cr}^{3+} > \text{Fe}^{3+}$ .

The binding trend is presented on the mass basis, (mg) metal binding per gram hydrogels, in Figure 4.13 and Figure 4.14 and these units are important in quantifying respective metal capacities in real terms. However, a more effective approach is to compare metal binding on a molar basis; this gives a measure of the total number of metal ions adsorbed, as opposed to total mass, and is an indication of the total number of binding sites available in the hydrogel to each metal. Additionally, the molar basis of calculation is the only accurate way of investigating competition in multi-component metal mixtures. The binding capacity of the Cd(II)-imprinted p(NIPA-MAC) hydrogels on molar basis is 3.60  $\mu\text{mol/g}$  for  $\text{Cd}^{2+}$ , 3.23  $\mu\text{mol/g}$  for  $\text{Cu}^{2+}$ , and 1.51  $\mu\text{mol/g}$  for  $\text{Pb}^{2+}$  (for the mixture of Cd(II), Pb(II), and Cu(II) solution containing 10 mg/L of each metal ion), and 4.63  $\mu\text{mol/g}$  for  $\text{Cd}^{2+}$ , 1.34  $\mu\text{mol}$  for  $\text{Cr}^{3+}$ , and 0.419  $\mu\text{mol/g}$  for  $\text{Fe}^{3+}$ , (for the mixture of Cd(II), Cr(III), and Fe(III) solution containing 10 mg/L of each metal ion). The binding capacity of the Cd(II) imprinted hydrogels on molar basis for the single metal solutions is 6.70  $\mu\text{mol/g}$  for  $\text{Cd}^{2+}$ , 4.88  $\mu\text{mol/g}$  for  $\text{Cu}^{2+}$ , 2.80  $\mu\text{mol/g}$  for  $\text{Pb}^{2+}$ , 2.68  $\mu\text{mol/g}$  for  $\text{Cr}^{3+}$ , and 0.429  $\mu\text{mol}$   $\text{Fe}^{3+}$ . On the other hand, the binding capacity of the non-imprinted p(NIPA-MAC) hydrogels on molar basis is 5.77  $\mu\text{mol/g}$  for  $\text{Cu}^{2+}$ , 5.13  $\mu\text{mol/g}$  for  $\text{Cd}^{2+}$ , and 2.47  $\mu\text{mol/g}$  for  $\text{Pb}^{2+}$  (for the mixture of Cd(II), Pb(II), and Cu(II) solution containing 10 mg/L of each metal ion), and 6.78  $\mu\text{mol/g}$  for

## Results and Discussion

$\text{Cd}^{2+}$ ,  $2.31 \mu\text{mol}$  for  $\text{Cr}^{3+}$ , and  $0.412 \mu\text{mol/g}$  for  $\text{Fe}^{3+}$ , (for the mixture of  $\text{Cd}(\text{II})$ ,  $\text{Cr}(\text{III})$ , and  $\text{Fe}(\text{III})$  solution containing  $10 \text{ mg/L}$  of each metal ion). The binding capacity of the non-imprinted hydrogels for the single metal solutions is  $11.43 \mu\text{mol/g}$  for  $\text{Cd}^{2+}$ ,  $9.91 \mu\text{mol/g}$  for  $\text{Cu}^{2+}$ ,  $6.38 \mu\text{mol/g}$  for  $\text{Pb}^{2+}$ ,  $6.08 \mu\text{mol/g}$  for  $\text{Fe}^{3+}$ , and  $5.96 \mu\text{mol/g}$  for  $\text{Cr}^{3+}$ .

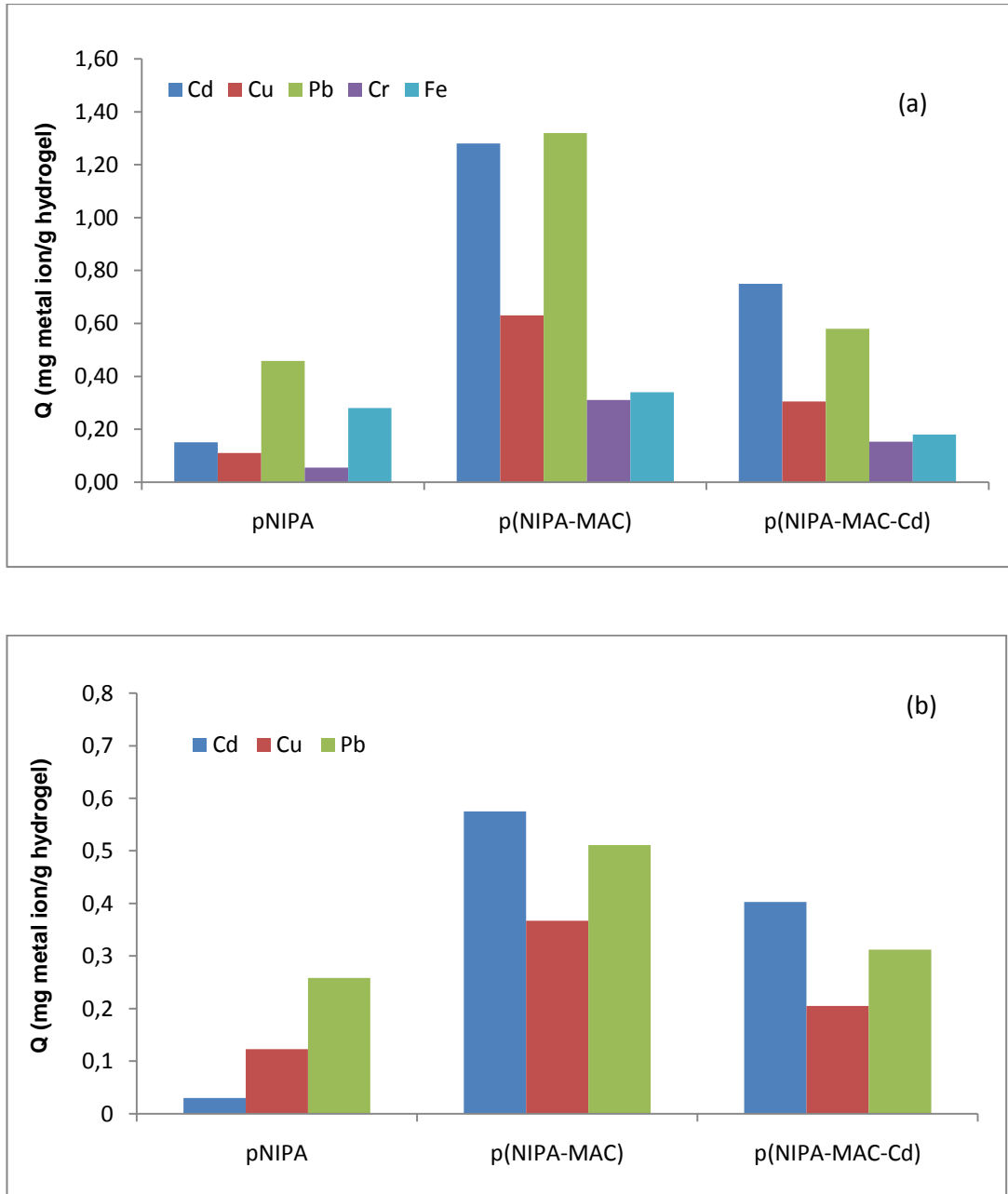


Figure 4.13. The amount of  $\text{Cd}^{2+}$ ,  $\text{Cu}^{2+}$ , and  $\text{Pb}^{2+}$  ions adsorbed by using pNIPA, non-imprinted p(NIPA-MAC) and Cd(II) imprinted p(NIPA-MAC) hydrogels (a) from each metal ion solution (noncompetitive) (b) from the mixtures of these metal ions (competitive).

As a result, on molar basis, Cd(II)-imprinted p(NIPA-MAC) hydrogels show the following metal ion affinity in order of Cd(II)>Cu(II)>Pb(II)>Cr(III)>Fe(III) while the non-imprinted hydrogels exhibit the following affinity in order of Cu(II)>Cd(II)>Pb(II)>Cr(III)>Fe(III).

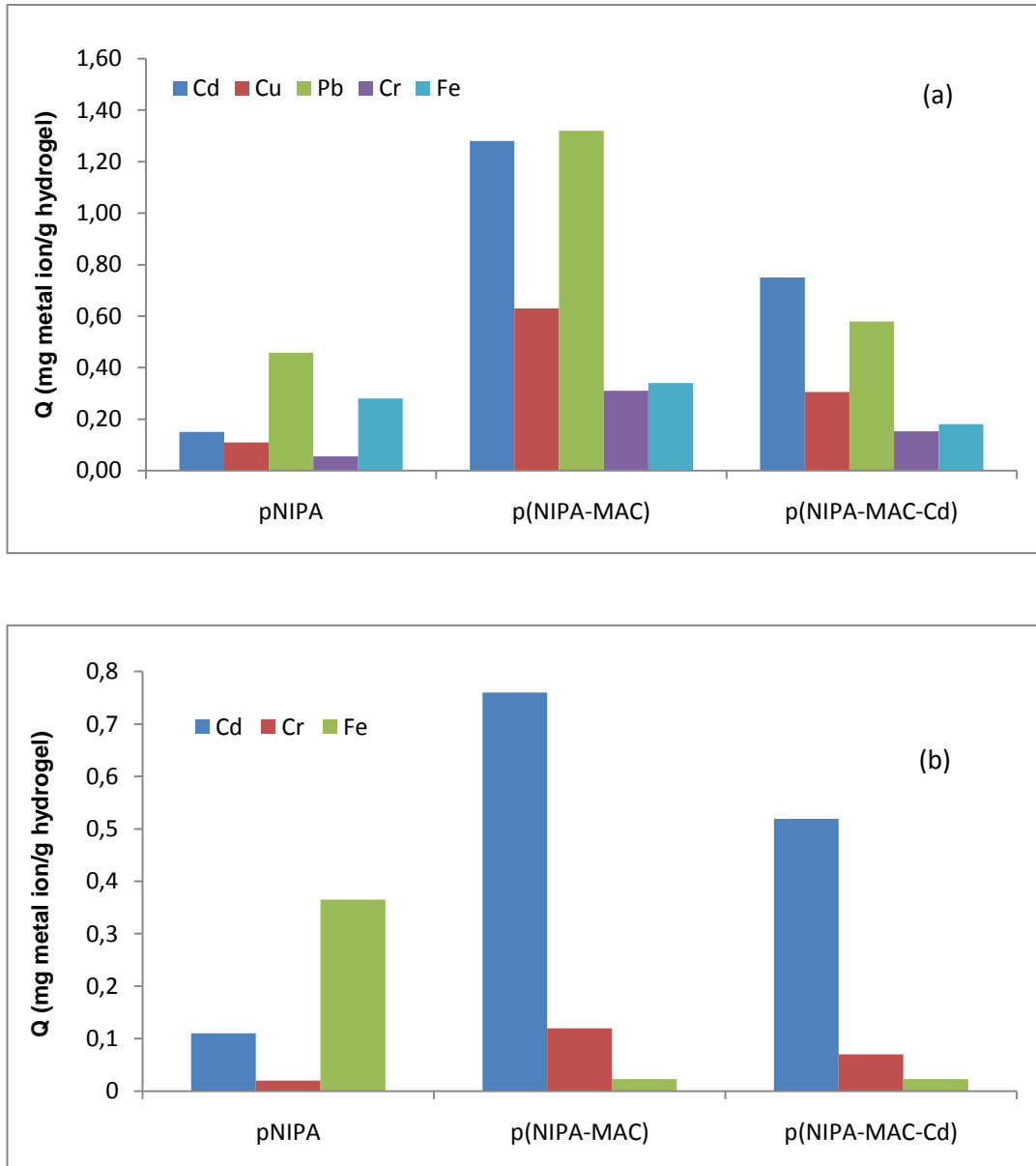


Figure 4.14. The amount of Cd<sup>2+</sup>, Cr<sup>3+</sup>, and Fe<sup>3+</sup> ions adsorbed by using pNIPA, non-imprinted p(NIPA-MAC) and Cd(II) imprinted p(NIPA-MAC) hydrogels (a) from each metal ion solution (noncompetitive) (b) from the mixtures of these metal ions (competitive).

From these results, it can be said that the hydrogel adsorbent imprinted with Cd(II) ions indicates the selectivity for the Cd<sup>2+</sup> ion as expected.

#### 4.3.6. Desorption and Reusability

With the aim of developing polymeric hydrogels sensitive to external (temperature) stimuli and able to reversibly adsorb and release  $\text{Cd}^{2+}$  ions, we tried to take out the  $\text{Cd}^{2+}$  ions from the  $\text{Cd(II)}$  imprinted p(NIPA-MAC) hydrogel- adsorbent by squeezing the gels above LCST. First, the non-imprinted and imprinted hydrogels were incubated in 10 ppm  $\text{Cd(II)}$  solution at  $22^\circ\text{C}$  for 12 h. After the adsorption was completed, adsorption medium was placed in a thermostatic water bath at  $50^\circ\text{C}$  for 24 h. Figure 4.15 shows the results of desorption of  $\text{Cd}^{2+}$  ions, by squeezing the non-imprinted and imprinted hydrogels at  $50^\circ\text{C}$ . According to our expectation, we could shrink the swollen hydrogels despite the presence of MAC- $\text{Cd}^{2+}$  complexes by raising the temperature to  $50^\circ\text{C}$ . Unfortunately, both the non-imprinted and the imprinted hydrogels released water when shrinking, but did not release  $\text{Cd}^{2+}$  ions at mentionable amount. The imprinted hydrogel released just 6.02% of the adsorbed  $\text{Cd(II)}$  ions, which means the squeezed hydrogel still keeps 93.98% of the bound  $\text{Cd(II)}$  ions in the polymeric hydrogel network, and the non-imprinted hydrogel released 13.49% of the adsorbed  $\text{Cd(II)}$  ions. The results can be concluded that there is a frustration for adsorbing monomers to come into proximity, which comes from the cross links and the polymer connection, so that the affinity is recovered upon shrinking. Consequently, the  $\text{Cd(II)}$  ions adsorbed on the hydrogels were completely desorbed from the hydrogels by means of acid treatment. 3 hours of interaction time with 0.1 M  $\text{HNO}_3$  was enough for complete desorption and the amounts of the stripping  $\text{Cd}^{2+}$  ions were almost the same with the adsorbed amounts in the experimental error limits (Table 4.3).

In order to investigate the reusability of the imprinted and non-imprinted p(NIPA-MAC) hydrogels, adsorption-desorption cycle was repeated three times using the same sorbent. The data are presented in Table 4.3. Resorption capacity of the hydrogels for  $\text{Cd(II)}$  ions did not change significantly during repeated adsorption-desorption operations. Thus, it is concluded that the non-imprinted and  $\text{Cd}^{2+}$ -imprinted p(NIPA-MAC) particles can be used many times without decreasing their adsorption capacities significantly.

Alvarez-Lorenzo et al. prepared copolymer gels of NIPA and methacrylic (MAA) monomers to reversibly adsorb and desorb divalent ions and  $\text{Ca}^{2+}$  was chosen as

a target divalent atom. To enhance the affinity to calcium, they applied imprinting technique using  $\text{Ca}^{2+}$  and  $\text{Pb}^{2+}$  as templates. They reported that (a) the affinity depends on the degree of gel swelling or shrinkage that can be switched on and off by temperature (b) in the shrunken state, affinity depends approximately linearly on the MAA concentration in the imprinted gels, whereas in the non-imprinted gels it is proportional to the square of MAA concentration (c) the imprinted gels adsorb more than the nonimprinted gels when MAA concentration is less than that of permanent cross linkers (Alvarez-Lorenzo et al., 2001). Yamashita et al. examined the preparation of IPN-type stimuli-responsive gel consisting of PNIPAm and PNaAAC for heavy-metal-ion adsorption/desorption.

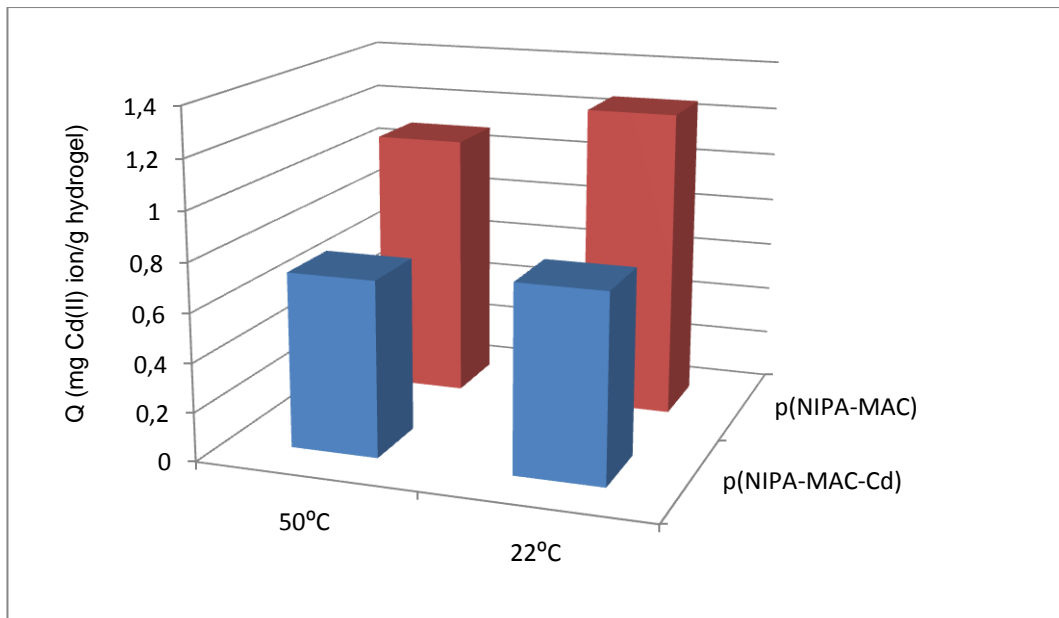


Figure 4.15. Desorption of Cd(II) ions from the non-imprinted and imprinted p(NIPA-MAC) hydrogels by raising the temperature above LCST, at 50°C, after the adsorption was carried out at 22°C.

They pronounced that the swelling IPN gel below the LCST quickly adsorbed the Cu(II) ions but did not release Cu(II) ions at all. In another study, Ju et al. showed the adsorption/desorption of lead(II) ions from aqueous solutions by using the P(NIPAM-co-BCAm) hydrogels. They observed complete desorption of Pb(II) ions above the LCST (Ju et al., 2009).



Table 4.3. Reusability of the imprinted and non-imprinted hydrogels; adsorption-desorption of Cd(II) ions from the hydrogels.

Adsorbent	Cd(II) ions adsorbed, mg/g			Desorption ratio %		
	First	Second	Third	First	Second	Third
Cd(II) imprinted p(NIPA-MAC)	0.727	0.691	0.709	98.9	98.6	99.2
Non-imprinted p(NIPA-MAC)	1.204	1.31	1.116	99.7	97.9	97.2

#### 4.3.7. Determination of Cd(II) ions in a Certified Sample

Using a certified water sample (NWTMDA-52.3 fortified water, obtained from LGC Standards), the recovery of the Cd(II) ions from the non-imprinted and the imprinted hydrogels was verified. The content of the certified sample is given in Table 4.4. The adsorption studies were carried out in 50 mL aliquots of the certified sample with a stirring rate of 300 rpm and adjusted the pH to 5.5 for 12 hours at 22°C. For the desorption of the Cd(II) ions 50 mL of 0.1 M HNO<sub>3</sub>(aq) was used. The certified value and the obtained results after desorption with HNO<sub>3</sub>(aq) are presented in Table 4.5. As can be seen from the data in Table 4.4 and Table 4.5, both non-imprinted and imprinted hydrogels exhibited a satisfactory recovery values in spite of the presence of other metal ions.

Table 4.4. The content of the certified water sample, NWTMDA-52.3.

Element	Concentration, µg/L	Element	Concentration, µg/L
Ag	20.8	Li	14.9
Al	310	Mn	198
As	25.3	Mo	208
Ba	148	Ni	274
Be	17.6	Pb	358
Bi	12.5	Sb	16.5
<b>Cd</b>	<b>190.9</b>	Se	21.8
Co	136	Sn	19.9
Cr	165	Sr	286
Cu	189	Ti	120
Fe	413	Tl	18.4

Table 4.5. Results for determination of Cd(II) ions in certified water sample. (N=2)

Hydrogel Sample	Certified value for Cd µg/L	Determined value for Cd µg/L	Recovery (%)
Cd(II) imprinted p(NIPA-MAC)	190.9	164.6	86.2
Non-imprinted p(NIPA-MAC)	190.9	178.3	93.3

## 5. CONCLUSION

With the aim of developing polymeric hydrogels sensitive to temperature and able to reversibly adsorb and release Cd(II) ions in aqueous solutions, copolymer hydrogels of NIPA and MAC monomers were prepared by using free radical polymerization technique. An imprinted thermosensitive hydrogel adsorbent was prepared by copolymerizing NIPA with a chelating monomer, MAC-Cd<sup>2+</sup> complex, in the presence of cadmium ion, as a target metal ion.

The effect of NIPA/MAC feed ratio on the swelling ratios of p(NIPA-MAC) hydrogels was investigated. The results showed that the increased swelling ratio was obtained with increasing MAC content in the feed composition of the prepared hydrogels. The swelling ratio of 21.98 was achieved with the NIPA/MAC molar ratio of 92/8 for the p(NIPA-MAC) hydrogel whereas the swelling ratio of 17.81 was obtained for the hydrogel which has molar ratio of 100/0. The obtained results also showed that the LCST of the p(NIPA-MAC) hydrogels are affected with NIPA/MAC feed ratio.

The LCST of pNIPA was around 33 °C. Introducing MAC monomer into the polymer structure, the LCST temperature shifted to a higher temperature, 35 °C, due to hydrophilic nature of the MAC groups.

The influence of the amount of crosslinker, MBAA, on the swelling ratios of p(NIPA-co-MAC) hydrogels was also examined. The amount of the cross linker did not affect the LCST and phase separation behavior of hydrogels evidently in the range of 1.0 - 4.0 wt%, however, the swelling ratio of the p(NIPA-MAC) hydrogels increased with decreasing MBAA amount. The swelling ratios of the p(NIPA-MAC) hydrogels were calculated as 34.42, 21.98, and 16.21 corresponding to 1.0, 2.0, and 4.0% MBAA, respectively.

The pNIPA, non-imprinted p(NIPA-MAC), and Cd(II) imprinted p(NIPA-MAC) hydrogels showed increasing swelling ratio at lower temperatures, but they deswelled at high temperatures because of the aggregation of the network chains. The highest LCST value was observed at 34°C for p(NIPA-MAC) gels, followed by

## *Conclusion*

template removed  $\text{Cd}^{2+}$ -imprinted p(NIPA-MAC) and pNIPA hydrogels with the LCST of 33 and 32°C, respectively.

The dry pNIPA, non-imprinted p(NIPA-MAC) and template removed  $\text{Cd}^{2+}$ -imprinted p(NIPA-MAC) hydrogels adsorbed about 40, 52 and 44% water within 240 min, respectively. This relationship suggests that water can diffuse into the hydrogel networks faster if the hydrogel has more hydrophilic (MAC monomer) contents.

The incorporation of MAC and MAC-Cd complex into the hydrogels were confirmed by using sulphur ratio obtained from the elemental analysis results. The determined sulphur amounts are 0.67, 2.36 and 1.83% for pNIPA, non-imprinted p(NIPA-MAC) and Cd(II) imprinted p(NIPA-MAC) hydrogels, respectively.

When the FTIR spectrum of pNIPA, non-imprinted p(NIPA-MAC), and  $\text{Cd}^{2+}$  imprinted p(NIPA-MAC) hydrogels were compared it can be seen that the characteristic double peaks at 1388 and 1366  $\text{cm}^{-1}$  for isopropyl group of NIPA appeared in all FT-IR spectra. Specifically, the appearance of the C-S peak around 620  $\text{cm}^{-1}$  in both FT-IR spectrum of p(NIPA-MAC) and  $\text{Cd}^{2+}$  imprinted p(NIPA-MAC) hydrogels denoted a successful incorporation of MAC groups into copolymeric hydrogels.

From comparative analysis of the EDS spectrums, the copolymerization of NIPA and MAC- $\text{Cd}^{2+}$  complex was confirmed due to the appearance of the Cd peaks in the range 3-4 keV in the EDS spectrum of  $\text{Cd}^{2+}$  imprinted p(NIPA-MAC) hydrogel but not in the spectrum of the non-imprinted p(NIPA-MAC) hydrogel. The feature peaks suggested a successful manufacturing of  $\text{Cd}^{2+}$  imprinted p(NIPA-MAC) copolymeric hydrogel.

Scanning electron microscope images showed that the pNIPA, non-imprinted p(NIPA-MAC), and  $\text{Cd}^{2+}$  imprinted p(NIPA-MAC) hydrogels have microporous network structure. According to the SEM images below LCST, moderately disorganized morphology and rather small pores observed for imprinted p(NIPA-MAC) hydrogel compared with the non-imprinted one may result the molecular structure difference between the MAC molecule and the MAC- $\text{Cd}^{2+}$  complex molecule. The

## *Conclusion*

SEM images above the LCST exhibited rather compact with small pores network structure when compared with their corresponding SEM images below LCST.

The adsorption and desorption properties of pNIPA, non-imprinted p(NIPA-MAC) and imprinted p(NIPA-MAC) hydrogels for  $\text{Cd}^{2+}$  ions were investigated in batch system.

High adsorption rates are observed at the beginning, and then plateau values (i.e., adsorption equilibrium) are gradually reached within 240 min for both non-imprinted p(NIPA-MAC), and  $\text{Cd}^{2+}$  imprinted p(NIPA-MAC) hydrogels. In the case of pNIPA, equilibrium adsorption rate is observed within 60 minutes which indicates that the Cd(II) ion adsorption is not affected with the expanded network structure of the pNIPA hydrogel compared to MAC incorporated hydrogels, due to poorer binding ability for Cd(II) ions of amide group in the NIPA.

The adsorption amount of  $\text{Cd}^{2+}$  ions on the pNIPA, non-imprinted p(NIPA-MAC) and the  $\text{Cd}^{2+}$  imprinted poly(NIPA-MAC) hydrogels were determined at the pH range between 2.5-7.5. In all of the cases, the adsorption amount increased with increasing pH, reaching a maximum value at around pH 5.5.

The adsorption amounts increased with increasing initial  $\text{Cd}^{2+}$  ion concentration, and the saturation value is achieved at ion concentration of 25 ppm for non-imprinted p(NIPA-MAC) hydrogel, and 10 ppm for imprinted p(NIPA-MAC) hydrogel, which represents saturation of the active binding sites of the polymeric hydrogels.

The adsorption capacities of  $\text{Cd}^{2+}$  imprinted p(NIPA-MAC), non-imprinted p(NIPA-MAC) and pNIPA hydrogels were found 0.975 mg Cd(II)/g, 1.324 mg Cd(II)/g and 0.20 mgCd(II)/g at pH 5.5.

The effect of temperature on the adsorption amount for Cd(II) ions of the non-imprinted and  $\text{Cd}^{2+}$  imprinted p(NIPA-MAC) hydrogels was also studied. The adsorbed amount of cadmium ions per unit mass of the hydrogels decreased from 1.09 mg/g at 22°C to 0.24 mg/g at 40°C for non-imprinted p(NIPA-MAC) and from 0.71 mg/g at 22°C to 0.11 mg/g at 40°C for imprinted p(NIPA-MAC) hydrogel.

## *Conclusion*

The selective adsorption for Cd(II) ions of Cd<sup>2+</sup> imprinted p(NIPA-MAC) hydrogel was confirmed by comparing the adsorption amounts of other metal ions, Pb(II), Cu(II), Cr(III) and Fe(III).

With the aim of developing polymeric hydrogels able to reversibly adsorb and release Cd<sup>2+</sup> ions by temperature swing (changing the temperature below and above the LCST), we tried to take out the Cd<sup>2+</sup> ions from the Cd(II) imprinted p(NIPA-MAC) hydrogel- adsorbent by squeezing the gels above LCST. Unfortunately, both the non-imprinted and the imprinted hydrogels released water when shrinking, but did not release Cd<sup>2+</sup> ions at mentionable amount.

The complete desorption of the adsorbed Cd(II) ions on the thermosensitive hydrogels was achieved by using 0.1 M HNO<sub>3</sub>(aq).

Resorption capacities of both non-imprinted and Cd(II) imprinted p(NIPA-MAC) hydrogels did not change significantly during repeated adsorption-desorption operations.

The removal of Cd(II) ions from aqueous solutions is carried out using p(NIPA-co-MAC) hydrogels. The prepared Cd<sup>2+</sup>-imprinted p(NIPA-MAC) hydrogel exhibits good ion-recognition and Cd(II) adsorption characteristics. Our results suggest that the Cd<sup>2+</sup>-imprinted p(NIPA-MAC) hydrogel and the non-imprinted p(NIPA-MAC) hydrogel can be a novel thermo-responsive smart Cd<sup>2+</sup> adsorbents and may have potential applications in environmental protections.

Recovery of Cd(II) ions from a certified water sample was investigated at optimized adsorption/desorption conditions. Results showed that both non-imprinted and imprinted hydrogels exhibit satisfactory recovery values (92.3% and 86.2%, respectively) in spite of the presence of other metal ions.

## REFERENCES

- Alvarez-Lorenzo, C., 2000, Polymer gels that memorize elements of molecular conformation, *Macromolecules*, 33, 8693-8699.
- Alvarez-Lorenzo, C., Guney, O., Oya, T., Sakai, Y., Kobayashi, M., Enoki, T., Takeoka, Y., Ishibashi, T., Kuroda, K., Tanaka, K., Wang, G. and Grosberg, A.Y., 2001, Reversible adsorption of calcium ions by imprinted temperature sensitive gels, *J. Chem. Phys.*, 114, 2812-2816.
- Alvarez-Lorenzo, C., Enoki, T., 2005, Temperature-sensitive chitosan-poly(*N*-isopropylacrylamide) interpenetrated networks with enhanced loading capacity and controlled release properties, *J. Control. Rel.*, 102, 629-637.
- Andersson, L.I., 2000, Molecular imprinting for drug bioanalysis: a review on the application of imprinted polymers to solid-phase extraction and binding assay, *J. Chromatogr. B*, 739, 163-172.
- Ansell, R.J., 2004, Molecularly imprinted polymers in pseudoimmunoassay, *J. Chromatogr. B*, 804, 151.
- Bae, Y.H., Okano, T., Kim, S.W., 1990, Temperature dependence of swelling of crosslinked poly (N,N-alkyl substituted acrylamide) in water, *J. Polym. Sci. Polym. Phys.*, 28, 923-936.
- Bradshaw, A.P. and Sturgeon, R.J., 1990, The synthesis of soluble polymer-ligand complexes for affinity precipitation studies, *Biotechnol. Techniq.*, 4, 254.
- Bryngelson, J.D. and Wolynes, P.G., 1987, Spin glasses and the statistical mechanics of protein folding, *Proc. Natl. Acad. Sci. USA*, 2, 7524.
- Burova, T., 2003, Effects of ligand binding on relative stability of subchain conformations of weakly charged *N* isopropylacrylamide gels in swollen and shrunken states, *Macromolecules*, 36, 9115.
- Byrne, M.E., Park, K., and Peppas, N.A., 2002, Molecular imprinting within hydrogels, *Adv. Drug Del. Rev.*, 54, 149.
- Charles, M., Coughlin, R.W., and Hasselberger, F.X., 1974, Soluble-insoluble enzyme catalysis, *Biotechnol. Bioeng.*, 16, 1553.

## References

- Connor, D.J.O., Sexton, B.A., Smart, R.S.C., 2003, *Surface Analysis Methods in Materials Science*, Springer-Verlag, New York.
- Denizli, A., Garipcan, B., Karabakan, A., Say, R., Emir, S., Patir, S., 2003, Metal-complexing ligand methacryloylamidocysteine containing polymer beads for Cd(II) removal, *Separation and Purification Technology*, 30, 3-10.
- D'Oleo, R., Alvarez-Lorenzo, C., and Sun, G., 2001 A new approach to design imprinted polymer gels without using a template, *Macromolecules*, 34, 4965.
- Enoki, T., Tanaka, K., Watanabe, T., 2000, Frustrations in polymer conformation in gels and their minimization through molecular imprinting, *Phys. Rev. Lett.*, 85, 5000.
- Filipcsei G., Feher J. and Zrinyi M., 2000, Electric field sensitive neutral polymer gels, *J Mol Struct* 554, 109–117.
- Galaev, I.Yu. and Mattiasson, B., 1993, Thermoreactive water-soluble polymers, nonionic surfactants, and hydrogels as reagents in biotechnology, *Enzyme Microb. Technol.*, 15, 354.
- Galaev, I.Yu., Gupta, M.N., and Mattiasson, B., 1996, Use smart polymers for bioseparations, *Chemtech*, 26, 19.
- Galaev, I.Yu. and Mattiasson, B., 1999, Smart polymers and what they could do in biotechnology and medicine, *Trends Biotechnol.*, 17, 335.
- Galaev, I.Yu. and Mattiasson, B., 2002, Affinity precipitation of proteins using smart polymers, in *Smart Polymers for Bioseparation and Bioprocessing*, Galaev, I.Yu. and Mattiasson, B., Eds., Taylor & Francis, London, 55–77.
- Gotoh, T., Nakatani, Y., Sakohara, S., 1998, Novel synthesis of thermosensitive porous hydrogels, *J of Applied Polymer Science*, 69, 895-906.
- Grinberg, N.V., 1999, Studies of the thermal volume transition of poly(*N*isopropylacrylamide) hydrogels by high-sensitivity differential scanning microcalorimetry, 1: dynamic effects, *Macromolecules*, 32, 1471.



## References

- Grinberg, V.Ya. et al., 2000, Studies of the thermal volume transition of poly(Misopropylacrylamide) hydrogels by high sensitivity microcalorimetry, 2: thermodynamic functions, *Macromolecules*, 33, 8685.
- Grosberg, A.Yu. and Khokhlov, A.R., 1997, *Giant Molecules*, Academic Press, San Diego.
- Güney, O., Yilmaz, Y., and Pekcan, O., 2002, Metal ion templated chemosensor for metal ions based on fluorescence quenching, *Sensors Actuators B*, 85, 86.
- Hillberg, A.L., Brain, K.R., and Allender, C.J., 2005, Molecular imprinted polymer sensors: implications for therapeutics, *Adv. Drug Del. Rev.*, 57, 1875.
- Hoffman, A.S., 1987, Application of thermally reversible polymers and hydrogels in therapeutics and diagnostic, *J. Controlled Release*, 6, 297.
- Hoffman, A.S., 1995, Intelligent polymers in medicine and biotechnology, *Macromol. Symp.*, 98, 645.
- Hoffman, A.S., 2001, New antibody purification procedure using thermally responsive poly(NIPA)-dextran derivative conjugate, *J. of Chromatography B, Biomedical Sciences and Applications*, 761, 247-254.
- [http://www.univie.ac.at/Mikrolabor/chn\\_eng.htm](http://www.univie.ac.at/Mikrolabor/chn_eng.htm)
- Ito, K. et al., 2004, Multiple contact adsorption of target molecules, *Macromol. Symp.*, 207, 1.
- Juodkazis S., Mukai N., Wakaki R., Yamaguchi A., Matsuo S. and Misawa H., 2000, Reversible phase transitions in polymer gels induced by radiation forces, *Nature*, 408, 178–181.
- Ju, X-J., Zhang, S-B., Zhou, M-Y., Xie, R., Yang, L. And Chu, L-Y., 2009, Novel heavy metal adsorption material: ion-recognition P(NIPAM-co-BCAm) hydrogels for removal of lead(II) ions, *J. Hazardous Materials*, 114-119.
- Kabanov V.A., 1994, Physicochemical basis and the prospects of using soluble interpolyelectrolyte complex, *Polym Sci* 36, 143–156.

## References

- Kanazawa, R., Mori, K., Tokuyama, H., and Sakohara, S., 2004, Preparation of thermosensitive microgel adsorbent for quick adsorption of heavy metal ions by a temperature change, *J. Chem. Eng. Japan*, 37, 80-807.
- Kikuchi, A. and Okano, T., 2002, Pulsatile drug release control using hydrogels, *Adv. Drug Del. Rev.*, 54, 53.
- Leclercq L., Boustta M. and Vert M., 2003, A physico-chemical approach of polyanion-polycation interactions aimed at better understanding the in vivo behaviour of polyelectrolyte-based drug delivery and gene transfection, *J Drug Target* 11, 129–138.
- Lee, S.J. and Park, K., 1996, Glucose-sensitive phase-reversible hydrogels, in *Hydrogels and Biodegradable Polymers for Bioapplications*, Ottenbrite, R.M., Huang, S.J., and Park, K., Eds., American Chemical Society, Washington, DC, 2–10.
- Lee, W.-F. and Shieh, C.H., 1999, pH-thermoreversible hydrogels, II: synthesis and swelling behaviours of *N* isopropylacrylamide-*co*-acrylic acid-*co*-sodium acrylate hydrogels, *J. Appl. Polym. Sci.*, 73, 1955.
- Lee, W-F. and Lin, Y-H., 2006, Swelling behavior and drug release of NIPAAm/PEGMEA copolymeric hydrogels with different crosslinkers, *J Mater. Sci.*, 41, 7333-7340.
- Lehto, J., Vaaramaa, K. and Vesterinen, E., 1998, uptake of zinc, nickel, and cadmium by N-isopropylacrylamide polymer gels, *J. Appld. Polymer Sci.*, 68, 355-362.
- Linné-Larsson, E. et al., 1992, Evaluation of alginate as a carrier in affinity precipitation, *Biotechnol. Appl. Biochem.*, 16, 48.
- Liu, F. et al., 1995, Development of a polymer-enzyme immunoassay method and its application, *Biotechnol. Appl. Biochem.*, 21, 257.
- Liu, X.Y. et al., 2004, Design of temperature sensitive imprinted polymer hydrogels based on multiple-point hydrogen bonding, *Macromol. Biosci.*, 4, 680.
- Liu, X.Y., 2004, Fabrication of temperature-sensitive imprinted polymer hydrogel, *Macromol. Biosci.*, 4, 412.

## References

- Lomadze N. and Schneider H.-J., 2005, Ternary complex formation inducing large expansions of chemomechanical polymers by metal chelators, aminoacids and peptides as effectors, *Tetrahedron Lett* 46,751–754.
- Mayes, A.G. and Whitcombe, M.J., 2005, Synthetic strategies for the generation of molecularly imprinted organic polymers, *Adv. Drug Del. Rev.*, 57, 1742.
- Miyata, T., Uragami, T., and Nakamae, K., 2002, Biomolecule-sensitive hydrogels, *Adv. Drug Del. Rev.*, 54, 79.
- Mori, S., Nakata, Y., and Endo, H., 1994, Purification of rabbit C-reactive protein by affinity precipitation with thermosensitive polymer, *Prot. Expr. Purif.*, 5, 151.
- Moritani, T. and Alvarez-Lorenzo, C., 2001, Conformational imprinting effect on stimuli-sensitive gels made with an imprinter monomer, *Macromolecules*, 34, 7796.
- Morris, G.E., Vincebt, B. and Snowden, M.J., 1997, Adsorption of lead ions onto N-isopropylacrylamide and acrylic acid copolymer microgels, *J. Colloid and Interface Science*, 190, 198-205.
- Nagarsekar, A. et al., 2003, Genetic engineering of stimuli-sensitive silk elastin-like protein block copolymers, *Biomacromolecules*, 4, 602.
- Oh, K.S. et al., 1998, Effect of cross-linking density on swelling behavior of NIPA gel particles, *Macromolecules*, 31, 7328.
- Okano T., 1993, Molecular design of temperature-responsive polymers as intelligent materials. In: K. Dusek, Editor, *Responsive gels: volume transitions vol. II*, Springer, Berlin, 180–197.
- Okay, O., 2000, Macroporous copolymer networks, *Prog. Polym. Sci.*, 25, 711.
- Omidian, H., Rocca, J.G., and Park, K., 2005, Advances in superporous hydrogels, *J. Contr. Rel.*, 102, 3.

## References

- Pande, V.S., Grosberg, A.Yu., and Tanaka, T., 2000, Heteropolymer freezing and design: towards physical models of protein folding, *Rev. Mod. Phys.*, 72, 259.
- Park, T.G. and Hoffman, A.S., 1994, Estimation of temperature-dependent pore size in poly(*N*-isopropylacrylamide) hydrogel beads, *Biotechnol. Prog.*, 10, 82.
- Petka, W.A. et al., 1998, Reversible hydrogels from self-assembling artificial proteins, *Science*, 281, 389.
- Piletsky, S.A. and Turner, A.P.F., 2002, Electrochemical sensors based on molecularly imprinted polymers, *Electroanalysis*, 14, 317.
- Qiu, Y. and Park, K., 2001, Environment-sensitive hydrogels for drug delivery, *Adv. Drug Del. Rev.*, 53, 321.
- Schild, H.G., 1992, Poly(*N*-isopropylacrylamide): experiment, theory and applications, *Prog. Polym. Sci.*, 17, 163.
- Sellergren, B., 2001, The non-covalent approach to molecular imprinting, in *Molecularly Imprinted Polymers*, Sellergren, B., Ed., Elsevier, Amsterdam, 113–184.
- Shibayama, M. and Tanaka, T., 1993, Volume phase transition and related phenomena of polymer gels, *Adv. Polym. Sci.*, 109, 1.
- Sibrian-Vazquez, M. and Spivak, D.A., 2003, Improving the strategy and performance of molecularly imprinted polymers using cross-linking functional monomers, *J. Org. Chem.*, 68, 9604.
- Skoog D.A., Leary, J.J., 1992, *Principles of Instrumental Analysis*, 4<sup>th</sup> Edition, Saunders College Publishing, New York.
- Solpan, D., Duran, S., and Guven, O., 2002, Synthesis and properties of radiation-induced acrylamide-acrylic acid hydrogels, *J. Appl. Polym. Sci.*, 86, 357.
- Stancil, K.A., Feld, M.S., and Kardar, M., 2005, Correlation and cross-linking effects in imprinting sites for divalent adsorption in gels, *J. Phys. Chem. B*, 109, 6636.

## References

- Tanaka, T. and Fillmore, D.J., 1979, Kinetics of swelling of gels, *J. Chem. Phys.*, 70, 1214.
- Tanaka, T. and Annaka, M., 1993, Multiple phases of gels and biological implications, *J. Intel. Mat. Syst. Struct.*, 4, 548.
- Tanaka, T., 1998, Reversible molecular adsorption as a tool to observe freezing and to perform design of heteropolymer gels, *Ber. Bunsenges. Phys. Chem.*, 102, 1529.
- Taylor L.D. and Gerankowski L.D., 1975, Preparation of films exhibiting balanced temperature dependence to permeation by aqueous solutions—a study of lower consolute behavior, *J Polymer Sci Polymer Chem Ed* 13, 2551–2570.
- Twaites B.R., Alarcon C.H., Cunliffe D., Lavigne M., Pennadam S. and Smith J.R., 2004, Thermo and pH responsive polymers as gene delivery vectors: effect of polymer architecture on DNA complexation in vitro, *J Control Release* 97, 551–566.
- Watanabe, M., Akahoshi, T., Tabata, Y., and Nakayama, D., 1998, Molecular specific swelling change of hydrogels in accordance with the concentration of guest molecules, *J. Am. Chem. Soc.*, 120, 5577.
- Welz, B., Sperling, M., 1999, *Atomic Absorption Spectrometry*, Wiley-VCH Verlag GmbH, D-69469, Federal Republic of Germany.
- Wulff, G., 1995, Molecular imprinting in cross-linked materials with the aid of molecular templates: a way towards artificial antibodies, *Angew. Chem. Int. Ed. Engl.*, 34, 1812.
- Xue, W. and Hamley, I.W., 2002, Thermoreversible swelling behaviour of hydrogels based on *N*-isopropylacrylamide with a hydrophobic comonomer, *Polymer*, 43, 3069.
- Yamashita, K., Nishimura, T., and Nango, M., 2003, Preparation of IPN-type stimuli responsive heavy-metal-ion adsorbent gel, *Polym. Adv. Technol.*, 14, 189.

## References

- Yan, M. and Ramström, O., 2005, Molecular imprinting: an introduction, in *Molecularly Imprinted Materials*, Yan, M. and Ramström, O., Eds., Marcel Dekker, New York, 1–12.
- Yusa S., Sakakibara A., Yamamoto T. and Morishima Y., 2002, Fluorescence studies of pH-responsive unimolecular micelles formed from amphiphilic polysulfonates possessing long-chain alkyl carboxyl pendants, *Macromolecules* 35, 10182–10188.
- Yu, Y., Chang, X., Ning, H., Zhang, S., 2008, Synthesis and characterization of thermoresponsive hydrogels cross-linked with chitosan, *Cent. Eur. J. Chem.*, 6(1), 107-113.
- Zhang, J. And Peppas, N.A., 2000, Synthesis and characterization of pH- and temperature sensitive poly(methacrylic acid)/poly(N-isopropylacrylamide) interpenetrating polymeric networks, *Macromolecules*, 33, 102-109.
- Zhang, X.Z., Zhuo, R.X., 2009, Composite microparticle drug delivery systems based on chitosan, alginate and pectin with improved pH sensitive drug release property, *J Colloid Interface Sci.*, 223, 311-313.
- Zhang, X.Z. and Chu, C.C., 2004, Preparation of thermosensitive PNIPAAm hydrogels with superfast response, *Chem. Commun.*, 350-351.
- Zhang, X.Z. and Chu, C.C., 2005, Fabrication and characterization of microgel-impregnated thermosensitive PNIPAAm hydrogels, *Polymer*, 46, 9664-9673.
- Zhang, X.Z. and Chu, C.C., 2007, Influence of polyelectrolyte on the thermosensitive property of PNIPAAm-based copolymer hydrogels, *J Matter Med*, 18, 1771-1779.
- Zrinyi M., 2000, Intelligent polymer gels controlled by magnetic fields, *Colloid Polym Sci* 278, 98–103.

## **CURRICULUM VITAE**

Name Surname : Ayşenur Sağlam

Place of Birth : Ankara

Date of Birth : 1975

Marital Status : Single

### Education and Academic Position

High School 1989-1992 Tinaztepe Lisesi (Ankara)

BSc 1994-1999 Hacettepe University, Department of Chemistry

MSc 2000-2003 Institute of Sciences of Hacettepe University

### Job Experience

2000-2010 Research Assistant at Hacettepe University, Department of Chemistry